Universitat Autònoma de Barcelona

Analytical design of feedback compensators based on Robustness/Performance and Servo/Regulator trade-offs

Utility in PID control applications

SUBMITTED IN PARTIAL FULFILMENT
OF THE REQUIREMENTS FOR THE DEGREE
OF DOCTOR ENGINEER AT UNIVERSITAT
AUTÒNOMA DE BARCELONA.

by

Salvador Alcántara

July, 2011

Dr. Carles Pedret i Ferré, Research Academic at Universitat Autònoma de Barcelona,

CERTIFIES:

That the thesis entitled **"Analytical design of feedback compensators based on Robustness/Performance and Servo/Regulator trade-offs: Utility in PID control applications"** by Salvador Alcántara Cano, presented in partial fulfilment of the requirements for the degree of Doctor Engineer, has been developed and written under his supervision.

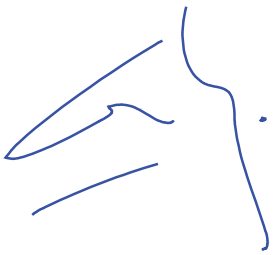

Dr. Carles Pedret i Ferré

Bellaterra, July 2011

Feedback is a central feature of life. The process of feedback governs how we grow, respond to stress and challenge, and regulate factors such as body temperature, blood pressure and cholesterol level.

Hoagland and Dodson (1995), The Way Life Works

A mechanical clock uses feedback,
but not for command following or disturbance rejection.
Instead, feedback provides a stable limit cycle [...]
The technology may be vintage, but the principles are timeless.

Bernstein (2011), Exquisite Coupling

Preface

The concept of (negative) feedback, albeit simple, is extremely powerful, and has since the Industrial Revolution changed our world dramatically. Nowadays, control systems are everywhere. In process industry, for example, they keep the manipulated variables close to the set-points in spite of disturbances and changes in the plant. Moreover, feedback provides the only means to *stabilize* unstable processes. This way, the feedback mechanism is essential for improving product quality and energy efficiency, which yields better (sustainable) economy.

The theme of this thesis is on analytical design of feedback compensators through linear control theory. The restriction to the Linear Time Invariant (LTI) case is not severe in the sense that most processes are well modeled locally by LTI systems. The operating range of the controller can then be extended using gain scheduling or adaptation (Astrom and Hagglund, 2005). Within this work, the standard single-loop feedback configuration is assumed. Among the control objectives, stability and robustness are important considerations because of the presence of uncertainty in practice. Apart from that, the controller faces servo (set-point tracking) and regulation (disturbance rejection) objectives.

In the considered scenario, it is well-known that there is an inherent compromise between robustness and performance. In general, the servo and regulation objectives are also conflicting and sometimes a balance is desirable. An example is in cascade configurations: the inner loop should be tuned based on tracking as it receives the set-points from the master loop. However, the inner loop may also need acceptable load disturbance suppression capabilities. Another good example is found in Model Predictive Control (MPC) applications due to frequent changes of set-points by the server. Finally, there may be a

trade-off between the response to disturbances entering at the input and at the output of the plant, which can be understood as a servo/regulator trade-off too.

The goal of this thesis is to provide model-based design procedures in terms of the *Robustness/Performance* and *Servo/Regulator* trade-offs, and give insight into how the tuning depends on the process parameters. In the presented methods, the designer is not required to choose weighting functions nor reference models as in other approaches, and the involved parameters have a clear meaning to facilitate the tuning process. Because PID controllers are prevalent in industry, application to PID tuning is considered most of the times. Although numerical methods for controller derivation may yield superior performance than analytical ones, the latter category has been preferred for several reasons. First, analytical procedures help understand the problem at hand. Second, when applied to low-order models, well-motivated tuning rules which are simple and easy to memorize can be obtained. These features are very desirable from the operator's point of view, and for teaching purposes too.

This work was started in October 2008 and it has resulted in the papers listed in Table 1. The thesis document is organized in the form of a brief introduction (Chapter 1), followed by six chapters (Chapters 2–7) based on the papers of Table 1. A final chapter (Chapter 8) summarizes the main conclusions and highlights some points for further research.

Publication	Chapter
Alcántara, S., C. Pedret, R. Vilanova and W. Zhang (2010). **Simple Analytical min-max Model Matching Approach to Robust Proportional-Integrative-Derivative Tuning with Smooth Set-Point Response**. Industrial & Engineering Chemistry Research 49(2), 690 – 700.	2
Alcántara, S., C. Pedret, R. Vilanova and P. Balaguer (2010). **Analytical $\mathcal{H}_\infty$ Sensitivity matching approach to Smooth PID design: Quantitative Servo/Regulator tuning guidelines**. Internal report.	3
Alcántara, S., C. Pedret and R. Vilanova (2010). **On the model matching approach to PID design: Analytical perspective for robust Servo/Regulator tradeoff tuning**. Journal of Process Control 20(5), 596–608.	4
Alcántara, S., C. Pedret, R. Vilanova and W. Zhang (2010). **Unified Servo/Regulator Design for Robust PID Tuning**. Proc. of IEEE Conference on Control Applications pp. 2432 – 2437.	5
Alcántara, S., W.D. Zhang, C. Pedret, R. Vilanova and S. Skogestad (2011). **IMC-like analytical $\mathcal{H}_\infty$ design with S/SP mixed sensitivity consideration: Utility in PID tuning guidance**. Journal of Process Control 21(6), 976–985.	6
Alcántara, S., S. Skogestad, C. Grimholt, C. Pedret and R. Vilanova (2011). **Tuning PI controllers based on $\mathcal{H}_\infty$ Weighted Sensitivity**. Proc. of the 19th Mediterranean Conference on Control and Automation.	6
Alcántara, S., C. Pedret, R. Vilanova and S. Skogestad (2011).**Generalized Internal Model Control for balancing input/output disturbance response**. Industrial & Engineering Chemistry Research 50(19), 11170–11180.	7

Table 1: Thesis publications.

Acknowledgements

First of all I want to thank my supervisor for his continuous encouragement and patience, and for teaching me how to be more self-starter and well-motivated to find my own way independently. Carles, thank you too for all the journeys you have financed, enabling me to be all over the world. In particular, I am specially thankful for the research stays

- at the Deparment of Automation of the Shanghai Jiao Tong University, under the supervision of Professor Weidong Zhang (Weidong, I will never forget your free-of-charge Saturday tour by Shanghai, nor any of your numerous gestures of generosity)
- and at the Deparment of Chemical Engineering of the Norwegian University of Science and Technology, working with Professor Sigurd Skogestad, probably the best intuitive-judgement professor in the world ;-).

Coming back to my home department, I cannot forget to express my gratitude

- to Ramon Vilanova, who was always there to help and whose works inspired this thesis, nor
- to Asier Ibeas, who I am lucky to count among my closest friends. Thank you for your love towards the academic world, without your genuine enthusiasm, bringing this thesis to an end would have been even harder.

Other colleagues who have shown me their support are: Montse, J. Serrano and P. Balaguer (now at *Universitat Jaume I*). It is also in place to say sorry to my office mates (Mota, Carlos, Alejandra, Catya and Rafa), to whom I have

continuously annoyed over the last years, specially to Dr. Mota and Carlos (*póngale cuidao*). Similar comments apply to Jorge, another victim upstairs. Thank you guys for the tea time and so many interesting discussions, mostly without any research relevance (but otherwise essential for life!).

And now the VIP list (turning to family/friends): *gracias a los que habéis puesto pausas a tantas horas de soledad:*

- *A mi padre, por ser tan trabajador y generoso (¿se puede ser mejor que eso?)*
- *...y a mi madre, por su enorme bondad: vuestros esfuerzos han sido mi comodidad.*
- *A mis hermanos Javi y Julián, y a la mujer del primero, Jessi.*
- *A mis tíos y primos "del pueblo", y a mi abuela Matilde, que tanto me quería.*
- *A mi abuelo (el único que me queda).*
- *A mi familia política (a Rosa por sus paellas, a Antonio por no meterse nunca con nadie, a David y Lola por las barbacoas en su terraza, aunque el trabajo sucio lo haga siempre Antonio...)*
- *A Óscar y Cristina.*
- *Al Dani, company de mates.*
- *A Maléfico (Álex), por pasarse de vez en cuando por el QC-0015 a ver qué tal me iba.*
- *A Asier, una vez más, por su gran amistad.*
- *Por último, gracias Rosi por darme tu amor y apoyarme siempre. Sin duda, tú eres lo mejor de mi vida.*

Bellaterra, July 2011

Salva

Contents

Preface **i**

Acknowledgements **v**

1 Introduction **3**
1.1 Two sources of inspiration: IMC (λ-tuning) and $\mathcal{H}_\infty$ control . . 4
1.1.1 Internal Model Control 4
1.1.2 $\mathcal{H}_\infty$ control 6
1.1.3 Blending IMC and $\mathcal{H}_\infty$ control 7
1.2 The starting point: a model matching design for PID tuning . . 9
1.2.1 A word about PID controllers 9
1.2.2 The Model Matching Problem within $\mathcal{H}_\infty$ control 12
1.2.3 Vilanova's (2008) design for robust PID tuning revisited 13
1.3 Outline/summary of the thesis 16

2 Simple model matching approach to robust PID tuning **29**
2.1 Introduction 29
2.2 Problem statement 31
2.2.1 The control framework 31
2.2.2 The Model Matching Problem 32
2.3 Analytical solution 33
2.4 Stability analysis 36
2.4.1 Nominal stability 36

2.4.2 Robust stability 39
2.5 Automatic PID tuning derivation 40
2.5.1 Control effort constraints 43
2.6 Simulation examples 46
2.7 Summary 53

3 Improving the load disturbance response (γ-tuning) 55
3.1 Introduction 55
3.2 Problem statement 57
3.2.1 The control framework 57
3.2.2 The Model Matching Problem 58
3.3 Model matching approach to PID design 59
3.4 Trade-off tuning interval for γ considering load disturbances . . 62
3.4.1 Nominal stability 64
3.5 Quantitative guidelines for the tuning of γ 68
3.6 Simulation examples 72
3.6.1 Example 1 72
3.6.2 Example 2 74
3.7 Summary 79

4 λ-tuning versus γ-tuning 81
4.1 Introduction 81
4.2 *Smooth/Tight* interval for λ 83
4.3 Comparison of the λ and γ-tuning approaches 85
4.4 Implementation aspects 88
4.5 Simulation examples 90
4.6 Summary 94
Appendix 4A 99

5 Combined $\lambda\gamma$ approach: a first $\mathcal{H}_\infty$ design **103**
5.1 Introduction . . . 103
5.2 The control framework . . . 104
5.3 Proposed $\lambda\gamma$-tuning . . . 105
5.3.1 Robustness considerations in terms of λ and γ . . . 108
5.3.2 IMC interpretation . . . 110
5.4 Simulation example . . . 112
5.5 Summary . . . 116

6 An improved $\mathcal{H}_\infty$ design **119**
6.1 Introduction . . . 119
6.2 Proposed design procedure . . . 122
6.2.1 Analytical solution . . . 122
6.2.2 Selection of W . . . 125
6.2.3 Stability and Robustness . . . 128
6.3 Application to PI tuning . . . 129
6.3.1 Stable/unstable plants . . . 129
6.3.2 Integrating plant case ($\tau \to \infty$) . . . 132
6.4 Simulation examples . . . 132
6.4.1 Example 1 . . . 133
6.4.2 Example 2 . . . 134
6.4.3 Example 3 . . . 136
6.4.4 Example 4 . . . 136
6.5 Summary . . . 140
Appendix 6A . . . 141

7 The $\mathcal{H}_2$ counterpart **147**
7.1 Introduction . . . 147
7.2 Problem statement and background material . . . 149
7.3 Proposed input/output regulator design . . . 151
7.3.1 Selection of W . . . 151
7.3.2 Analytical solution . . . 153

7.3.3 Nominal performance and robust stability/performance 158
7.4 Simulation examples 161
7.5 Summary 168

8 Conclusions and perspectives **169**
8.1 Conclusions 169
8.2 Perspectives 170

Bibliography **186**

Chapter 1

Introduction

The aim of this introduction is to guide the reader through the contributions made in Chapters 2–7. The discussion that follows is based on the unity feedback, LTI and Single-Input-Single-Output (SISO) continuous-time system of Figure 1.1, where P is the plant and K the feedback controller to be designed. The output signals y, u represent, respectively, the plant output and the control action. Two exogenous inputs to the system are considered: d and r. Here, d represents a disturbance affecting the plant input, and the term *regulator mode* refers to the case when this is the main exogenous input. The term

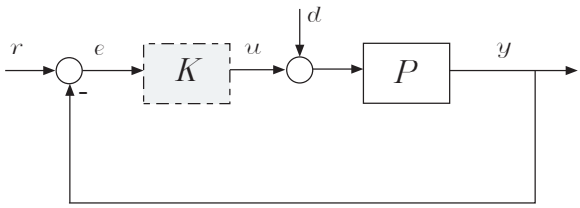

Figure 1.1: Conventional feedback configuration.

servo mode refers to the case when the set-point change r is the main concern. Although the reference tracking can be improved by using a two-degree-of-freedom (2DOF) controller (Skogestad and Postlethwaite, 2005; Astrom and Hagglund, 2005), there will always be some unmeasured disturbance directly affecting the plant output, which may be represented as an unmeasured signal

r (in this case, the plant output would be the control error $e = r - y$). In summary, there is a fundamental trade-off between the regulator (input disturbance) and servo (output disturbance) modes. The closed-loop mapping for the system in Figure 1.1 is given by

$$\begin{bmatrix} y \\ u \end{bmatrix} = \begin{bmatrix} T & SP \\ KS & S \end{bmatrix} \begin{bmatrix} r \\ d \end{bmatrix} \doteq H(P,K) \begin{bmatrix} r \\ d \end{bmatrix} \tag{1.1}$$

where $S \doteq \frac{1}{1+PK}$ and $T \doteq \frac{PK}{1+PK}$ denote the sensitivity and complementary sensitivity functions (Skogestad and Postlethwaite, 2005), respectively (note that $S+T = 1$). In terms of the performance for the regulator and servo modes, the closed-loop effect of disturbance and set-point changes on the output error is given by

$$y - r = -e = -Sr + SPd \tag{1.2}$$

The most basic requirement for the controller K is *internal stability*, which means that all the relations in $H(P,K)$ are stable. The set of all internally stabilizing feedback controllers will be hereafter denoted by $\mathcal{C}$. At this point, it is also convenient to introduce a special notation for the set of stable transfer functions, or $\mathcal{RH}_\infty$ for short. Many times, arguments in signals and transfer functions will be dropped for simplicity, i.e., we will write y instead of $y(t)$ or $y(s)$, and P instead of $P(s)$. We also note here that P will be normally used to refer both to the real plant and the model of it. Depending on the context, however, we will also use the notation $\tilde{P}$ for the real (uncertain) plant in order to distinguish it from the model.

1.1 Two sources of inspiration: IMC (λ-tuning) and $\mathcal{H}_\infty$ control

This work has received the influence of Internal Model Control (IMC) and $\mathcal{H}_\infty$ control. These two paradigms are briefly outlined next. A design method that puts them together will also be reviewed.

1.1.1 Internal Model Control

Let us start factoring the plant as $P = P_a P_m$, where $P_a \in \mathcal{RH}_\infty$ is all-pass and P_m is minimum-phase (MP). As reported in (Skogestad and Postlethwaite,

2005; Dehghani *et al.*, 2006), the broad objective of the IMC procedure (Morari and Zafiriou, 1989) is to specify the closed-loop relation $T_{yr} = T = P_a f$, where f is the so-called IMC filter. Assuming that P has k unstable poles, the filter is chosen as follows:

$$f(s) = \frac{\sum_{i=1}^{k} a_i s^i + 1}{(\lambda s + 1)^{n+k}} \tag{1.3}$$

The purpose of f is twofold: first, to ensure the properness of the controller and the internal stability requirement (to this double aim, n must be equal or greater than the relative degree of P, whereas the $a_1, \ldots, a_k$ coefficients impose $S = 0$ at the k unstable poles of P). Second, the λ parameter is used to find a compromise between robustness and performance. Roughly speaking, the choice $T = P_a f$ is motivated by $\mathcal{H}_2$ optimization[1], in such a way that when $\lambda \to 0$ the closed-loop minimizes $\|S\frac{1}{s}\|_2$. By using Parseval's theorem and the fact that $S = T_{er}$, as it is clear from (1.2), minimizing $\|S\frac{1}{s}\|_2$ is equivalent to minimizing the Integrated Square Error (ISE) over time due to a set-point change. Starting with a small value of λ, optimality can then be sacrificed for the sake of robustness (this process is referred to as *detuning*). In general, the larger the value of λ, the more robust (and slow) the resulting system. For example, in the stable plant case —i.e., $k = 0$ in (1.3)— it is readily seen that λ is closely related to the closed-loop bandwidth since $|T| = |P_a f| = |f| = \frac{1}{|(\lambda j\omega + 1)^n|}$.

The main advantages of IMC are its simplicity and analytical character, while some of its drawbacks are listed below [2]:

[1] For a SISO (strictly proper) LTI system $G(s)$, the $\mathcal{H}_2$ norm is defined as

$$\|G(s)\|_2 \doteq \left(\frac{1}{2\pi}\int_{-\infty}^{\infty} |G(j\omega)|^2 d\omega\right)^{1/2}$$

Parseval's theorem says that

$$\|G(s)\|_2^2 = \|g(t)\|_2^2 \doteq \int_0^{\infty} |g(t)|^2 dt$$

where $g(t) = \mathcal{L}^{-1}(G(s))$ denotes the impulse response of G. Therefore, $\|G(s)\|_2$ can be interpreted in terms of the Integrated Square Error of the impulse response. For more performance interpretations (both deterministic and stochastic), and a definition covering the multivariable case, consult (Skogestad and Postlethwaite, 2005).

[2] For an exhaustive list of the IMC shortcomings, consult (Dehghani *et al.*, 2006, Section 3). Here, only the points relevant to the thesis are considered.

- For stable plants, the poles of P are cancelled by the zeros of the controller K. This yields good results in terms of set-point tracking but results into sluggish disturbance attenuation when P has slow/integrating poles (Chien and Fruehauf, 1990; Horn *et al.*, 1996; Skogestad, 2003; Shamsuzzoha and Lee, 2007).

- For unstable plants, the pole-zero pattern of (1.3) can lead to large peaks on the sensitivity functions, which in turn means poor robustness and large overshoots in the transient response (Campi *et al.*, 1994).

- In general, poor servo/regulator performance compromise is obtained (Skogestad, 2003).

1.1.2 $\mathcal{H}_\infty$ control

Modern $\mathcal{H}_\infty$ control theory (Skogestad and Postlethwaite, 2005) is based on the general feedback setup depicted in Figure 1.2, composed of the generalized plant G and the feedback controller K. Once the problem has been posed in this form, the optimization process aims at finding a controller K which makes the feedback system in Figure 1.2 stable, and minimizes the $\mathcal{H}_\infty$-norm[3] (sometimes referred to as *min-max* or supremum norm) of the closed-loop relation from w to z. Mathematically, the synthesis problem can be expressed as

$$\min_{K\in\mathcal{C}} \|\mathcal{N}\|_\infty = \min_{K\in\mathcal{C}} \|\mathcal{F}_l(G,K)\|_\infty \tag{1.4}$$

where

$$\mathcal{N} = \mathcal{F}_l(G,K) \doteq G_{11} + G_{12}K(I - G_{22}K)^{-1}G_{21} = T_{zw} \tag{1.5}$$

An important feature of the $\mathcal{H}_\infty$-norm is that not only captures performance but also robustness objectives. More concretely, uncertainty (usually denoted by Δ) can be explicitly considered in the general control configuration, see

[3] For a (proper) LTI system $G(s)$, the $\mathcal{H}_\infty$ norm is defined as

$$\|G(s)\|_\infty \doteq \max_\omega \bar{\sigma}(G(j\omega))$$

where $\bar{\sigma}$ denotes the largest singular value (induced 2-norm). In the SISO case, $\bar{\sigma}(G(j\omega)) = |G(j\omega)|$. Thus, the $\mathcal{H}_\infty$ norm is simply the peak of the transfer function magnitude. By introducing weights, the $\mathcal{H}_\infty$ norm can be interpreted as the magnitude of some closed-loop transfer function(s) relative to a specified upper bound (Skogestad and Postlethwaite, 2005).

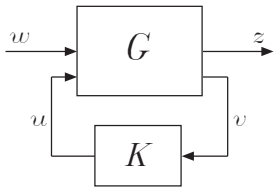

Figure 1.2: Generalized control setup.

Figure 1.3. Then, if $\|\mathcal{N}_{11}\|_\infty < 1$, the Small-Gain theorem guarantees that the closed-loop remains stable for every (normalized) perturbation such that $\|\Delta\|_\infty < 1$ (this is referred to as *Robust Stability*). Thus, using the $\mathcal{H}_\infty$ norm, it is possible to deal with performance and robustness issues simultaneously by means of the so-called mixed sensitivity problems. From this point of view, the basic idea behind the $\mathcal{H}_\infty$ design methodology is to press down the peaks of several closed-loop transfer functions; some may be related to performance and some others to robustness. The main difficulty with the $\mathcal{H}_\infty$ methodology

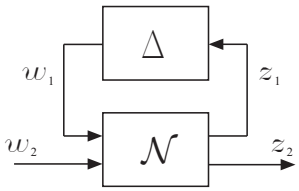

Figure 1.3: Generalized control setup including uncertainty.

is that the designer has to select suitable frequency weights included in G (this point will be exemplified shortly later), which may require considerable trial and error. Furthermore, for stacked problems involving three or more closed-loop transfer functions, the shaping becomes considerably difficult for the designer (Skogestad and Postlethwaite, 2005).

1.1.3 Blending IMC and $\mathcal{H}_\infty$ control

In (Dehghani *et al.*, 2006), a systematic $\mathcal{H}_\infty$ procedure to generalize IMC is presented. The idea is to avoid the limitations of the IMC design method when these are present, but retain its desirable features and simplicity when these shortcomings are absent. To achieve this goal, the following problem is

posed to be solved numerically:

$$\begin{aligned}\rho &= \min_{K\in\mathcal{C}}\|\mathcal{N}\|_\infty \\ &= \min_{K\in\mathcal{C}}\left\|\mathcal{F}_l\left(\left[\begin{array}{cc:c} -P_af & \epsilon_2P & P \\ 0 & \epsilon_1\epsilon_2 & \epsilon_1 \\ \hdashline 1 & -\epsilon_2P & -P \end{array}\right], K\right)\right\|_\infty \\ &= \min_{K\in\mathcal{C}}\left\| \begin{array}{cc} T-P_af & \epsilon_2SP \\ \epsilon_1KS & \epsilon_1\epsilon_2S \end{array} \right\|_\infty \end{aligned} \tag{1.6}$$

where ϵ_1 and ϵ_2 are stable, MP and proper weighting functions. The basic philosophy is to minimize the closeness between the input-to-output relation and a specified reference model, which is set as P_af along the lines (but with more flexibility) of the standard IMC. At the same time, the (1,2) term of (1.6) limits the size of $SP = T_{yd}$, whereas the (2,1) term limits the size of $KS = T_{ur}$. The index in (1.6) automatically guarantees that

$$|T(j\omega) - P_af(j\omega)| \leqslant \rho \ \forall\omega, \tag{1.7}$$

$$|SP(j\omega)| \leqslant \rho/|\epsilon_2(j\omega)| \ \forall\omega, \tag{1.8}$$

$$|KS(j\omega)| \leqslant \rho/|\epsilon_1(j\omega)| \ \forall\omega \tag{1.9}$$

Now, if the design specifications are written as $\|T - P_af\|_\infty \leqslant \alpha$, $|SP(j\omega)| \leqslant \beta_p^i \ \forall\omega \in [w_1^i, w_2^i]$, and $|KS(j\omega)| \leqslant \beta_k^i \ \forall\omega \in [\omega_3^i, \omega_4^i]$ where $\alpha, \beta_p^i, \beta_k^i, w_1^i, w_2^i, w_3^i$ and w_4^i are positive real numbers representing the closed-loop objectives, ϵ_1 and ϵ_2 can be chosen as

$$|\epsilon_1(j\omega)| \geqslant \alpha/\beta_k^i \ \forall\omega \in [\omega_3^i, \omega_4^i] \quad \text{and} \quad |\epsilon_2(j\omega)| \geqslant \alpha/\beta_p^i \ \forall\omega \in [\omega_1^i, \omega_2^i] \tag{1.10}$$

Then, if $\rho \leqslant \alpha$, the design specifications are certainly met[4]. Note that by selecting $\epsilon_1 = \epsilon_2 = 0$ (corresponding to $\beta_k^i, \beta_p^i \to \infty$) and f as in (1.3), the design reduces, essentially, to the original IMC procedure.

[4]Notice that if $\rho > \alpha$ one cannot conclude anything about achieving the performance objectives.

The revised design method has great versatility, blending IMC and $\mathcal{H}_\infty$ ideas elegantly[5]. In exchange, the resulting procedure inevitably loses part of the IMC simplicity (even if $f, \epsilon_1, \epsilon_2$ can be chosen in a systematic way) and its analytical character. Without some caution, this may translate into design pitfalls as noted in (Lee and Shi, 2008). Another disadvantage of the $\mathcal{H}_\infty$ machinery is that it usually gives high-order controllers, requiring the use of model order reduction techniques (Skogestad and Postlethwaite, 2005).

As it was pointed out in Section 1.1, some basic problems with IMC are related to servo/regulation issues. In this thesis, the design methodology will share the analytical character of IMC and much of its simplicity. This will be achieved by considering a simple weighted sensitivity formulation. Apart from considering the inherent compromise between robustness and performance, extra design parameters will be finally introduced into the weight to deal with the trade-off between the servo and regulatory performance.

1.2 The starting point: a model matching design for PID tuning

Vilanova (2008) proposed a robust PID tuning that was the starting point for this thesis. After passing through some preliminary concepts, this section reviews the aforementioned solution and introduces the first proposed design, which arose from a simplification of the settings in (Vilanova, 2008).

1.2.1 A word about PID controllers

Proportional, Integral and Derivative (PID) controllers have been around in process industry for more than seven decades (O'Dwyer, 2006). In spite of their old existence, current surveys estimate that the great majority of the controllers are (still) of PID type. For example, in (Kano and Ogawa, 2010), the process control state of the art in Japan is surveyed, and it is reported that the ratio of applications of PID control, conventional advanced control,

[5] The reader may be aware of other techniques with strong links to the size of $H(P, K)$. One is the H_∞ loop-shaping method (McFarlane and Glover, 1992; Skogestad and Postlethwaite, 2005), which has points in common with the design philosophy in (Dehghani *et al.*, 2006). Note, however, that the frequency cost functions ϵ_1 and ϵ_2 capture the design objectives differently.

and MPC is 100:10:1. The main reasons for the great success of PID controllers are that they are well-performing in many applications, and that they are easy to understand and implement. Furthermore, today's technology provides additional features like automatic tuning or gain scheduling (Astrom and Hagglund, 2005). Add to this a long history of proven operation, and it is not difficult to understand the decision.

Originally, the PID algorithm was conceived as the combination of three basic control actions, hence its name, so that the control law can be ideally expressed as

$$u(t) = K_c \left(e(t) + \frac{1}{T_i} \int_0^t e(\tau) d\tau + T_d \frac{de(t)}{dt} \right) \tag{1.11}$$

where the tuning parameters K_c, T_i, T_d are known as the proportional gain, integral and derivative times, respectively. Accordingly, the ideal PID law is based on the present ($e(t)$), past ($\int_0^t e(\tau)d\tau$) and estimated future ($\dot{e}(t)$) error information. PID controllers can also be understood in terms of lead-lag compensation. Even for such a simple strategy, it is not easy to find good settings for K_c, T_i, T_d without a systematic procedure (Pedret *et al.*, 2002; Ogunnaike and Mukati, 2006). In this regard, a visit to a process plant will usually show poorly tuned PID controllers (Skogestad, 2003).

Because pure derivative action cannot be implemented, the following *commercial* PID transfer function is usually considered:

$$K = K_c \left(1 + \frac{1}{sT_i} + \frac{sT_d}{1 + sT_d/N} \right) \tag{1.12}$$

In the (noninteractive) industrial ISA form (1.12), N is the derivative filter parameter. Although N is normally fixed by the manufacturer (or restricted to a limited range), the advantages of considering N an extra tuning parameter have been stressed in different works (Luyben, 2001; Isaakson and Graebe, 2002; Leva and Maggio, 2011). Adhering to this recommendation, N will be considered tunable. In fact, disregarding N at the design stage is in part responsible for the myth that derivation action does not work (it is common to find PID controllers acting as PI controllers, namely $T_d = 0$, to avoid noise sensitivity problems). As reported in (Kristiansson and Lennartson, 2006; Larsson and Hagglund, 2011), improved filtering of PID controllers has a great potential to show industry the benefits of derivative action.

From a modern perspective, a PID controller is simply a controller of up to second order containing an integrator:

$$K = \frac{c_1 s^2 + c_2 s + c_3}{s(d_1 s + 1)} \tag{1.13}$$

where c_1, c_2, c_3, d_1 are positive real constants. Considering the general second order form (1.13) is quite natural (Isaakson and Graebe, 2002), and helps to avoid the computational oddities that may exist in the PID algorithms of common vendors. For example, N and T_d may be negative when going from (1.13) to (1.12). This problem is avoided if the *practical* output-filtered form (1.14) introduced in (Morari and Zafiriou, 1989) is used for implementation:

$$K = K_c \left(1 + \frac{1}{sT_i} + sT_d\right) \frac{1}{T_F s + 1} \tag{1.14}$$

where T_F is a fourth tuning parameter. A general reformulation of the PID controller along the lines of (1.13), but including up to 5 tuning parameters, can be found in (Kristiansson and Lennartson, 2006).

Although it is surprising that such a simple structure (1.13) works so well, the simplicity entails limitations too, implying that in some applications better performance can be obtained using more sophisticated strategies. For example, for processes with long time delays it should be better to combine the PID controller with a dead-time compensator like the Smith-Predictor. Another situation where the the PID controller (alone) is not recommended is for oscillatory processes (Astrom and Hagglund, 2005). Even in such cases, a PID controller properly augmented with an additional low-pass filter may yield acceptable results in practice (Kristiansson and Lennartson, 2006). Consequently, although simple candidates to replace the PID compensator have appeared in the literature (Pannocchia *et al.*, 2005; Ogunnaike and Mukati, 2006), it seems that PID control has a future yet. Definitely, it still constitutes an active research field, including topics such as PID (automatic) tuning methodologies (Leva and Maggio, 2011), adaptive and robust PID control (El Rifai, 2009), stabilizing PID parameters (Hohenbichler, 2009), Fractional PID control (Padula and Visioli, 2011) or event-based PID control (Sánchez *et al.*, 2011).

1.2.2 The Model Matching Problem within $\mathcal{H}_\infty$ control

The (SISO) Model Matching Problem (MMP) (Doyle *et al.*, 1992) consists of:

$$\min_{Q\in\mathcal{RH}_\infty} \|T_1 - T_2Q\|_\infty \tag{1.15}$$

where $T_1, T_2 \in \mathcal{RH}_\infty$. Let $\{z_1, z_2, \ldots, z_\nu\}$ be the distinct Right Half-Plane (RHP) zeros of T_2. Then,

Lemma 1.2.1. *The optimal matching error $\mathcal{E}^o = T_1 - T_2Q$ in (1.15) is an all-pass function (Francis, 1987; Doyle* et al.*, 1992; Vilanova, 2008), more precisely:*

$$\mathcal{E}^o(s) = \begin{cases} \rho\frac{q(-s)}{q(s)} & \text{if } \nu \geq 1 \\ 0 & \text{if } \nu = 0 \end{cases} \tag{1.16}$$

where $q(s) = 1 + q_1 s + \cdots + q_{\nu-1}s^{\nu-1}$ is a strictly hurwitz polynomial. Furthermore, the constants ρ and $\{q_i\}_{i=1}^{\nu-1}$ are real and are uniquely determined by the interpolation constraints

$$\mathcal{E}(z_i) = T_1(z_i) \qquad i = 1 \ldots \nu \tag{1.17}$$

Remark 1.2.1. *For $\nu = 1$ or $\nu = 2$, Lemma 1.2.1 can be directly used to obtain explicit formulae for the solution of (1.15) (Zames and Francis, 1983). However, because the interpolation conditions (1.17) constitute a nonlinear system, for $\nu \geq 3$ it should be better to find $\mathcal{E}^o$ by using a more systematic procedure like the Nevanlinna-Pick's algorithm (Doyle* et al.*, 1992).*

The importance of the MMP relies on the fact that any generalized control problem can be expressed as a MMP[6]. This is achieved by means of the celebrated Youla-Kucera parameterization (Youla *et al.*, 1976; Vidyasagar, 1985; Skogestad and Postlethwaite, 2005), which states that any $K \in \mathcal{C}$ can be parameterized as

$$K = \frac{Y + MQ}{X - NQ} \tag{1.18}$$

being $Q \in \mathcal{RH}_\infty$ a free parameter, and $X, Y, M, N \in \mathcal{RH}_\infty$ a coprime factorization of P, implying that $P = NM^{-1}$ and $XM + YN = 1$ (Vidyasagar, 1985;

[6] In general, in the multivariable case, the MMP is expressed as $\min_{Q\in\mathcal{RH}_\infty} \|T_1 - T_2QT_3\|_\infty$, where $Q, T_1, T_2, T_3 \in \mathcal{RH}_\infty$ are matrix transfer functions.

Skogestad and Postlethwaite, 2005; Kwok and Davison, 2007). The above result allows to express any closed-loop transfer function affinely in Q in the form of a MMP. For example, a basic problem in $\mathcal{H}_\infty$ (of main importance in this thesis) is the Weighted Sensitivity Problem (WSP) (Skogestad and Postlethwaite, 2005, Section 2.8.2):

$$\min_{K \in \mathcal{C}} \|WS\|_\infty \tag{1.19}$$

where W is a performance weight in charge of shaping S conveniently. With respect to Figure 1.2, the WSP corresponds to the generalized plant

$$G = \left[\begin{array}{c:c} W & -WP \\ \hdashline 1 & -P \end{array}\right] \tag{1.20}$$

Using (1.18), the sensitivity function can be parameterized as $S = M(X - NQ)$, and the WSP (1.19) can then be cast into the MMP form by selecting $T_1 = WMX, T_2 = WMN$, where $T_1, T_2 \in \mathcal{RH}_\infty$ as long as $W \in \mathcal{RH}_\infty$.

1.2.3 Vilanova's (2008) design for robust PID tuning revisited

Let us consider the following problem

$$\min_{K \in \mathcal{C}} \|W(T_d - T)\|_\infty \tag{1.21}$$

where T_d represents the desired complementary sensitivity (the input-to-output response: T_{yr}) and W is a frequency weight (see Figure 1.4). The idea in

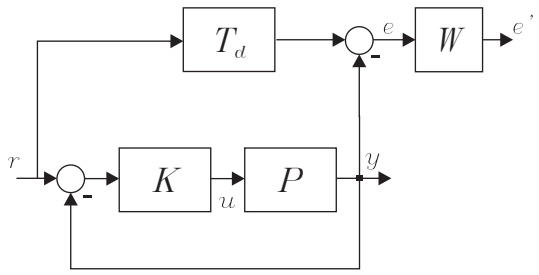

Figure 1.4: Diagram for problem (1.21). Here, e denotes the error between the desired and actual outputs.

(Vilanova, 2008) is to use simple settings in order to obtain a PID controller:

- $T_d = \frac{1}{T_M s+1}$, where the T_M parameter specifies the desired *speed of response.*
- $W = \frac{zs+1}{s}$. The integrator forces integral action by requiring perfect matching between T and T_d at zero frequency. The z parameter is used to adjust the robustness margins: the larger the value of z, the more robust the resulting system.

In addition, many processes have rather simple dynamics and are often modeled using low-order models of the form

$$P = K_g \frac{e^{-sh}}{\tau s + 1} \tag{1.22}$$

called First Order Plus Time Delay or just FOPTD systems, where K_g, h, τ are, respectively, the gain, the (apparent) delay, and the time constant of the process. These models can be obtained easily through open-loop and closed-loop step response tests (Shamsuzzohaa and Skogestad, 2010). Alternatively, one can start from an accurate description of the process and apply then some model reduction technique. In this regard, Skogestad's (2003) *Half-Rule* provides a simple analytic approach. Supported by these considerations, an stable FOPTD model is used in (Vilanova, 2008). However, for derivation purposes, the time delay in (1.22) is approximated using a first order Taylor expansion:

- $P = K_g \frac{-sh+1}{\tau s+1}$

Note that the problem at hand could now be posed in terms of the general control setup (see Figure 1.5) to be solved numerically for particular values of the tuning parameters. For such a simple problem, however, the solution can be obtained analytically. First, note that for stable plants we can take $X = 1, M = 1, N = P, Y = 0$ in (1.18), and express all stabilizing controllers as

$$K = \frac{Q}{1 - PQ} \tag{1.23}$$

Then, in terms of Q, $T = PQ$, and (1.21) is equivalent to

$$\min_{Q \in \mathcal{RH}_\infty} \|W(T_d - PQ)\|_\infty \tag{1.24}$$

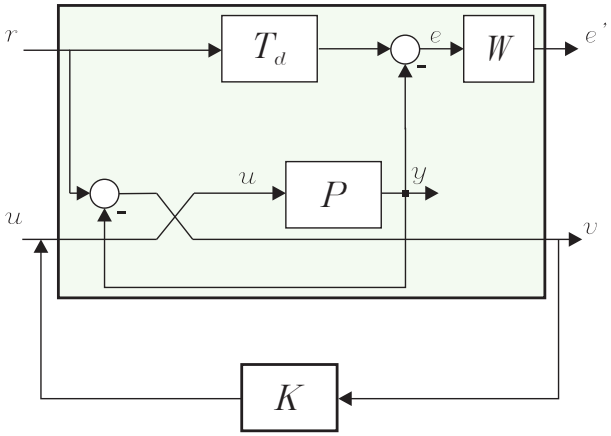

Figure 1.5: Problem (1.21) rearranged in the general control form.

which is a MMP (1.15) with $T_1 = WT_d, T_2 = WP$. The solution to (1.24) follows immediately from Lemma 1.2.1 (with $\nu = 1$) and, after straightforward algebra, the resulting feedback compensator obtained using (1.23) turns out to be a PID controller:

$$K = \frac{1}{K_g(\rho + T_M)} \frac{(1+\tau s)(1+\chi s)}{s(1+\frac{zT_M+h\chi}{\rho+T_M}s)} \tag{1.25}$$

where

$$\rho = \frac{h+z}{h+T_M}h \qquad \chi = h + z - \rho \tag{1.26}$$

The tuning parameters T_m, z can be fixed for auto-tuning purposes:

$$T_M = 2h \qquad z = \sqrt{2}h \tag{1.27}$$

With these values for z, T_M, which are chosen according to robustness considerations, the tuning rule (in ISA-PID form) can be expressed as

$$\begin{aligned} K_p &= \frac{T_i}{K_g h 2.65} \\ T_i &= \tau + 0.03h \\ \frac{T_d}{N} &= 1.72h \\ N+1 &= \frac{\tau}{T_i} \end{aligned} \tag{1.28}$$

Vilanova's (2008) tuning rule has been found to work well in practice, exhibiting a robust behaviour in the face of process abnormalities including model mismatch, valve stiction and sensor noise (Amiri and Shah, 2009).

1.3 Outline/summary of the thesis

Chapter 2: Simple model matching approach to robust PID tuning

The following observation can be made regarding the design in (Vilanova, 2008) revised in Section 1.2.3:

- The tuning parameters z and T_M have a very similar effect on the final controller and are somehow redundant.

This means that the settings used for analytical derivation can be simplified to make the final solution dependent on a single tuning parameter. The corresponding simplified design can be found in Chapter 2. In particular, the settings below are suggested:

- $T_d = 1$. For this reference model, the problem is a sensitivity problem, see Figure 1.4. Now, e is the conventional error between the reference and the actual output, and problem (1.24) is a WSP:

$$\min_{Q\in\mathcal{RH}_\infty} \|W(T_d - PQ)\|_\infty = \min_{Q\in\mathcal{RH}_\infty} \|W(1 - PQ)\|_\infty = \min_{Q\in\mathcal{RH}_\infty} \|WS\|_\infty \tag{1.29}$$

- $W = \frac{1}{s}$. This weight is used to force integral action ($S(0) = 0$). Note that the resulting performance objective is

$$\min \left\| S\frac{1}{s} \right\|_\infty = \min \max_\omega \left| S(j\omega)\frac{1}{j\omega} \right| \tag{1.30}$$

  Although (1.30) has often been used as a general performance criterion for control design, it is particularly suitable for the servo mode. This can be understood from (1.2). The relation between the reference r and the error $e = r - y$ is given by $T_{er} = S = \frac{1}{1+PK}$. At low frequencies (where feedback is effective), $|L| = |PK| \gg 1$, and $S \approx P^{-1}K^{-1}(j\omega) \approx$

$P^{-1}(j\omega)\frac{1}{k_i}j\omega$, where k_i represents the integral gain of the controller (in case it is of PID type, $k_i = \frac{K_c}{T_i}$). Therefore, when $\omega \to 0$ in (1.30), $S(j\omega)\frac{1}{j\omega} \to P^{-1}(j\omega)\frac{1}{k_i}$.

- $P = K_g \frac{-\frac{h}{2}s+1}{(\tau s+1)(\frac{h}{2}s+1)}$, which results from using a first order Padé approximation for the time delay in the FOPTD model (1.22).

For this setup, the optimal Q parameter is not proper, which leads to an improver K. To circumvent this problem, Q is augmented using the filter $f = \frac{1}{(\lambda s+1)^2}$, where λ is the only tuning parameter. The resulting design is very similar to IMC, and λ is used in the same way to detune the optimal controller. If one assumes multiplicative uncertainty Δ, the Small-Gain theorem ensures the closed-loop stability provided that $|T| = |PQ| < 1/|\Delta| \; \forall\omega$. Therefore, increasing λ reduces the closed-loop bandwidth and contributes to high-frequency robustness against model uncertainty. Another reason to keep $|T|$ small at high frequencies is that sensor noise is transferred to the output by T (Skogestad and Postlethwaite, 2005). In terms of λ, the final feedback controller is given by

$$K = \frac{1}{K_g\left(2\lambda + \frac{h}{2}\right)} \frac{(\frac{h}{2}s+1)(\tau s+1)}{s\left(\frac{\lambda^2}{2\lambda+\frac{h}{2}}s+1\right)} \tag{1.31}$$

Note that the gain of the controller K (i.e., $|K(j\omega)|$) gets reduced by increasing λ. Because $T_{ur} = KS$, large values of λ will yield moderate levels of control activity. Taking all these considerations into account, λ is finally fixed to get an automatic rule that directly gives the controller parameters in terms of the process model information. The choice $\lambda = h$, which results into the ISA-PID tuning rule

$$\begin{aligned} K_p &= \frac{0.4T_i}{K_g h} \\ T_i &= \tau + 0.1h \\ \frac{T_d}{N} &= 0.4h \\ N+1 &= 1.25\frac{\tau}{T_i} \end{aligned} \tag{1.32}$$

yields very similar results to (1.28). Both (1.28) and (1.32) are aimed at *smooth* set-point response, yielding $M_S \approx 1.42$, which is a good robustness indicator[7]. By *smooth* control we mean the slowest possible control with acceptable disturbance rejection (Skogestad, 2006). Of course, the definition may depend on the application at hand, and the term *smooth* is sometimes used in this thesis merely as a synonym of *robust*.

Chapter 3: Improving the load disturbance response (γ-tuning)

A common drawback of Vilanova's (2008) and the design in Chapter 2 is that poor disturbance attenuation is obtained for *lag-dominant* plants[8]. This phenomenon occurs because of pole-zero cancellation between the plant P and the controller K. Effectively, both (1.25) and (1.31) have a zero at the plant pole at $s = -1/\tau$. In order to prevent this to happen, a modification of (Vilanova, 2008) is presented in (Vilanova and Arrieta, 2007) which consists of specifying a different target closed-loop , taken now as:

$$T_d = \frac{(T_M - \gamma)s + 1}{1 + T_M s} \tag{1.34}$$

Equivalently, the new T_d corresponds to the desired sensitivity function

$$S_d = 1 - T_d = \frac{\gamma s}{T_M s + 1} \tag{1.35}$$

With this change, the solution to (1.21) is

$$K = \frac{1}{K_g(\rho + \gamma)} \frac{(1 + \tau s)(1 + \chi s)}{s(1 + \frac{zT_M + h\chi}{\rho + \gamma} s)} \tag{1.36}$$

[7] Mid-frequency sensitivity to modelling errors can be captured by the peak of the sensitivity function:

$$M_S \doteq \|S(j\omega)\|_\infty \doteq \max_\omega \left| \frac{1}{1 + L(j\omega)} \right| \tag{1.33}$$

M_S indicates the inverse of the shortest distance from the Nyquist plot to the critical point $-1 + 0j$ (Skogestad and Postlethwaite, 2005).

[8] With respect to the FOPTD model (1.22), a process is said to be lag-dominant if τ/h is larger than about 10 (integrating plants fit into this category as an extreme example). Sometimes, however, by lag-dominant we just mean $\tau/h > 1$, including plants with relatively balanced lag/delay ratio.

where

$$\rho = \frac{h+z}{h+T_M}(h+T_M-\gamma) \qquad \chi = h+z-\rho+T_M-\gamma \tag{1.37}$$

Note that when $\gamma = T_M$, the design coincides with that revised in Section 1.2.3. In particular, (1.36) and (1.37) simplify to (1.25) and (1.26). By fixing z, T_m as in (1.27), γ turns out to be the only tuning parameter now. The role of γ is to balance the performance between the servo and regulator modes:

- Setting $T_M = \sqrt{2}$ corresponds to the servo mode (good set-point tracking).
- Setting $T_M > \sqrt{2}$ allows improvement of the regulatory performance (better disturbance attenuation).

The above points are fully addressed in Chapter 3, where the *servo/regulator* interval for γ is found to be:

$$\sqrt{2}h \leq \gamma \leq \frac{12.36h(\tau - \sqrt{2}h)}{h+\tau} \tag{1.38}$$

and it is assumed that $\tau \geq 1.7262h$ so that (1.38) makes sense.

Chapter 4: λ-tuning versus γ-tuning

The design in Chapter 2 depends on a single tuning parameter: λ, used to adjust the robustness/performance trade-off. Regarding the design discussed in Chapter 3 (Alcántara *et al.*, 2010*b*), the only tuning parameter is γ, and its role is to adjust the servo/regulator trade-off. In Chapter 4, these two strategies are compared from a balanced servo/regulator point of view: first, an interval for λ is defined based on the *smooth* and *tight* control concepts (Skogestad, 2006; Ali and Majhi, 2009):

- *Smooth* control, as already commented, is the slowest possible control with acceptable disturbance rejection. In (Alcántara *et al.*, 2010*a*), $\lambda = h$ for smooth control, yielding $M_S \approx 1.42$.
- *Tight* control is the fastest possible control with acceptable robustness. In (Alcántara *et al.*, 2010*a*), $\lambda = 0.56h$ for tight control, resulting in $M_S \approx 1.75$.

Then, the trade-off value $\lambda = 0.7h$ is picked up to be used for balanced servo/regulator operation. The conclusion of Chapter 4 is that one can use the tuning $\lambda = 0.7h$ for plants such that $h/\tau \geq 0.1$. In these cases, the γ-tuning method of Chapter 3 provides no real advantage. However, for more lag-dominant plants, the γ-tuning technique allows better suppression of load disturbances with the same degree of robustness.

Chapter 5: Combined $\lambda\gamma$ approach: a first $\mathcal{H}_\infty$ design

A general conclusion of Chapter 4 (Alcántara *et al.*, 2010*d*) is that it would be convenient to consider at least two design parameters: one to adjust the robustness/performance trade-off and the other one to balance the performance between the servo and regulator modes. With this idea in mind, in Chapter 5, the λ-tuning design of Chapter 2 (Alcántara *et al.*, 2010*c*) is modified to introduce an extra design parameter to deal with servo/regulation issues. The WSP (1.19) is considered again, but now:

- $P = K_g \frac{-sh+1}{\tau s+1}$, which results from a first order Taylor approximation of the time delay in the FOPTD model (1.22).
- The weight $W = \frac{1}{s}$ is replaced with

$$W = \frac{(\lambda s + 1)^2}{s(\alpha s + 1)} \tag{1.39}$$

where $\alpha \in [\lambda, \tau]$. The resulting feedback compensator is

$$K = \frac{1}{K_g(2\lambda + h - \gamma)} \frac{(\tau s + 1)(\gamma s + 1)}{s\left(\left(\frac{\lambda^2 + h\gamma}{2\lambda + h - \gamma}\right) s + 1\right)} \tag{1.40}$$

where

$$\gamma = \frac{h\alpha + 2\lambda\alpha - \lambda^2}{\alpha + h} \tag{1.41}$$

The rationale behind W in (1.39) is as follows:

- When $\alpha = \lambda$, $W = \frac{\lambda+1}{s}$. For $\lambda \approx 0$, the performance objective is $\min \left\| \frac{1}{s} S \right\|_\infty$ which is suitable for the servo mode. By augmenting λ, the WSP minimizes $|S|$ in a wider frequency range. This makes the closed-loop slower and helps to reduce M_S (the peak on $|S|$). Thus, the role of λ is to detune the controller if necessary.

- When $\alpha = \tau$, $W = \frac{(\lambda+1)^2}{s(\tau s+1)}$. Now, provided that $\lambda < \tau$, W penalizes less the magnitude of S at middle-high frequencies because $\left|\frac{\lambda j\omega+1}{\tau j\omega+1}\right| < 1$. Thus, the resulting S is bound to have a larger peak (M_S value). By a waterbed effect argument (Skogestad and Postlethwaite, 2005), $|S|$ will in turn decrease at low frequencies (around the slow pole at $s = -1/\tau$), favouring the disturbance rejection task.

In summary, we can use λ for detuning the controller and α for servo/regulator purposes. If $\alpha = \lambda$, the design corresponds to the servo mode, whereas $\alpha = \tau$ represents the regulator mode. Intermediate values of α result into balanced performance between the set-point tracking and disturbance suppression tasks. In terms of γ (1.41), the extreme values are

- $\gamma = \lambda$ (servo). For this value of γ, the controller (1.40) is of PI type

$$K = \frac{1}{K_g(\lambda + h)} \frac{\tau s + 1}{s} \tag{1.42}$$

  and it is based on pole-zero cancellation (the pole at $s = -1/\tau$ in P is cancelled by the zero of K).

- $\gamma = \gamma_{ld} = -\frac{\lambda^2 - 2\lambda\tau - h\tau}{h+\tau}$ (regulation). For this value of γ, a PI controller is also obtained:

$$K = \frac{1}{K_g(2\lambda + h - \gamma)} \frac{\gamma s + 1}{s} \tag{1.43}$$

  For the regulator mode, the pole at $s = -1/\tau$ of P is no longer cancelled by K. Instead, the slow pole is cancelled by S, i.e. $S(-1/\tau) = 0$. This is easy to understand, recall from (1.2) that $T_{yd} = SP$. Consequently, S must cancel the slow pole to avoid *sluggishness* in the disturbance response.

Figure 1.6 illustrates the design for the system $\frac{e^{-s}}{20s+1}$. The experiment considers a unity set-point change at $t = 0$ and a load disturbance of magnitude 5 entering at $t = 25$. For the case $\lambda = 1$, we have that $M_S \approx 1.6$ ($\gamma = \tau$) and $M_S \approx 2.5314$ ($\gamma = \gamma_{ld}$). Therefore, the improvement of the regulatory performance has been achieved at the cost of a large peak on $|S|$. A large value of M_S normally correlates with a large value of M_T (the peak on $|T|$); for the case at hand, $M_T = 1$ ($\lambda = \tau$) and $M_T \approx 2.53$ ($\gamma = \gamma_{ld}$). The latter

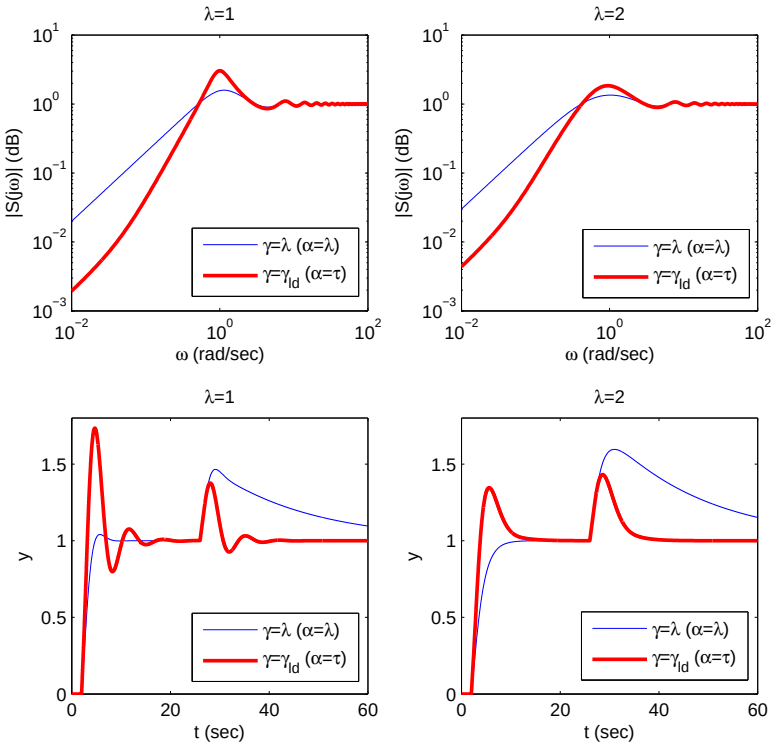

Figure 1.6: Sensitivity function (top) and set-point/load disturbance responses (bottom) for different values of λ and γ.

value is consistent with the large overshoot exhibited in Figure 1.6 (bottom) (Skogestad and Postlethwaite, 2005). In order to yield less aggressive solutions, λ can be augmented. In Figure 1.6 (right column), the choice $\lambda = 2$ is made. The same kind of conclusions follow with respect to the extreme values of γ, but now the time responses are smoother as expected. The corresponding peaks on the sensitivity functions are $M_S \approx 1.35, M_T = 1$ $(\gamma = \tau)$ and $M_S \approx 1.84, M_T \approx 1.42$ $(\gamma = \gamma_{ld})$.

Chapter 6: An improved $\mathcal{H}_\infty$ design

There are two important problems with the design in Chapter 5 (Alcántara *et al.*, 2010*d*) imputable to the weight (1.39):

1. We saw that the PI controllers (1.42) and (1.43) were obtained for the extreme values of γ. However, the general expression for K is given in (1.40), which is a (*filtered*) PID compensator. Hence, the order of K increases (unnecessarily) for intermediate values of γ.

2. The method is not applicable to unstable plants; the resulting closed-loop system would be internally unstable.

An improved selection of W to undergo these problems is presented in Chapter 6. According to (Alcántara *et al.*, 2011*c*), the weight W in the WSP (1.19) can be chosen as follows:

$$W(s) = \frac{(\lambda s + 1)(\gamma_1 s + 1) \cdots (\gamma_k s + 1)}{s(\tau_1 s + 1) \cdots (\tau_k s + 1)} \tag{1.44}$$

where $\tau_1, \ldots, \tau_k$ are the time constants of the unstable or slow poles of P, $\lambda > 0$, and

$$\gamma_i \in [\lambda, |\tau_i|] \tag{1.45}$$

As before, λ is used to adjust the robustness/performance trade-off. The γ_i parameters permit to balance the servo/regulator performance (Alcántara *et al.*, 2011*c*). For the sake of clarity, set $\lambda \approx 0$ and $\tau_i > 0$ (stable plant case). By similar arguments as those used for Chapter 5 we have that:

- If $\gamma_i = \tau_i, i = 1, \ldots, k$, the corresponding weight is $W = \frac{1}{s}$, and the WSP is equivalent to the performance objective $\min \left\| \frac{1}{s} S \right\|_\infty$, which is suitable for the servo mode.

- If $\gamma_i = \lambda, i = 1, \ldots, k$, the resulting weight W reduces $|S|$ at low frequencies to improve the disturbance rejection properties. Note that, heuristically, the choice $\gamma_i = \lambda$ can be understood (for small values of λ and neglecting the effect of the zeros of P) in terms of the performance objective $\min \left\| \frac{1}{s} T_{yd} \right\|_\infty = \min \left\| \frac{1}{s} SP \right\|_\infty$. This performance objective is suitable for regulatory purposes (Kristiansson and Lennartson, 2006). In particular, when $\omega \to 0$, one has that $\frac{1}{j\omega} S(j\omega) P(j\omega) \to \frac{1}{k_i}$, which is coherent with the well-known fact that the integral gain of the controller gives a measure of the system's ability to reject low-frequency load disturbances[9].

[9]For example, for a PID controller Astrom and Hagglund (2005) show that a unit step

A good point of the weight (1.44) is that it is also valid for unstable plants ($\tau_i < 0$ for some i). As it is shown in (Alcántara *et al.*, 2011*c*; Alcántara *et al.*, 2011*b*), the use of the possibly unstable weight (1.44) avoids any notion of coprime factorization. Let us assume that P is purely rational and contains at least one RHP zero, in such a way that:

$$P = \frac{n_p}{d_p} = \frac{n_p^+ n_p^-}{d_p^+ d_p^-} \tag{1.46}$$

where n_p^+, d_p^+ contain the unstable (or slow in the case of d_p^+) zeros of n_p, d_p and n_p^-, d_p^- contain the stable zeros of n_p, d_p. The weight (1.44) can be factored similarly

$$W = \frac{n_w}{d_w} = \frac{n_w}{d_p^+ d_w'} \tag{1.47}$$

Then, the optimal weighted sensitivity for problem (1.19) using the weight (1.47) is given by

$$\mathcal{N}^o = \rho \frac{q(-s)}{q(s)} \tag{1.48}$$

where ρ and $q = 1 + q_1 s + \cdots + q_{\nu-1} s^{\nu-1}$ (a hurwitz polynomial) are uniquely determined by the interpolation constraints:

$$W(z_i) = \mathcal{N}^o(z_i) \qquad i = 1 \ldots \nu, \tag{1.49}$$

being $z_1 \ldots z_\nu$ ($\nu \geq 1$) the RHP zeros of P. The corresponding controller is:

$$K = \frac{d_p \chi}{\rho n_p^- q(-s) d_w} = \frac{d_p^- \chi}{\rho n_p^- q(-s) d_w'} \tag{1.50}$$

where χ is a polynomial satisfying

$$q(s) n_w - \rho q(-s) d_w = n_p^+ \chi \tag{1.51}$$

Based on simple models for the plant, the described procedure can be applied to PID tuning. In particular, Table 1.1 collects the tuning rules associated with first and second order models. In the second order model case, it is

disturbance applied at the plant input yields an integral of the error (IE) equal to $-1/k_i$, i.e.:

$$\text{IE} = \int_0^\infty e(\tau) d\tau = -\frac{T_i}{K} = \frac{-1}{k_i}$$

Indeed, the result holds for any controller including integral action. For a robust design exhibiting a non-oscillatory response, one has that $|\text{IE}| = 1/k_i \approx \text{IAE} = \int_0^\infty |e(\tau)| d\tau$.

Table 1.1: PI/D tuning rules based on $\mathcal{H}_\infty$ Weighted Sensitivity.

Model	K_c	T_i	T_d	
$K_g \frac{e^{-sh}}{\tau s+1}$	$\frac{1}{K_g}\frac{T_i}{\lambda+\gamma+h-T_i}$	$\frac{\tau(h+\lambda+\gamma)-\lambda\gamma}{\tau+h}$	-	$\gamma \in [\lambda, \lvert\tau\rvert]$
$K_g \frac{e^{-sh}}{(\tau_1 s+1)(\tau_2 s+1)}$	$\frac{1}{K_g}\frac{T_i}{\lambda+\gamma+h-T_i}$	$\frac{\tau_1(h+\lambda+\gamma)-\lambda\gamma}{\tau_1+h}$	$T_d = \tau_2$	$\gamma \in [\lambda, \lvert\tau_1\rvert]$

assumed that $|\tau_1| > \tau_2 > h > 0$, and that a series form PID controller is used for implementation:

$$K = K_c \left(1 + \frac{1}{T_i s}\right)(T_d s + 1) \tag{1.52}$$

The use of the series form is convenient here because it allows a simplification of the tuning expressions (Skogestad, 2003); in particular, we get the simple relationship $T_d = \tau_2$ for the derivative time. For implementation purposes, the derivative filter present in the real PID forms should also be designed. In order to convert the ideal PID law into the real one in the best possible way, it is advisable to follow the indications given in (Leva and Maggio, 2011).

Chapter 7: The $\mathcal{H}_2$ counterpart

The frequency domain design in Chapter 6 uses the $\mathcal{H}_\infty$ norm. However, the same kind of WSP can be posed in terms of the $\mathcal{H}_2$ norm to make the resulting design closer to conventional IMC. This is the purpose of Chapter 7, where the $\mathcal{H}_\infty$ WSP is replaced with

$$\min_{K \in \mathcal{C}} \|WS\|_2 \tag{1.53}$$

Now, the servo/regulator modes are understood in terms of input/output disturbances. With respect to Chapter 6, there are several other differences: first, the weight depends on the input type (e.g., steps, ramps, etc); second, P may contain a time delay (in this case, a dead time compensator is directly obtained). In addition, the extension to plants with complex conjugate poles is addressed; for oscillating plants, it is specially important to distinguish between the servo and regulatory tasks (Kristiansson and Lennartson, 1998; Alcántara *et al.*, 2011*a*).

For illustration purposes, let us assume that the inputs to the system are step signals and denote by $s = -1/\tau_1, \ldots, -1/\tau_k$ the unstable/slow poles of P (we restrict here to non-repeated real poles). Then, the weight in (1.53) is taken as

$$W(s) = \frac{(\lambda s + 1)^n (\gamma_1 s + 1) \cdots (\gamma_k s + 1)}{s(\tau_1 s + 1) \cdots (\tau_k s + 1)} \tag{1.54}$$

The only difference with (1.44) is the term $(\lambda s + 1)^n$, where n is used to ensure the properness of the final controller. In the case at hand, n must be at least equal to the relative degree of P (Alcántara *et al.*, 2011*a*). The other parameters: $\lambda > 0$ and $\gamma_1, \ldots, \gamma_k \in [\lambda, |\tau|]$, have the same meaning as in Chapter 6. Because the WSP problem is now posed in terms of the $\mathcal{H}_2$ norm, the performance interpretation changes accordingly; for negligible values of λ:

- If $\gamma_i = |\tau|$, $|W| \approx \left|\frac{1}{s}\right|$. In this case, the WSP (1.53) minimizes the ISE with respect to a step disturbance entering at the plant output (which is equivalent to minimizing the ISE for a set-point change).
- If $\gamma_i = \lambda$, $W \approx \frac{1}{s(\tau_1 s+1)\cdots(\tau_k+1)}$, and the WSP (1.53) minimizes now the ISE with respect to a step disturbance passing through the conflictive poles of P (input/load disturbances).

Set $P = P_a P_m$, where $P_a \in \mathcal{RH}_\infty$ is all-pass and P_m is MP. By using the IMC parameterization (1.23) for K, a *quasi-optimal* proper solution to (1.53) is given by:

$$Q = (P_m W)^{-1} \left\{ P_a^{-1} W \right\}_\star \tag{1.55}$$

where the operator $\{\}_\star$ denotes that after a partial fraction expansion (PFE) of the operand, the non-strictly proper terms and all the terms involving the poles of P_a^{-1} are omitted[10]. Equation (1.55) can be expressed as

$$Q = P_m^{-1} f \tag{1.56}$$

with $f = W^{-1} \left\{ P_a^{-1} W \right\}_\star$. Taking $W = \frac{n_w}{d_w}$, we can alternatively write f as

$$f = \frac{\chi}{n_w} = \frac{\sum_{i=0}^{\delta(d_w)-1} a_i s^i}{(\lambda s + 1)^n \prod_{i=1}^{k} (\gamma_i s + 1)} \tag{1.57}$$

[10]Note that the operator $\{\}_\star$ is slightly different from the operator $\{\}_*$ defined by Morari and Zafiriou (1989, Theorem 5.2-1).

where $\delta(d_w)$ denotes the degree of d_w and $a_0, \ldots, a_k$ are determined from the following system of linear equations

$$T|_{s=\pi_i} = PQ|_{s=\pi_i} = P_a f|_{s=\pi_i} = 1 \qquad i = 1 \ldots \delta(d_w) \tag{1.58}$$

being $\pi_i, i = 1, \ldots, \delta(d_w)$ the poles of W. As long as the a_i coefficients satisfy (1.58), the filter time constants λ and γ_i can be selected freely without any concern for nominal stability or asymptotic tracking. By using Lagrange-Type interpolation theory (Morari and Zafiriou, 1989), it is possible to develop an expression for (1.57) explicitly:

$$f = \frac{1}{n_w} \sum_{j=1}^{\delta(d_w)} (P_a^{-1} n_w)|_{s=\pi_j} \prod_{\substack{i=1 \\ i \neq j}}^{\delta(d_w)} \frac{s - \pi_i}{\pi_j - \pi_i} \tag{1.59}$$

The filter (1.59), or (1.57), represents a generalization of the conventional filter (1.3) used within IMC. In the case at hand, the γ_i parameters are used to balance the regulatory performance between step-like input/output disturbances.

Chapter 2

Simple model matching approach to robust PID tuning

Based on (Alcántara et al.*, 2010c)*

This chapter addresses PID tuning for robust set-point response from a min-max model matching formulation. Within the considered context, several setups result in a PID controller. This work investigates the simplest one, leading to a PID controller solely dependent on a single design parameter. Attending to common performance/robustness indicators, the free parameter is finally fixed to provide an automatic tuning in terms of the model information. Simulation examples are given to evaluate the proposed settings.

2.1 Introduction

In spite of the modern control theory state of the art, PID controllers continue to be the most common option in the realm of control applications, with an absolute dominance within the process control industry (Astrom and Hagglund, 2004; Astrom and Hagglund, 2005; Shamsuzzohaa and Skogestad, 2010). This is explained due to their simplicity both in implementation and in understanding. As a matter of fact, in most of the situations a PID can perform reasonably well and is indeed all that is required.

Recent advances in optimal methods have boosted the control solutions based on optimization procedures. In particular, a plethora of PID designs based on direct optimization have been reported in the literature during the last years, see, for example (Astrom *et al.*, 1998; Panagopoulos *et al.*, 2002; Ge *et al.*, 2002; Toscano, 2005). However, many of them, although effective, rely on somewhat complex numerical optimization procedures (several local minima may exist) and/or fail to provide tuning rules (Vilanova, 2008; Sanchís *et al.*, 2010). A different approach is to derive PID solutions based on a simplified (first or second order) model of the plant. Tuning rules obtained in this way through numerical optimization can be consulted in (Zhuang and Atherton, 1993; Visioli, 2001; Astrom and Hagglund, 2004; Tavakoli *et al.*, 2007), whereas an analytical approach is followed in other works such as (Rivera *et al.*, 1986; Skogestad, 2003; Zhang *et al.*, 2006*c*; Vilanova, 2008).

Following the latter perspective, this chapter addresses the analytical derivation, within a min-max model matching context, of PID tuning rules for smooth set-point response. To achieve results as close as possible to the industrial situation, the widely used ISA PID structure (Astrom and Hagglund, 2005) is chosen for the control law. The analytical min-max model matching approach to PID design was already conducted in (Vilanova, 2008), but the derived solution involved two tuning parameters. In this work, simpler settings depending on a single tuning parameter (and yielding the same degree of robustness/performance) are proposed. The tuning parameter is finally fixed to provide an automatic tuning solely dependent on the model information. For design purposes, a FOPTD model is employed; although a FOPTD model does not capture all the features of a high order system (it cannot represent well a system with oscillating step response), it has been shown to represent reasonably well an important category of industrial processes (Astrom and Hagglund, 2005).

The chapter is organized as follows: Section 2.2 is devoted to the problem statement. In Section 2.3, the general min-max model matching problem (MMP) is solved for a particular setup leading to a PID compensator with a single tuning parameter. Section 2.4 addresses the stability of the derived controller. In Section 2.5, the tuning parameter is conveniently fixed, thus providing automatic tuning. Simulation examples to show the applicability of the proposed method are provided in Section 2.6 while concluding remarks are collected in Section 2.7.

2.2 Problem statement

In this section, the control framework and the MMP on which the controller derivation is based are introduced. The latter obeys to a min-max optimization problem that captures the performance objective.

2.2.1 The control framework

The customary unity feedback controller is depicted in Figure 1.1. Closed-loop performance and robustness are typically evaluated in terms of the sensitivity S and the complementary sensitivity T transfer functions (Skogestad and Postlethwaite, 2005), respectively:

$$S \doteq \frac{1}{1+L} \tag{2.1}$$

$$T \doteq 1 - S = \frac{L}{1+L} \tag{2.2}$$

where $L \doteq PK(s)$ is the loop transfer function. As it has already been stated, the model of the plant is given by:

$$P = K_g \frac{e^{-sh}}{\tau s + 1} \tag{2.3}$$

For design purposes, it is convenient to approximate the delay term in (2.3) so as to achieve a purely rational process model. By using the first order Padé expansion $e^{-sh} \approx \frac{-(h/2)s+1}{(h/2)s+1}$, (2.3) can be approximated as follows

$$P \approx K_g \frac{-\frac{h}{2}s + 1}{(\tau s + 1)(\frac{h}{2}s + 1)} \tag{2.4}$$

Regarding the control law, the following ISA PID form (Astrom and Hagglund, 2005) is chosen:

$$u = K_p \left(1 + \frac{1}{sT_i} + \frac{sT_d}{1 + sT_d/N}\right) e \tag{2.5}$$

where $e(s) = r(s) - y(s)$, being $r(s)$, $y(s)$ and $u(s)$ the Laplace transforms of the reference, process output and control signal, respectively. K_p is the PID gain, whereas T_i and T_d are its integral and derivative time constants.

Finally, N is the ratio between T_d and the time constant of an additional pole introduced to assure the properness of the controller. This way, the following transfer function for the controller K is assumed:

$$K = K_p \frac{1 + s(T_i + \frac{T_d}{N}) + s^2 T_i \frac{T_d}{N}(N+1)}{sT_i(1 + s\frac{T_d}{N})} \tag{2.6}$$

2.2.2 The Model Matching Problem

The controller design will be based on a desired input-output response. Mathematically, the following min-max optimization problem is posed to capture the performance objective:

$$\min_{K \in \mathcal{C}} \|W(T_d - T)\|_\infty \tag{2.7}$$

where $T_d(s)$ is a desired reference model for the closed-loop system response, $W(s)$ is a weighting function and $T(s)$ is the complementary sensitivity function, which corresponds to the transfer function from the input to the output. In Section 2.3, the control problem (2.7) will be solved for a suitable particular case yielding a regulator K of the form (2.6). The Youla parametrization (Morari and Zafiriou, 1989) for stable plants will be used to simplify the search of the optimal stabilizing controller in (2.7). According to Figure 1.1, this result states that any *internally stabilizing* controller K can be expressed as

$$K = \frac{Q}{1 - PQ} \tag{2.8}$$

where $Q(s)$ is any stable transfer function. The role of Q is better understood within the IMC configuration (Morari and Zafiriou, 1989) depicted in Figure 2.1. In the context of the IMC structure, Q is the parameter to be designed. The main advantage of this approach comes from the fact the all the closed-loop feedback relations become *affine* in the Q parameter. For instance, $H(P, K)$ in (1.1) simplifies to:

$$\begin{pmatrix} y \\ u \end{pmatrix} = \begin{pmatrix} PQ & P(1-PQ) \\ Q & -PQ \end{pmatrix} \begin{pmatrix} r \\ d \end{pmatrix} \tag{2.9}$$

In particular, one has that:

$$S = 1 - PQ \tag{2.10}$$

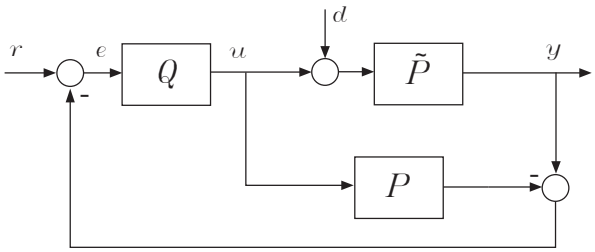

Figure 2.1: IMC configuration. Here, $\tilde{P}$ represents the real (uncertain) plant, whereas P denotes the available model. In the nominal scenario, the model is assumed to be perfect, i.e., $\tilde{P} = P$.

and

$$T = PQ \tag{2.11}$$

With all these considerations in mind, the constrained problem (2.7) can be posed in terms of Q as follows:

$$\min_{Q \in \mathcal{RH}_\infty} \|W\left(T_d - PQ\right)\|_\infty \tag{2.12}$$

Once the problem above has been solved, the equivalent unity feedback controller is obtained from (2.8).

2.3 Analytical solution

We are now concerned with finding a simple solution to problem (2.12), which aims at minimizing the functional

$$\mathcal{E} = \|W(T_d - T)\|_\infty \tag{2.13}$$

Several methods could be followed in order to solve this $\mathcal{H}_\infty$ general problem. See, for example, (Francis, 1987; Vilanova and Serra, 1999). However, our interest focuses on simple instances of the problem (2.7) leading to a controller of the form (2.6). Following this rationale, the above min-max problem was solved in (Vilanova, 2008) for the following particular setup: $W = \frac{1+zs}{s}, T_d = \frac{1}{1+T_M s}$. Additionally, a first order Taylor approximation for

the delay in (2.3) was taken into account. The resulting controller depends on two tuning parameters: z, T_M. The role of T_M is clear: it specifies the desired speed of response whereas z allows for adjustment of the robustness of the control system. In what follows, a different setup is suggested, resulting in a single-parameter PID control law which provides very similar performance.

The suggested settings for minimizing (2.13) are:

$$P = K_g \frac{-\frac{h}{2}s + 1}{(\frac{h}{2}s + 1)(\tau s + 1)} \quad T_d = 1 \quad W = \frac{1}{s} \tag{2.14}$$

The weight $W = \frac{1}{s}$ is the simplest one ensuring integral action in the design, whereas the selected reference model $T_d = 1$ specifies the ideal input-to-output relation. Needless to say, this is not achievable in practice: if a very quick response is desired, this would be normally at the expense of a large overshoot in the output transient and poor robustness margins. As it will be seen, controlling the overshoot will be an easy task once the optimum controller has been derived. Substituting the expressions for W and T_d into (2.12) we finally arrive at

$$\min_{Q \in \mathcal{RH}_\infty} \left\| \frac{1}{s}(1 - PQ) \right\|_\infty \tag{2.15}$$

Note that problem (2.15) is indeed a sensitivity one because $1 - PQ = S$. In addition, (2.15) corresponds to a MMP (recall Section 1.2.2) with $T_1 = 1/s, T_2 = P/s$. Because T_2 (equivalently P) has only one RHP zero ($\nu = 1$) at $s = h/2$, Lemma 1.2.1 implies that the optimal $\mathcal{E}$ in (2.13) is[1]

$$\mathcal{E}^o = \rho \frac{q(-s)}{q(s)} = \rho \tag{2.16}$$

where the constant ρ is determined from the interpolation constraint

$$\mathcal{E}\left(\frac{2}{h}\right) = W\left(\frac{2}{h}\right) T_d\left(\frac{2}{h}\right) = W\left(\frac{2}{h}\right) = \frac{h}{2} \tag{2.17}$$

[1]For the case of a single RHP zero in T_2, the MMP (1.15) can also be solved by direct application of the maximum modulus principle of complex variable (Churchill and Brown, 1986; Skogestad and Postlethwaite, 2005; Alcántara *et al.*, 2009).

Consequently, from (2.17), $\rho = \frac{h}{2}$. This means that the optimal IMC controller Q is such that

$$\mathcal{E}^o = \rho = \frac{h}{2} = W(T_d - PQ) = \frac{1}{s}(1 - PQ) \tag{2.18}$$

By isolating Q from (2.18) we arrive at

$$Q = \left(-\frac{h}{2}s + 1\right) P^{-1} = \frac{1}{K_g}\left(\frac{h}{2}s + 1\right)(\tau s + 1) \tag{2.19}$$

From (2.19), we see that the optimal Q solving the minimization problem is not proper. In order to yield a realizable compensator, it is necessary to augment it with a filter:

$$Q = \frac{1}{K_g}\left(\frac{h}{2}s + 1\right)(\tau s + 1) f(s) = \frac{1}{K_g}\frac{(\frac{h}{2}s + 1)(\tau s + 1)}{(\lambda s + 1)^2} \tag{2.20}$$

By making $\lambda \to 0$, the optimal behaviour is recovered. The equivalent unity feedback controller K is given by (2.8)

$$K = \frac{1}{K_g}\frac{(\frac{h}{2}s + 1)(\tau s + 1)}{s(\lambda^2 s + 2\lambda + \frac{h}{2})} \tag{2.21}$$

and can be cast into the commercial form (2.6) according to the following tuning rule:

$$\begin{aligned} K_p &= \frac{\chi(\lambda)}{K_g(4\lambda + h)} \\ T_i &= \frac{\chi(\lambda)}{2} \\ \frac{T_d}{N} &= \frac{2\lambda^2}{4\lambda + h} \\ N + 1 &= \frac{\tau h(4\lambda + h)}{2\lambda^2 \chi(\lambda)} \end{aligned} \tag{2.22}$$

where

$$\chi(\lambda) = \frac{4\lambda(2\tau + h) + (\tau + h)^2 - \tau^2 - 4\lambda^2}{4\lambda + h} \tag{2.23}$$

Remark 2.3.1. *Although the focus in this chapter is on the FOPTD model, the above analytical procedure is readily applicable to other low-order stable*[2] *models:*

- *Second Order Processes with Time Delay (SOPTD):* $K_g \frac{e^{-hs}}{(\tau_1 s+1)(\tau_2 s+1)} \approx K_g \frac{-hs+1}{(\tau_1 s+1)(\tau_2 s+1)}$.
- *Second Order Processes with Inverse Response (SOPIR):* $K_g \frac{-\alpha s+1}{(\tau_1 s+1)(\tau_2 s+1)}$. *The latter case was considered in (Alcántara* et al.*, 2009).*

2.4 Stability analysis

This section addresses how the λ parameter influences both the nominal and the robust stability of the proposed controller. The main objective is to prepare the groundwork for assisting in the selection of the tuning parameter based on robustness considerations. This task is finally accomplished in Section 2.5, where a *free-of-*λ tuning rule is proposed.

2.4.1 Nominal stability

Since we have considered the approximation (2.4) for the adopted FOPTD model, the basic requirement of nominal stability is not guaranteed for a FOPTD plant even when all its parameters are perfectly known. The nominal stability issue is dealt with here by means of the Dual Locus technique along the lines of (Zhong, 2003). This technique, based upon the Argument Principle (Churchill and Brown, 1986), can be regarded as a *modified* version of the well-known Nyquist criterion (Skogestad and Postlethwaite, 2005). Taking the controller from (2.21) together with the model (2.3) results in the following characteristic equation:

$$1 + L = 1 + \frac{\frac{h}{2}s + 1}{\lambda^2 s^2 + (2\lambda + \frac{h}{2})s} e^{-sh} = 0 \tag{2.24}$$

[2]The design, as it has been presented here, is not applicable to unstable plants since it would result in an unstable pole/zero cancellation between the plant P and the controller K.

which can be rewritten in the form

$$L_1 - L_2 = 0 \tag{2.25}$$

by making the following assignments:

$$L_1 = -\frac{\lambda^2 s^2 + (2\lambda + \frac{h}{2})s}{\frac{h}{2}s + 1} \qquad L_2 = e^{-sh}$$

The Dual Locus diagram technique is now applied: briefly stated, the closed-loop system is stable if the locus of L_1 reaches the intersection point earlier than L_2. The loci of L_1 and L_2 have been displayed in Figure 2.2 for positive frequencies of the imaginary axis.

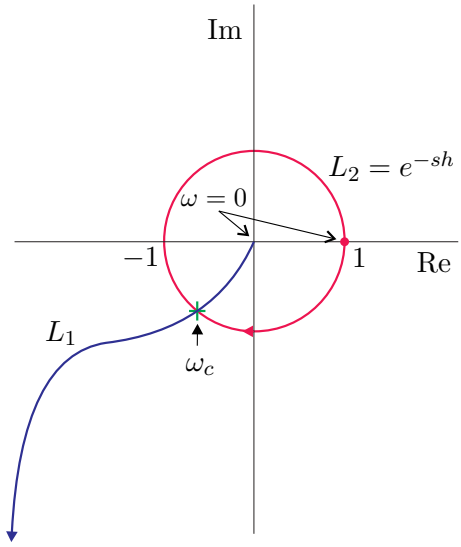

Figure 2.2: Dual Locus diagram.

The intersection frequency can be determined by solving the equation:

$$\left| -\frac{\lambda^2 s^2 + (2\lambda + \frac{h}{2})s}{\frac{h}{2}s + 1} \right|_{s=j\omega} = 1 \tag{2.26}$$

from which the positive frequency of interest can be seen to be:

$$\omega_c = \frac{\sqrt{-4 - 2\mu + \sqrt{(-4 - 2\mu)^2 + 4}}}{\sqrt{2}\lambda} \tag{2.27}$$

where $\mu = \frac{h}{\lambda}$. The phase angles of L_1 and L_2 at ω_c are, respectively:

$$\phi_1 = \arctan -\frac{2 + \frac{1}{2}\mu}{\lambda\omega_c} - \arctan \frac{1}{2}\mu\lambda\omega_c \tag{2.28}$$

and

$$\phi_2 = -h\omega_c \tag{2.29}$$

The stability condition is satisfied only when the phase angle of L_1 is larger (in absolute value) than that of L_2 at ω_c, i.e, if $\phi_1 - \phi_2 < 0$. From the fact that $\mu = \frac{h}{\lambda}$ and (2.27) it can be seen that the function $\phi_1 - \phi_2$ is ultimately only a function of μ.

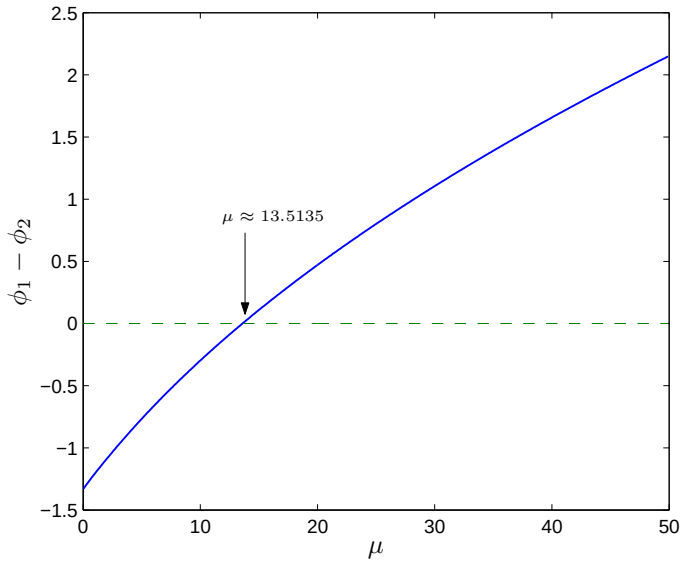

Figure 2.3: $\phi_1 - \phi_2$ vs $\mu = \frac{h}{\lambda}$.

The function $\phi_1 - \phi_2$ is plotted against the μ parameter in Figure 2.3. It can be concluded that the resulting closed loop system is stable provided that $\lambda = \frac{h}{\mu}$ is chosen such that

$$\lambda > \frac{1}{13.5135}h \approx 0.074h \tag{2.30}$$

2.4.2 Robust stability

To account for model uncertainty we will assume that the dynamic behaviour of a plant is described not only by a single LTI model but by a whole family, usually referred to as the *uncertainty set*. More precisely, we will consider the possible plants at hand belonging to the following set:

$$\mathcal{F} = \left\{ \tilde{P} = P(1 + \Delta_m) \right\} \tag{2.31}$$

where Δ_m is the relative (multiplicative) model error

$$\Delta_m \doteq \frac{\tilde{P} - P}{P} \tag{2.32}$$

satisfying $|\Delta_m(j\omega)| \leq |W_m(j\omega)|$. $W_m(s)$ is a frequency weight bounding the model error (plant/model mismatch). It is well-known (Skogestad and Postlethwaite, 2005; Morari and Zafiriou, 1989) that a controller K that stabilizes the nominal plant P, also stabilizes all the plants in (2.31) provided that

$$\|W_m T\|_\infty < 1 \tag{2.33}$$

Condition (2.33) evaluates robust stability in terms of the nominal complementary sensitivity function T. We need to compute the relative model error between the model (2.3) and the real plant, which is considered to be

$$\tilde{P} = K_g(1 + r_k)\frac{e^{-h(1+r_h)s}}{(1 + r_\tau)\tau s + 1} \tag{2.34}$$

for r_k, r_τ, r_h in the interval $(-1, +1)$. It can be seen that if we denote by $\delta_k, \delta_\tau, \delta_h$ the maximum (positive) values of r_k, r_τ, r_h, respectively, then the worst case relative error Δ_m, corresponding to the most difficult plant to stabilize, is given by:

$$\Delta_m^* = (1 + \delta_k)\frac{\tau s + 1}{(1 - \delta_\tau)\tau s + 1}e^{-sh\delta_h} - 1 \tag{2.35}$$

From (2.4) and (2.20), the nominal complementary sensitivity function is

$$T = PQ = \frac{-\frac{h}{2}s + 1}{(\lambda s + 1)^2} \tag{2.36}$$

In our case, the robust stability condition (2.33) holds if and only if

$$|T(j\omega)| < \frac{1}{|\Delta_m^*(j\omega)|}\ ,\forall\omega \tag{2.37}$$

From the nominal stability analysis we know that by choosing $\lambda > 0.074$ the closed-loop is stable for a perfectly known FOPTD system. The necessary minimum λ — thus, providing the fastest response — yielding robust stability can be determined graphically by plotting the magnitudes of (2.36) and (2.35) for a given parametric uncertainty pattern, increasing λ until (2.37) is satisfied. This method could be followed by the control system designer in order to conveniently adjust the robustness/performance trade-off. In order to make this procedure completely automatic, the following section proposes a way to fix λ, providing thus an auto-tuning of the proposed controller.

2.5 Automatic PID tuning derivation

This section is aimed at conveniently fixing the value of λ in the tuning relations (2.22), giving rise to a tuning rule solely dependent on the model. So far, the particular MMP (2.15) has been solved. Its solution (2.22) has been found to depend on the FOPTD model in addition to an extra tuning parameter: λ. The lower the value of λ, the lower the value of the functional (2.13). However, an excessively low value for λ providing very fast responses is not desirable since it is bound to produce large overshoots in the step response. This is not taken into account by the adopted performance criterion. Besides, from the stability analysis of Section 2.4, in order to make the closed loop robust, λ has to provide the necessary detuning and cannot be so small in practice. In accordance with this, we summarize below the requirements to be met:

- *Performance:* A sufficiently fast, *free-of-overshoot* nominal set-point response. This performance specification obeys the fact that in many processes such as chemical or mechanical systems an excessive overshoot is not acceptable. Consequently, λ has to produce a small value for the functional (2.13) while ensuring smooth set-point response.

- *Robustness:* As the controller is obtained from the model, it has to be chosen in such a way that the closed-loop is not too sensitive to variations in process dynamics. Making direct use of the robust stability

condition (2.37) is not easy and would be restricted to parametric uncertainty. Instead, a more general and simpler robustness measure will be used. In spite of this, condition (2.37) will be used at a later stage to assess robustness in the face of parametric uncertainty. Sensitivity to modelling errors can alternatively be captured by the peak of the sensitivity function:

$$M_S \doteq \|S(j\omega)\|_\infty \doteq \max_\omega \left| \frac{1}{1+L(j\omega)} \right| \tag{2.38}$$

which indicates the inverse of the shortest distance from the Nyquist plot to the critical point. Having $M_S < 2$ is a traditional robustness indicator (Skogestad and Postlethwaite, 2005).

It is evident that both the overshoot and the sensitivity peak will depend on the loop function L. On the other hand, as $T = \frac{L}{1+L} = \frac{-(h/2)s+1}{(\lambda s+1)^2}$ is a function of just h and λ, L depends only on h, λ as well. Consequently, if we define q_1="*overshoot*", q_2="*sensitivity peak*" it is clear that there exist functional relations f_1, f_2 such that $q_i = f_i(h, \lambda),\ i = 1, 2$. In these functional relations we have two variables and only one independent unit (time). By applying the Buckingham Pi Theorem from Dimensional Analysis, consult for instance (Tavakoli *et al.*, 2007; Balaguer *et al.*, 2009), it is possible to describe the same relationships by using only one dimensionless parameter. In particular, relations $q_i = f_i(h, \lambda)$ can be expressed more compactly as $\pi_i = \phi_i(\frac{\lambda}{h})$ where π_i contains the quantity of interest q_i, proving that both the overshoot and the sensitivity peak depend only on $\frac{\lambda}{h}$. This dependence can be seen in Figure 2.4, from which the zero overshoot requirement is met for $\lambda > 0.6h$. However, at $\frac{\lambda}{h} = 0.6$ the sensitivity peak curve slope is still significant. For the sake of an improvement in robustness, some extra nominal performance in terms of closed-loop bandwidth is sacrificed by choosing $\lambda = h$, point on which $M_S \approx 1.42$ and the sensitivity curve has a slope of almost zero. This indicates that it is not worth slowing down the nominal response further. With the choice $\lambda = h$, the tuning rule (2.22) becomes that of Table 2.1. Condition (2.37) can be used now to give an idea of the achieved robustness with $\lambda = h$ in terms of parametric uncertainty. For $\lambda = h$, (2.36) becomes

$$T = \frac{-\frac{h}{2}s + 1}{(hs+1)^2} \tag{2.39}$$

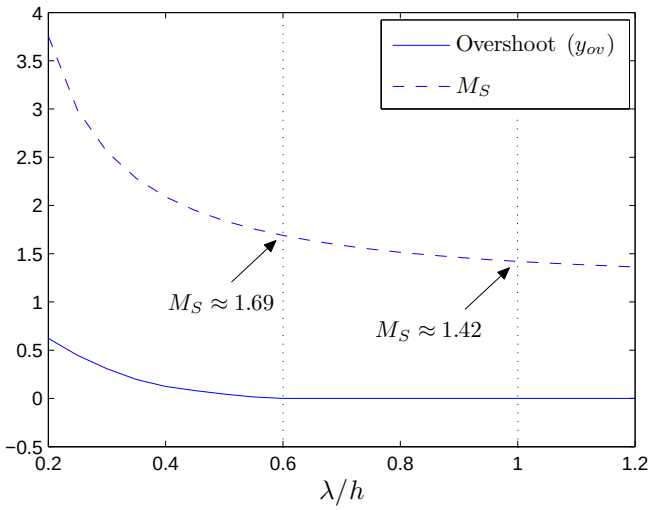

Figure 2.4: Output overshoot (y_{ov}) and sensitivity peak (M_S) against λ/h.

Table 2.1: Proposed ISA PID tuning.

$\mathbf{K_p}$	$\mathbf{T_i}$	$\mathbf{T_d/N}$	$\mathbf{N+1}$
$\frac{0.4T_i}{K_g h}$	$\tau + 0.1h$	$0.4h$	$1.25\frac{\tau}{T_i}$

Let us consider the worst case uncertainty Δ_m^* in (2.35) with $\delta_k = \delta_\tau = \delta_h = \delta = 0.65$ — i.e, assume 65% of simultaneous parametric uncertainty — and T in (2.39) and define the variable q_3="*frequency distance between bode plots of* T *and* $1/\Delta_m^*$". It is clear that $q_3 = f(h, \tau)$. By invoking again the Buckingham Pi Theorem, the same functional relationship can be expressed in the more compact form $\pi_3 = \phi(h/\tau)$, where π_3 contains the quantity of interest q_3. One can try out different values for h/τ until the magnitude bode plots of $1/\Delta_m^*$ and T almost intersect. This has been found to happen for $h/\tau = 0.63$, see Figure 2.5. Consequently, it can be claimed that 65% of parametric uncertainty is allowed for any FOPTD system for which $h/\tau = 0.63$. The described procedure can be repeated for different values of δ. This experiment yields the bounds shown in Table 2.2. It is worth noting that the

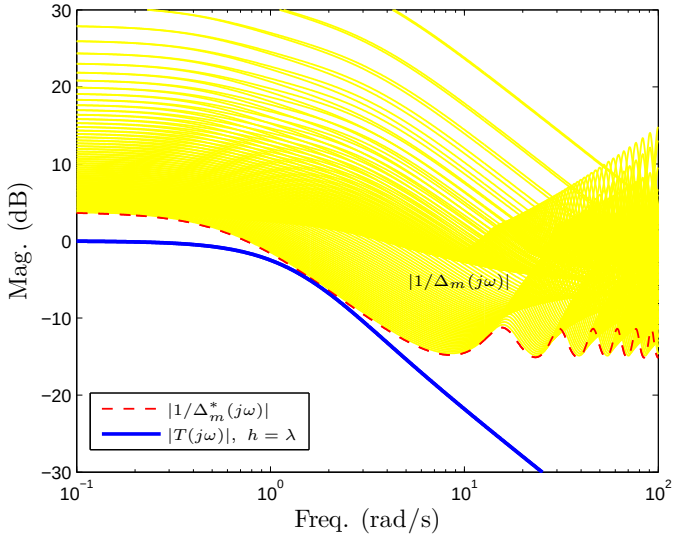

Figure 2.5: Robust stability condition for the nominal plant $\frac{e^{-0.63s}}{s+1}$, assuming 65% of parametric uncertainty in K_g, τ, h.

Table 2.2: Permissible simultaneous parametric uncertainty in K_g, τ, h.

h/τ	0.1	0.25	0.5	0.63	1	5	10
$\delta \times 100$	38%	45%	59%	65%	84%	97%	98%

proposed tuning rule is robust for lead-dominant systems, tolerating almost 100% of uncertainty in the plant parameters. Proceeding likewise, the worst case overshoots for different values of δ have been plotted in Figure 2.6.

2.5.1 Control effort constraints

As it will be seen in Section 2.6, moderate control usage is required by the proposed controller in Table 2.1. However, as the control effort is important in practical applications, we provide here quantitative guidelines for selecting λ according to saturation limits and slew rate constraints.

From (2.9) and (2.20), the control signal associated with a set-point change

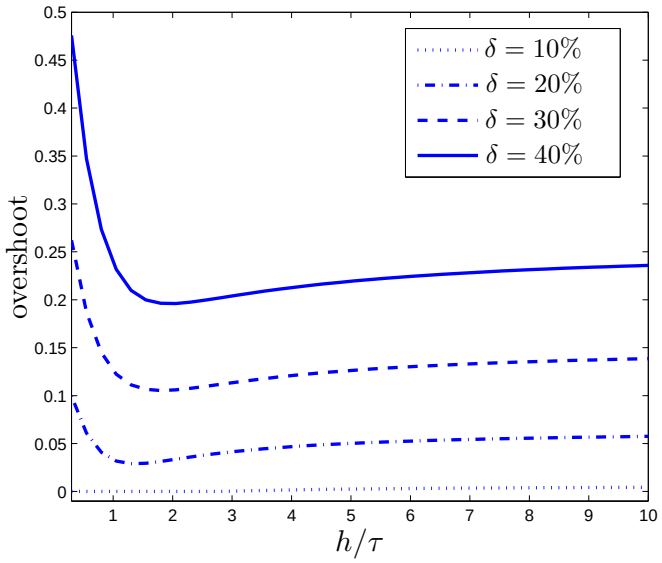

Figure 2.6: Worst case overshoots for different levels of parametric uncertainty.

is given by

$$u(t) = \mathcal{L}^{-1}\left\{Q\frac{1}{s}\right\} = \mathcal{L}^{-1}\left\{\frac{1}{K_g}\frac{(\tau s+1)(\frac{h}{2}s+1)}{(\lambda s+1)^2}\frac{1}{s}\right\} \tag{2.40}$$

where $\mathcal{L}^{-1}$ denotes the inverse Laplace transform. By calculating (2.40) the maximum value for $u(t)$ can be found to be

$$\|u(t)\|_\infty = \begin{cases} \frac{1}{K_g}\left(1 - \frac{\tau h - 2\tau\lambda - h\lambda + 2\lambda^2}{2\lambda^2} e^{-\frac{2\tau h - 2\tau\lambda - h\lambda}{(-2\lambda+h)(\tau-\lambda)}}\right) & \text{if} \quad \tau > \lambda \\ \frac{1}{K_g} & \text{if} \quad \tau \leq \lambda \end{cases} \tag{2.41}$$

From this point on, it is assumed that $\lambda/h > 0.5$ (indeed, it was shown in Figure 2.4 that $\lambda/h \geq 0.6$ for zero nominal overshoot). From (2.41) it can be seen that $\|K_g u(t)\|_\infty$ only depends on $\frac{h}{\tau}$ and $\frac{\lambda}{h}$. Thus, once a given plant has been modelled according to a FOPTD description, a particular $\frac{h}{\tau}$ relation is obtained. With this in mind, $\|K_g u(t)\|_\infty$ only depends on $\frac{\lambda}{h}$ and λ can be tuned so as to obtain acceptable peaks on the control signal. On the other hand, if

$\frac{\lambda}{h}$ is fixed first, then $\|K_g u(t)\|_\infty$ becomes a function of $\frac{h}{\tau}$. This function can be used to give an idea of the maximum control effort required along different *lead-lag* ratios. In our case, we fixed $\frac{\lambda}{h} = 1$. Substituting $\lambda = h$ in (2.41) leads to

$$\|u(t)\|_\infty = \begin{cases} \frac{1}{K_g}\left(1 - \frac{1}{2}\left(\frac{-\tau+h}{h}\right)e^{\frac{h}{-\tau+h}}\right) & \text{if} \quad h < \tau \\ \frac{1}{K_g} & \text{if} \quad h \geq \tau \end{cases} \tag{2.42}$$

which can be easily expressed as a function of K_g and $\frac{h}{\tau}$.

Slew rate constraints can be similarly tackled. From (2.40) the derivative of the control signal is

$$\dot{u}(t) = \mathcal{L}^{-1}\{Q\} = \mathcal{L}^{-1}\left\{\frac{1}{K_g}\frac{(\tau s+1)(\frac{h}{2}s+1)}{(\lambda s+1)^2}\right\} \tag{2.43}$$

By calculating (2.43) and considering the following decomposition[3]

$$\dot{u}(t) = \dot{u}_+(t) + \dot{u}_-(t) \tag{2.44}$$

where

$$\dot{u}_+(t) \doteq \begin{cases} \dot{u}(t) & \text{if} \quad \dot{u}(t) > 0 \\ 0 & \text{if} \quad \dot{u}(t) \leq 0 \end{cases} \qquad \text{and} \qquad \dot{u}_-(t) \doteq \begin{cases} -\dot{u}(t) & \text{if} \quad \dot{u}(t) < 0 \\ 0 & \text{if} \quad \dot{u}(t) \geq 0 \end{cases} \tag{2.45}$$

the following expressions can be easily obtained

$$\|\dot{u}_+(t)\|_\infty = -\frac{1}{2}\frac{2\tau h - 2\tau\lambda - h\lambda}{K_g\lambda^3} \tag{2.46}$$

and

$$\|\dot{u}_-(t)\|_\infty = \begin{cases} \frac{1}{2}\frac{2\lambda^2-2\tau\lambda-h\lambda+\tau h}{K_g\lambda^3}e^{-\frac{3\tau h+2\lambda^2-4\tau\lambda-2h\lambda}{(-2\lambda+h)(\tau-\lambda)}} & \text{if} \quad \tau > \lambda \\ 0 & \text{if} \quad \tau \leq \lambda \end{cases} \tag{2.47}$$

which represent, respectively, the highest rates of change in the increasing and decreasing directions. For the proposed tuning rule $\lambda = h$ the above two expressions simplify to

$$\|\dot{u}_+(t)\|_\infty = \frac{1}{2K_g h} \tag{2.48}$$

[3] A similar decomposition was not used for $u(t)$ in (2.40) due to the fact that $u(t) \geq 0$ for $t \geq 0$.

and

$$\|\dot{u}_-(t)\|_\infty = \begin{cases} \frac{1}{2}\frac{h-\tau}{K_g h^2} e^{-\frac{\tau}{\tau-h}} & \text{if} \quad h < \tau \\ 0 & \text{if} \quad h \geq \tau \end{cases} \tag{2.49}$$

2.6 Simulation examples

In this section we will evaluate the proposed simple automatic tuning rule of Table 2.1 through simulations. The objective is to cover a representative set of examples so as to properly obtain conclusions regarding the performance and robustness of the suggested method. Table 2.3 collects the information of the experimental setup. Firstly, four linear processes are considered including the lag-dominant, lead-dominant and balanced lag and delay cases. The first one consists of a FOPTD plant for which there is only parametric uncertainty whereas the other three systems are linear processes modelled as FOPTD plants. These three last examples are taken from (Astrom and Hagglund, 2004). Additionally, a fifth non-linear system is taken into account. This last process represents the isothermal series/paralel Van de Vusse reaction (de Vusse, 1964) taking place in an isothermal continuous stirred tank reactor (CSTR). The corresponding approximate FOPTD model has been derived assuming the system in a stationary point.

For the sake of comparison, other approaches to PID design considering FOPTD models are examined. Since a complete comparison is not possible due to the large number of existing tuning rules (see (O'Dwyer, 2006)) we will concentrate on two existing methods also conceived in the spirit of simplicity:

- SIMC tuning rule (leading to a PI). A really simple and effective tuning proposed in (Skogestad, 2003).
- AMIGO tuning rule (leading to a PID). A rule along the lines of the classical Ziegler-Nichols method. See (Astrom and Hagglund, 2004).

In order to evaluate the robustness and the performance obtained with the different methods at hand, the following standard measures will be used:

- *Robustness*: The peak of the Sensitivity function, M_S, is the inverse of the minimum distance from the Nyquist plot to the critial point and constitutes a quite standard robustness indicator (Skogestad and Postlethwaite, 2005).

Table 2.3: Processes within the experimental setup together with their FOPTD approximations. P_{1-4} are linear processes. Regarding P_5, $\mathbf{f}(\mathbf{x},u) = (f_1(\mathbf{x},u), f_2(\mathbf{x},u)) = (-50x_1 - 10x_1^2 + (10-x_1)u, 50x_1 - 100x_2 - x_2u)$. The assumed working point is $(\mathbf{x}^*, u^*) = (3, 1.117, 34.2805)$.

Real process	**FOPTD Model**
$P_1 = \frac{1.2e^{-1.2s}}{0.8s+1}$	$\frac{e^{-s}}{s+1}$
$P_2 = \frac{1}{(1+s)(1+0.1s)(1+0.01s)(1+0.001s)}$	$\frac{e^{-0.073s}}{1.073s+1}$
$P_3 = \frac{e^{-s}}{(1+0.05s)^2}$	$\frac{e^{-s}}{0.093s+1}$
$P_4 = \frac{1}{(1+s)^4}$	$\frac{e^{-1.42s}}{2.9s+1}$
$P_5 \equiv \begin{cases} \dot{\mathbf{x}} &= \mathbf{f}(\mathbf{x},u) \\ y &= x_2 \end{cases}$	$\frac{0.0126e^{-0.0085s}}{0.01s+1}$

- *Output performance*: The Integrated Absolute Error (IAE) of the error $e = r - y$ will be computed.

  $$\text{IAE} = \int_0^\infty |e(t)|dt$$

- *Input performance*: To evaluate the manipulated input usage, the total variation (TV) of the control signal $u(t)$ will be computed.

  $$\text{TV} = \int_0^\infty |\dot{u}(t)|dt$$

To provide a more global and complete comparison framework, the performance measures above will be calculated for both a set-point change and load disturbance. In addition, the percent overshoot of the output $y(t)$, denoted by y_{ov}, will be taken into account for set-point output performance. Similarly, the peak of the control signal $u(t)$, i.e. $\|u(t)\|_\infty$, will be indicated for load disturbance performance. Table 2.4 summarizes the results obtained.

Table 2.4: Results of performance/robustness evaluation for the set of plants $\{P_i\}_{i=1}^{5}$. As the system P_5 is nonlinear, the robustness indicator M_S has been computed with respect to its linearization on the working point, which turns out to be $\frac{-1.117s+188.8}{s^2+278.6s+1.937e04}$.

Plant	**Tuning**	**Robustness**	**Performance**					
			set-point			**disturbance**		
		M_S	IAE	TV	y_{ov}	IAE	TV	$\|u(t)\|_\infty$
$\mathbf{P_1}$	Proposed	1.74	2.15	1.1	3.3	1.25	0.55	0.51
	SIMC	2.12	2.4	1.64	20.95	1.235	0.79	0.6
	AMIGO	1.85	1.7	6.13	10.96	0.91	0.72	0.56
$\mathbf{P_2}$	Proposed	1.33	0.21	11.03	6.36	0.09	0.57	0.53
	SIMC	1.56	0.24	16.11	23.42	0.04	0.75	0.62
	AMIGO	1.31	0.24	11.56	23.55	0.027	0.75	0.62
$\mathbf{P_3}$	Proposed	1.42	2.5	1	0	1.25	0.5	0.5
	SIMC	1.6	2.18	1.09	4.27	1.09	0.54	0.52
	AMIGO	1.46	1.94	1.46	0	0.97	0.56	0.5
$\mathbf{P_4}$	Proposed	1.66	3.76	1.78	5.1	1.77	0.61	0.53
	SIMC	2	4.08	2.68	18.77	1.54	0.82	0.6
	AMIGO	1.62	3.23	2.02	15.54	1.26	0.67	0.58
$\mathbf{P_5}$	Proposed	1.4	0.0026	11.1	0.4	0.0005	2.3	34.46
	SIMC	1.57	0.0026	15.6	1.6	0.0047	2.5	34.48
	AMIGO	1.38	0.0022	51.4	1.1	0.0041	3	34.73

It follows from Figures 2.7–2.11 that the proposed tuning rule generates quite smooth responses requiring moderate control action level[4]. Table 2.4 shows that the required control usage is lower than the associated with the other two methods. In particular, for plants P_1 and P_5 the proposed tuning control usage is far below that of the AMIGO tuning. It can also be seen that the proposed method provides, generally, both the minimum output overshoots and the control signal peaks. With respect to set-point evaluation, the AMIGO tuning rule gives better IAEs. However, if one inspects Figures 2.7–2.11 it is clear that the set-point responses of the proposed method exhibit less overshoot than those of the AMIGO tuning.

Regarding disturbance rejection, the proposed method provides an inferior performance with respect to the SIMC and AMIGO proposals. This is a quite expected result since the proposed tuning rule was derived for smooth set-point. Nevertheless, disregarding the lag-dominant plant P_2, the disturbance rejection responses are not significantly inferior, and in the case of the SIMC, they are indeed quite comparable. This is explained in part due to the fact that the optimization problem in (2.15) is, as a matter of fact, a sensitivity optimization problem. A deeper analysis of the *servo/regulator* trade-off tuning within a generalized version of the presented framework is being currently conducted and will be the topic of a future work.

Lastly, Table 2.4 shows that for the five considered systems the robustness indicator for the proposed method is always very close to that associated with the best method. This robustness is in accordance with the smoothness of the corresponding control and output signals.

[4]Indeed, the results obtained are very similar to those presented in (Vilanova, 2008) for the automatic tuning (1.28). That is why the method in (Vilanova, 2008) has been excluded from Table 2.4.

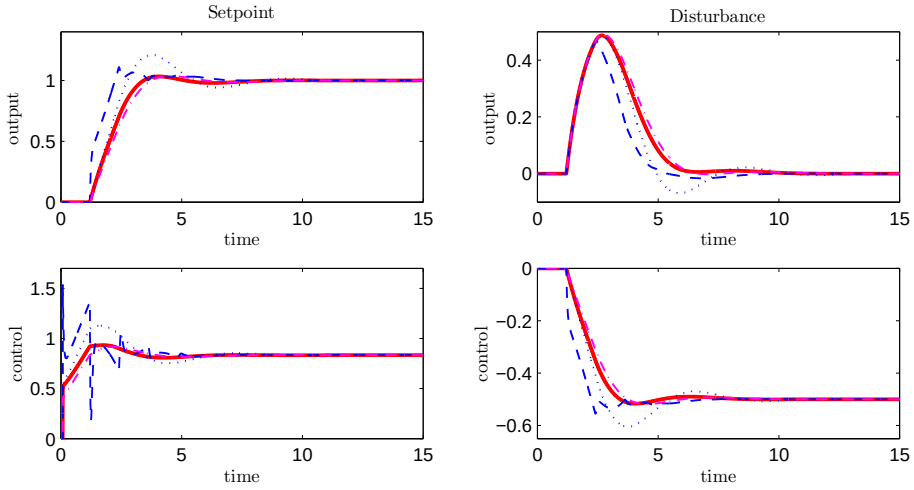

Figure 2.7: P_1 time responses for set-point change and load disturbance for the proposed (solid), SIMC (dotted), AMIGO (dashed) and Vilanova's (2008) (dashdot) tuning rules.

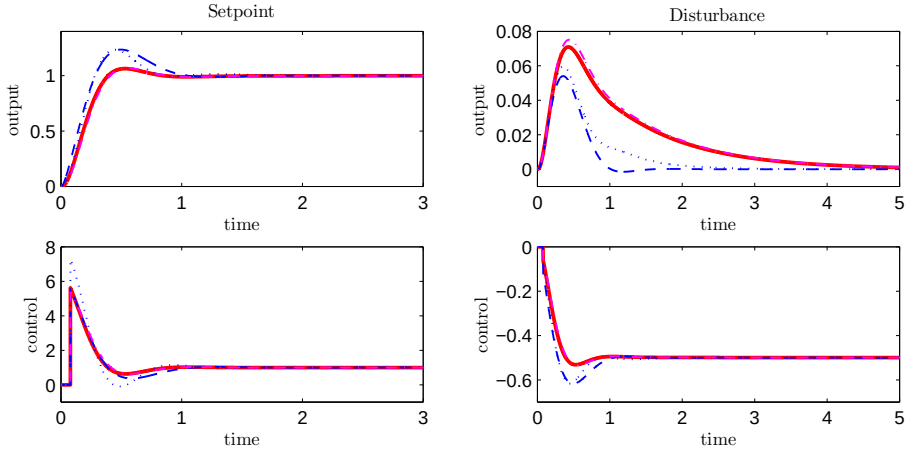

Figure 2.8: P_2 time responses for set-point change and load disturbance for the proposed (solid), SIMC (dotted), AMIGO (dashed) and Vilanova's (2008) (dashdot) tuning rules.

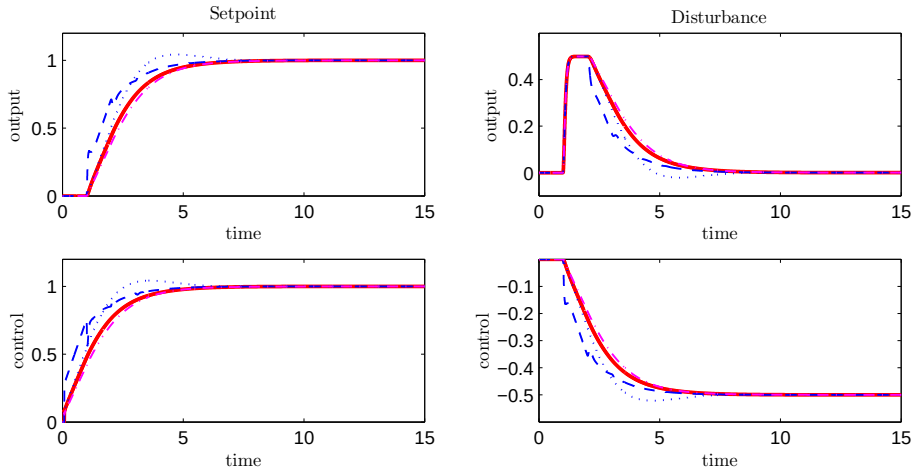

Figure 2.9: P_3 time responses for set-point change and load disturbance for the proposed (solid), SIMC (dotted), AMIGO (dashed) and Vilanova's (2008) (dashdot) tuning rules.

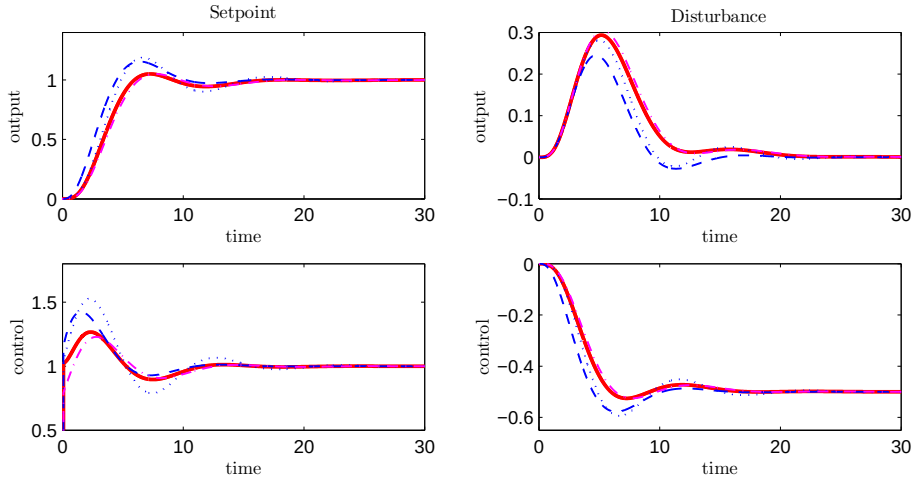

Figure 2.10: P_4 time responses for set-point change and load disturbance for the proposed (solid), SIMC (dotted), AMIGO (dashed) and Vilanova's (2008) (dashdot) tuning rules.

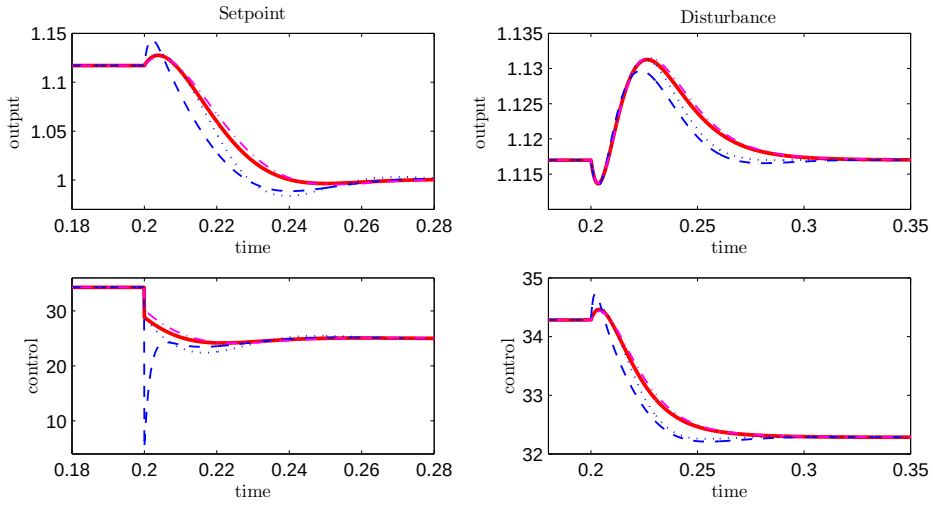

Figure 2.11: P_5 time responses for set-point change and load disturbance for the proposed (solid), SIMC (dotted), AMIGO (dashed) and Vilanova's (2008) (dashdot) tuning rules.

2.7 Summary

Starting by considering a general MMP in the supremum norm, tuning relations for PID design have been presented modelling the plant as a FOPTD system. For the derivation of the suggested tuning, the general MMP has been customized so as to arrive at a PID control solution. The concrete MMP finally solved corresponds to a sensitivity one and leads to a single tuning parameter. Since the controller is derived by means of a purely rational approximation, the nominal stability region for this parameter has been determined. Finally, an automatic robust tuning rule has been derived for smooth set-point following.

The primary goal of the presented method has been to obtain smooth set-point response. Because responses to set-points and load disturbances are usually conflicting, future work is conducted to show how the trade-off between the servo and regulator modes can be tackled within the adopted (weighted sensitivity) framework.

Chapter 3

Improving the load disturbance response (γ-tuning)

Based on (Alcántara et al.*, 2010*b*)*

Due to the fact that sometimes a one-degree-of-freedom (1DOF) PID has to deal with both set-point changes and load disturbances, it would be desirable to have at one's disposal simple methods to achieve a good compromise in this situation. Based on the well-established min-max model matching theory, this chapter addresses the smooth tuning of a 1DOF PID controller for both acceptable load disturbance attenuation and set-point tracking. As the design specifications are commonly given in the form of maximum allowed overshoot, peak on the sensitivity function and other popular measures, the analysis to carry out the design quantitatively based on these indexes is also provided.

3.1 Introduction

It is well-known that most of the control systems in industry are operated by PID controllers still nowadays (Astrom and Hagglund, 2005; Shamsuzzohaa and Skogestad, 2010). This is somehow explained due to their simplicity and acceptable performance in practice. Consequently, given the widespread

use of PID compensators, it is clear that even a small improvement over the already existing tuning methods could represent a benefit in process control. Fortunately, the gap between the theory and practice in control engineering has been reduced during the last twenty years in an attempt of incorporating the methods of optimal and robust control theory to the PID area. As a consequence, new theoretical results as well as several PID designs have been reported (He *et al.*, 2000; Skogestad, 2003; Astrom and Hagglund, 2004; Vilanova, 2008; Hohenbichler, 2009; Sanchís *et al.*, 2010), confirming a trend that endures.

Among the well-established analytical methods, the design of compensators by means of a desired closed-loop specification is a quite common one. Regarding PID controllers, some model matching based approaches have appeared during the last years (Aguirre, 1992; Vilanova, 2008). The problem with the approach in (Aguirre, 1992) is that robustness is not considered explicitly and no tuning rule is finally provided. Avoiding these problems, in (Vilanova, 2008) an analytical model matching based robust PID design is proposed for smooth set-point tracking. In this chapter, we extend this approach, completing the preliminary work initiated in (Vilanova and Arrieta, 2007), so that the controller can be tuned somewhere in between the *servo* and the *regulator* operating modes by means of adjusting a single design parameter: γ. Obviously, within the 1DOF context is not possible to have both optimal set-point and load disturbance attenuation simultaneously (Skogestad and Postlethwaite, 2005). Thus, some kind of trade-off is necessary in order to minimize the overall performance degradation. From a numerical point of view, the underlying idea was originally presented in (Arrieta and Vilanova, 2007), and further developed in (Arrieta *et al.*, 2010). The contributions of the present chapter are summarized below:

- First, the interval for the γ parameter in (Vilanova and Arrieta, 2007) is determined considering that the disturbances enter at the input of the plant (i.e., load disturbances). Additionally, the nominal stability analysis is conducted.
- Second, once the interval for γ is known, quantitative tuning guidelines based on common robustness/performance indexes are given.

In (Astrom and Hagglund, 2005), it is claimed that many analytical methods for PID design produce pole-zero cancellations, which makes them unsuit-

able for regulator purposes. This is one of the drawbacks of the conventional IMC method (Morari and Zafiriou, 1989; Skogestad, 2003) and some IMC-like approaches (Zhang *et al.*, 2002; Vilanova, 2008; Ali and Majhi, 2009; Alcántara *et al.*, 2010*c*). These approaches are suitable for servo operation but may exhibit poor disturbance attenuation. On the contrary, the presented method is aimed at providing good responses in both servo and regulator mode.

This chapter is organized as follows: Section 3.2 is devoted to the problem statement. Section 3.3 reviews the model matching analytical γ-tuning design. The exact interval for γ considering load disturbances is determined in Section 3.4, which also concerns the stability analysis. In Section 3.5, the quantitative tuning of γ is addressed according to standard robustness/performance indexes. Section 3.6 illustrates by example the suggested methodology for balancing servo and regulator performance. Finally, Section 3.7 concludes the chapter drawing some final conclusions.

3.2 Problem statement

In this section, the control framework and the problem formulation are introduced.

3.2.1 The control framework

The conventional 1DOF scenario of Figure 3.1 is assumed, where a distinction is made between input (d_i) and output (d_o) disturbances. A FOPTD model

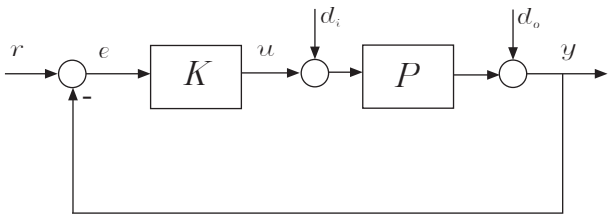

Figure 3.1: Feedback control scheme.

for the plant P is used, i.e.:

$$P = K_g \frac{e^{-sh}}{\tau s + 1} \tag{3.1}$$

For design purposes, it is convenient to approximate the delay term in (3.1) so as to achieve a purely rational process model. By using the first order Taylor expansion $e^{-sh} \approx 1 - sh$, the model in (3.1) can be approximated as follows

$$P \approx K_g \frac{-sh + 1}{\tau s + 1} \tag{3.2}$$

Regarding the control law, the ISA PID form (Astrom and Hagglund, 2005) is considered:

$$u = K_p \left(1 + \frac{1}{sT_i} + \frac{sT_d}{1 + sT_d/N}\right) e \tag{3.3}$$

where $e(s) = r(s) - y(s)$, being $r(s)$, $y(s)$ and $u(s)$ the Laplace transforms of the reference, process output and control signal, respectively. K_p is the PID gain, whereas T_i and T_d are its integral and derivative time constants, respectively. Finally, N is the ratio between T_d and the time constant of an additional pole introduced to assure the properness of the controller. Therefore, the transfer function representation of the chosen controller K is given by

$$K = K_p \frac{1 + s(T_i + \frac{T_d}{N}) + s^2 T_i \frac{T_d}{N}(N+1)}{sT_i(1 + s\frac{T_d}{N})} \tag{3.4}$$

3.2.2 The Model Matching Problem

In this section the min-max model matching approach to controller design is presented. The controller derivation will be based on a desired model for a given closed-loop transfer function. Mathematically, a min-max optimization problem of the form

$$\min_{K \in \mathcal{C}} \|W(X_d - X)\|_\infty \tag{3.5}$$

is posed to capture the performance objective. $W(s)$ is a weighting function, $X(s)$ is a given closed-loop system relation and $X_d(s)$ is the target model for $X(s)$. For instance, one could choose $X = T$, the complementary sensitivity function. In this case $X_d = T_d$ would specify a desired input-to-output response for the closed-loop system. Another possibility is to choose $X = S$, the sensitivity function. In this case $X_d = S_d$ would represent the desired sensitivity shape in frequency. Note that

$$\begin{aligned} \min_{K\in\mathcal{C}} \|\mathcal{E}\|_\infty &= \min_{K\in\mathcal{C}} \|W\,(T_d - T)\|_\infty \qquad (3.6)\\ &= \min_{K\in\mathcal{C}} \|W\,((1-S_d)-(1-S))\|_\infty \\ &= \min_{K\in\mathcal{C}} \|W\,(S_d - S)\|_\infty \qquad (3.7) \end{aligned}$$

Consequently, (3.6) and (3.7) ultimately amount to the same optimization problem. However, depending on the choice of the desired relations, the optimization will be better regarded as a complementary sensitivity problem for set-point tracking purposes or as a sensitivity one for disturbance rejection. By using the Youla parameterization (1.23), the constrained problem (3.6) can be recast in the more convenient form:

$$\min_{Q\in\mathcal{RH}_\infty} \|\mathcal{E}\|_\infty = \min_{Q\in\mathcal{RH}_\infty} \|W\,(T_d - PQ)\|_\infty \qquad (3.8)$$

3.3 Model matching approach to PID design

With the purpose of making the present work more self-contained, this section briefly outlines the PID-oriented solution to (3.8) presented in (Vilanova, 2008; Vilanova and Arrieta, 2007). In order to constrain the solution of (3.8) to be a PID compensator, the following setting was proposed:

$$T_d = \frac{(T_M - \gamma)s + 1}{1 + T_M s} \qquad (3.9)$$

which corresponds to a desired sensitivity function S_d of the form

$$S_d = \frac{\gamma s}{T_M s + 1} \qquad (3.10)$$

with respect to the sensitivity problem (3.7). Regarding the weighting function in (3.8), the following choice was made:

$$W = \frac{1 + zs}{s} \qquad (3.11)$$

in order to automatically include integral action and keep it as simple as possible. The solution to the model matching problem (MMP) (3.8) can be

obtained applying Lemma 1.2.1 with $T_1 = T_d$ and $T_2 = PQ$, where P is taken as in (3.2). In this case, there is only one RHP zero in P ($\nu = 1$) at $s = \frac{1}{h}$. Consequently, the optimum error is given by $\mathcal{E}^o = \rho$, being ρ determined from a single interpolation constraint:

$$\mathcal{E}^o(1/h) = \rho = W(1/h)T_d(1/h) \Longrightarrow \rho = \frac{1 + \frac{z}{h}}{\frac{1}{h}} \frac{(T_M - \gamma)\frac{1}{h} + 1}{1 + \frac{T_M}{h}}, \tag{3.12}$$

or more compactly:

$$\rho = \frac{h + z}{h + T_M} (T_M + h - \gamma) \tag{3.13}$$

Now, the optimum Q can be easily computed

$$\rho = \mathcal{E}^o = W(T_d - PQ) \Longrightarrow Q = \left(T_d - \rho W^{-1}\right) P^{-1} \tag{3.14}$$

By taking P as in (3.2) and substituting (3.9), (3.11) and (3.13) into (3.14), the optimal Q is

$$Q = \frac{1}{K_g} \frac{(1 + \tau s)(1 + \chi s)}{(1 + T_M s)(1 + z s)} \tag{3.15}$$

with

$$\chi = z + h - \rho + T_M - \gamma \tag{3.16}$$

The equivalent unity feedback controller is given by (2.8):

$$K = \frac{1}{K_g(\rho + \gamma)} \frac{(1 + \tau s)(1 + \chi s)}{s(1 + \frac{z T_M + h\chi}{\rho + \gamma} s)} \tag{3.17}$$

The compensator in (3.17) can be cast into (3.4) in accordance with:

$$\begin{aligned} K_p &= \frac{T_i}{K_g(\rho + \gamma)} \\ T_i &= \tau + \chi - \frac{z T_M + h\chi}{\rho + \gamma} \\ \frac{T_d}{N} &= \frac{z T_M + h\chi}{\rho + \gamma} \\ N + 1 &= \frac{\tau}{T_i} \chi \frac{\rho + \gamma}{z T_M + h\chi} \end{aligned} \tag{3.18}$$

It can be seen that there are three design parameters: T_M, z and γ. The meaning of T_M and z can be easily understood by considering the choice $\gamma = T_M$. This way, γ disappears and T_d in (3.9) becomes

$$T_d = \frac{1}{1 + T_M s} \tag{3.19}$$

Accordingly, (3.8) represents now a MMP with respect to the desired input-to-output relation T_d in (3.19). Based on this particular scenario, z and T_M can be fixed to obtain smooth set-point responses (Vilanova, 2008). The role of T_M is clear: it captures the desired closed-loop bandwidth. The role of z is to provide tolerance to model uncertainty. Let us assume first that the dynamic behaviour of the plant under control is described not only by the nominal model but by a whole family of possible plants:

$$\mathcal{F} = \left\{ \tilde{P} = P(1 + \Delta_m) \right\} \tag{3.20}$$

where Δ_m is the relative (multiplicative) model error

$$\Delta_m \doteq \frac{\tilde{P} - P}{P} \tag{3.21}$$

satisfying $|\Delta_m(j\omega)| \leq |W_m(j\omega)|$ and W_m is a frequency weight bounding the modelling error. It is well-known (Skogestad and Postlethwaite, 2005; Morari and Zafiriou, 1989) that a controller K that stabilizes the nominal plant P, also stabilizes all the plants in (3.20) provided that

$$\|W_m T\|_\infty < 1 \tag{3.22}$$

From (3.2), (3.15) and the fact that $T = PQ$, the robust stability condition (3.22) can be written as

$$\left| \frac{(1 - sh)(1 + \chi_1 s)}{(1 + T_m j\omega)(1 + zj\omega)} \right| < \left| \frac{1}{W_m(j\omega)} \right| \ \forall\omega \tag{3.23}$$

where $\chi_1 = z + \tau - \rho$. Let us consider $|W_m(j\omega)| = 1$ in (3.23), giving rise to the following condition:

$$\left| \frac{(1 - sh)(1 + \chi_1 s)}{(1 + T_m j\omega)(1 + zj\omega)} \right| < 1 \ \forall\omega \tag{3.24}$$

Although this may seem conservative, mid and high frequency uncertainty will be allowed. The constraint (3.24) imposes that the closed-loop transfer function does not have *spikes* and behaves as a low pass filter. By choosing

$$T_M = \sqrt{2}h \qquad z = 2h \tag{3.25}$$

a suitable pole-zero pattern is obtained, leading to a complementary sensitivity function with the desired low-pass shape. Selecting T_M and z as in (3.25) (with $\gamma = \gamma_{sp} = T_M$) yields smooth set-point response. Nevertheless, as it was pointed out in (Vilanova, 2008), this design can lead to poor disturbance rejection. Improving the disturbance rejection is precisely the role of the γ parameter.

In (Vilanova and Arrieta, 2007) it is shown that by choosing $\gamma > T_M = \sqrt{2}h$, the disturbance attenuation can be improved. However, the analysis in (Vilanova and Arrieta, 2007) only takes into account disturbances entering at the output of the plant, remaining open how to select γ if the disturbance enters at the input. Another missing aspect is the stability analysis. These points are the subject matter of the next subsection.

Remark 3.3.1. *In what follows, z and T_M will remain fixed as indicated in (3.25). Therefore, the tuning rule (3.18) depends on a single tuning parameter: γ. As it will be illustrated in the next subsection, $\gamma = \gamma_{sp} = \sqrt{2}h$ corresponds to the servo operation. From this point on, increasing the value of γ allows improvement of the regulatory performance. In this sense, (3.18) can be considered as a (robust) unified servo/regulator tuning rule.*

3.4 Trade-off tuning interval for γ considering load disturbances

First, we will review how to select γ for optimal step disturbance rejection at the output of the plant. Assuming that $P = \tilde{P}$ in Figure 2.1, we have that $y = (1 - PQ)d_o$. Taking $d_o = \frac{1}{s}$, P as in (3.2) and Q from (3.15) finally gives

$$y = S\frac{1}{s} \approx \left(1 - \frac{(1 - sh)(1 + \left(\sqrt{2}h + 0.24\gamma\right)s)}{(1 + \sqrt{2}hs)(1 + 2hs)}\right)\frac{1}{s} \tag{3.26}$$

We can choose γ according to the Integral Squared Error, defined as

$$ISE \doteq \int_0^\infty (r(t) - y(t))^2 \, dt \tag{3.27}$$

As we are concerned with the output disturbance rejection, we can assume that the reference is zero ($r(t) = 0$), which leads to

$$ISE(\gamma, h) = \int_0^\infty y^2(t)dt = \|y\|_2^2 \tag{3.28}$$

By applying the Parseval's theorem (Morari and Zafiriou, 1989), this calculation can be rewritten as

$$ISE(\gamma, h) = \frac{1}{2\pi} \int_{-\infty}^{\infty} y(j\omega)y(-j\omega)d\omega = \frac{1}{2\pi j} \oint y(s)y(-s)ds \tag{3.29}$$

Application of the residue theorem (Churchill and Brown, 1986) to solve (3.29) yields

$$ISE(\gamma, h) \approx 2.25h - 0.1065\gamma + \frac{0.0112}{h}\gamma^2 \tag{3.30}$$

By taking the derivative with respect to γ we can obtain the optimal value that minimizes the ISE criterion

$$\frac{\partial ISE(\gamma, h)}{\partial \gamma} = 0 \Rightarrow \gamma_{ldo} \approx 4.56h \tag{3.31}$$

In (Vilanova and Arrieta, 2007) it was shown that if the disturbance occurs at the input of the plant, the disturbance rejection produced by taking γ as in (3.31) may still be improved significantly, but the exact tuning was not given. In what follows, we will address how to choose γ for disturbances at the input of the plant. In this situation, the disturbance to output relation is

$$y = PSd_i \tag{3.32}$$

Instead of optimizing the ISE criterion as before, a more *heuristic* approach is taken. In the *lag-dominant* case, it is evident that a sluggish response will be obtained unless S cancels the slow dynamic of P. In fact, the impossibility of producing such a cancellation is the reason why the IMC-like design in (Ali and Majhi, 2009) cannot be used for regulator purposes. Thus, it would be necessary for good input disturbance attenuation that

$$S|_{s=-\frac{1}{\tau}} = 0 \tag{3.33}$$

Taking S as in (3.26), the following value for γ is finally obtained

$$\gamma_{ldi} \approx -\frac{12.36h(-\tau + \sqrt{2}h)}{h + \tau} \tag{3.34}$$

It is clear that γ_{ldi} in (3.34) can be regarded as a function of just $\frac{\tau}{h}$. Provided that $\tau \geq 3h$, the following chain of inequalities holds

$$\gamma_{sp} = \sqrt{2}h < \gamma_{ldo} \approx 4.56h < \gamma_{ldi} \tag{3.35}$$

For example, if $\frac{\tau}{h} = 10$, $\gamma_{ldi} \approx 9.65h$. We will assume from this point on that disturbances enter at the input of the plant. Thus, we will tune γ as in (3.34) for the regulator mode. Consequently, we are finally considering the following interval for the γ parameter:

$$\gamma \in [\gamma_{sp} = \sqrt{2}h, \gamma_{ld} = \gamma_{ldi}] \tag{3.36}$$

where the extremes represent the tuning for servo ($\gamma = \gamma_{sp}$) and regulator ($\gamma = \gamma_{ld}$) operation.

3.4.1 Nominal stability

Since we have considered the approximation (3.2) for the FOPTD model, the basic requirement of nominal stability is not guaranteed for a FOPTD plant even when all its parameters are perfectly known. The nominal stability issue is dealt with here by means of the Dual Locus technique along the lines of (Zhong, 2003). Taking the unity feedback controller from (3.17) together with the model (3.1) results in the following loop transfer function

$$L \approx \frac{1 + \left(\sqrt{2}h + 0.24\gamma\right) s}{\left(3h - 0.24\gamma\right) s + \left(3\sqrt{2}h^2 + 0.24h\gamma\right) s^2} e^{-sh} \tag{3.37}$$

The characteristic equation $1 + L = 0$ can then be rewritten in the form

$$L_1 - L_2 = 0 \tag{3.38}$$

by making the following assignments:

$$L_1 = -\frac{\left(3h - 0.24\gamma\right) s + \left(3\sqrt{2}h^2 + 0.24h\gamma\right) s^2}{1 + \left(\sqrt{2}h + 0.24\gamma\right) s} \qquad L_2 = e^{-sh}$$

The Dual Locus diagram technique states that the closed-loop system is stable if the Nyquist locus of L_1 reaches the intersection point with the locus of L_2 before L_2 does so. In this situation, the number of encirclements of $L_1 - L_2$ around the origin when traversing the Nyquist contour[1] is zero. Thus, by the Argument Principle (Churchill and Brown, 1986), there is no RHP pole in the closed-loop system. The idea is illustrated for a particular case in Figure 3.2. The phase angles of L_1 and L_2 at ω_c (the intersection frequency) are,

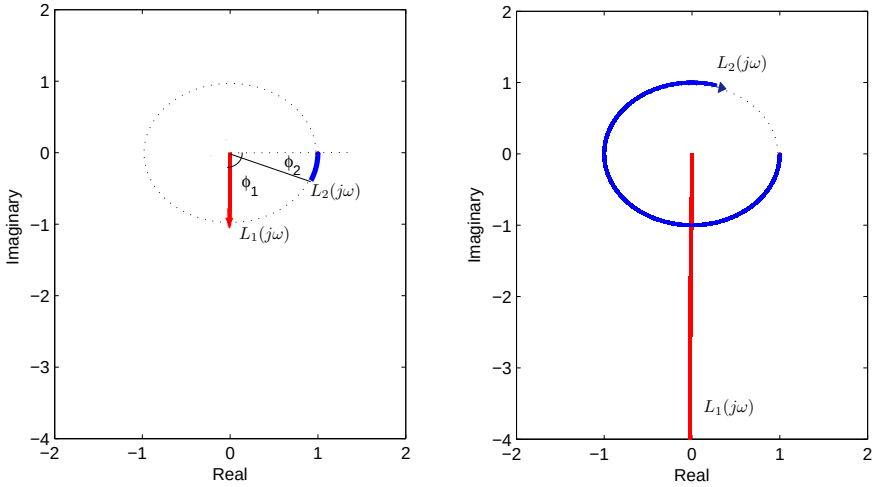

(a) $0 < \omega(\text{rad/s}) \leq 0.4$ (b) $0 < \omega(\text{rad/s}) \leq 5$

Figure 3.2: Dual locus diagram (restricted to the positive imaginary axis only) for $h = 1$,$\gamma = \sqrt{2}$. The closed-loop is stable because $\phi_1 - \phi_2 < 0$ at the intersection frequency ω_c, approximately 0.4 rad/s.

respectively:

$$\phi_1 = \arctan \frac{-3h + 0.24\gamma}{\left(3\sqrt{2}h^2 + 0.24h\gamma\right)\omega_c} - \arctan\left(\sqrt{2}h + 0.24\gamma\right)\omega_c \qquad (3.39)$$

[1] In our case, L has a pole at the origin and the conventional Nyquist contour must be modified to avoid passing through the point $0 + j0$ when traversing the imaginary axis. One way to do it is to construct a semicircular arc with infinitely small radius r around $0 + j0$, that starts at $0+j(0-r)$ and travels anticlockwise to $0+j(0+r)$. For our purposes, however, it is enough to consider the Nyquist contour on the positive imaginary axis.

and

$$\phi_2 = -h\omega_c \tag{3.40}$$

The stability condition is satisfied only when the phase angle of L_1 is larger (in absolute value) than that of L_2, i.e., if $\phi_1 - \phi_2 < 0$ (see Figure 3.2). Since $|L_2(j\omega)| = 1$, the intersection frequency can be determined from

$$\left| -\frac{(3h - 0.24\gamma)\, s + \left(3\sqrt{2}h^2 + 0.24h\gamma\right) s^2}{1 + \left(\sqrt{2}h + 0.24\gamma\right) s} \right|_{s=j\omega_c} = 1 \tag{3.41}$$

Solving (3.41) leads to

$$\omega_c = \frac{1}{h\left(6 + 0.24\sqrt{2}\eta\right)} \sqrt{-(B^2 - C^2)^2 + \sqrt{(B^2 - C^2)^2 + 4A^2}} \tag{3.42}$$

where

$$\begin{aligned} A &= 3\sqrt{2} + 0.24\eta \\ B &= 3 - 0.24\eta \\ C &= \sqrt{2} + 0.24\eta \end{aligned} \tag{3.43}$$

and $\eta \doteq \frac{\gamma}{h}$. It can be seen from (3.42) and (3.43) that $\omega_c h$ can be expressed as a function of $\frac{\gamma}{h}$. From (3.39) and (3.40), this in turn shows that $\phi_1 - \phi_2$ depends solely on $\frac{\gamma}{h}$. As we are considering the interval in (3.36), then $\frac{\gamma}{h} \in [\sqrt{2}, \frac{12.36(\tau/h - \sqrt{2})}{1+\tau/h}]$. The maximal interval corresponds to the situation in which $\tau/h \to \infty$, which yields $\sqrt{2} \leq \frac{\gamma}{h} < 12.36$. In Figure 3.3, $\phi_1 - \phi_2$ is plotted against $\frac{\gamma}{h}$. It can be concluded that the closed-loop system remains stable within the considered maximal interval. Hence, the nominal stability is always guaranteed.

So far, we have verified that the control system is stable with respect to the FOPTD model. Sometimes, however, the available model of the plant does not correspond to a FOPTD process. In these cases, we adopt a simple FOPTD model for the sake of simplicity: a low-order model will yield a low-order controller. Consequently, in theses cases, the nominal stability must consider the mismatch between the approximate FOPTD model (3.2) and the one precisely describing the dynamics of the real process. If we assume that the real plant $\tilde{P}$ is perfectly known, we can take Δ_m as in (3.21) and use the

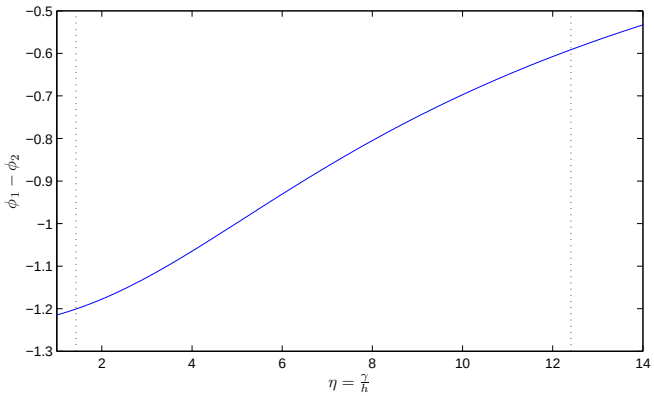

Figure 3.3: The closed-loop is stable because $(\phi_1 - \phi_2)(\eta) < 0$.

robust stability condition (3.22) for nominal stability purposes. As in this specific case we are considering that Δ_m is perfectly known (we know both $\tilde{P}$ and P) we can apply (3.22) taking $W_m = \Delta_m$ and restricted to the phase crossover frequency only:

$$|T(j\omega_{180})\Delta_m(j\omega_{180})| < 1 \tag{3.44}$$

where ω_{180} verifies

$$\angle\left(T(j\omega_{180})\Delta(j\omega_{180})\right) = -180^\circ \tag{3.45}$$

This can be readily understood by looking at Figure 3.4: the first feedback loop is stable if and only if the second one is stable. As $T\Delta = PQ\frac{\tilde{P}-P}{P} = Q(\tilde{P}-P)$ is stable (we are considering stable plants), condition (3.44) coincides with the Nyquist stability criterion (Skogestad and Postlethwaite, 2005) when $\angle(T(j\omega)\Delta(j\omega))$ crosses -180° only once. If it crosses -180° several times (this would seldom happen in practice), then (3.44) must account for all the phase crossover frequencies and becomes only a sufficient condition.

In the next subsection, guidelines for the tuning of γ are given. In particular, robustness is captured in terms of the peak on the sensitivity function.

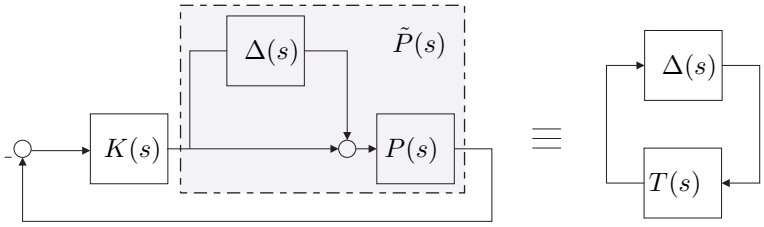

Figure 3.4: Equivalent Stability Loops.

3.5 Quantitative guidelines for the tuning of γ

In classical control theory, the performance of a control system is usually characterized in terms of the transient and steady-state time domain responses. Well-known time domain performance indicators are, among others, the overshoot and the settling time. On the other hand, the classical frequency domain approach provides typical robustness indexes as for example the GM (Gain Margin), the PM (Phase Margin) or the peak on the sensitivity function (M_S). These and other common standard measures usually capture the design specifications in practical designs and have something in common: they all depend only on the finally achieved loop function $L \doteq PK$.

This section is aimed at showing that the optimization procedure used to derive the presented controller can be ultimately put in connection with the classical robustness/performance indicators. For the sake of space limitations, only the overshoot and the M_S specifications will be considered, for which the following qualitative facts hold:

- The greater the value of γ, the greater the overshoot. This point is important because some plants have a strict limitation on the overshoot.
- Augmenting γ also reduces the stability margins, i.e., augments M_S. Recall that M_S, defined as

$$M_S \doteq \|S(j\omega)\|_\infty \doteq \max_\omega \left| \frac{1}{1+L(j\omega)} \right|,$$

  corresponds to the inverse of the shortest distance from the Nyquist plot to the critical point. This constitutes a more reliable robustness indicator than the popular Gain and Phase Margins. This is because a

control system with good Gain and Phase Margins can be very close to instability. On the contrary, it can be seen (Skogestad and Postlethwaite, 2005) that

$$GM \geq \frac{M_S}{M_S - 1} \qquad PM \geq 2 \arcsin\left(\frac{1}{2M_S}\right)$$

From (3.37), it is easily observed that L depends solely on h and γ in the nominal case. This means that the classical measures depending on L can be finally expressed as functions of the variables h and γ. Moreover, by applying the Buckingham Pi Theorem (Balaguer *et al.*, 2009) from Dimensional Analysis, both the overshoot and M_S can be expressed in terms of the single dimensionless relation γ/h. This result has several implications:

- First, it shows that the single parameter γ allows a quantitative tuning of the classical indicators.
- Second, it shows that it is not necessary to calculate explicitly the corresponding measures of interest (overshoot, M_S, etc) since the exact graphs of the corresponding (general) functions can be obtained through a single simulation experiment.

Figure 3.5 depicts the nominal overshoot and M_S as functions of γ/h. In order to facilitate the usage of this information for design purposes, the following linear approximations (valid in the range $\gamma \geq 5h$) have been obtained

$$M_S = 0.06913\frac{\gamma}{h} + 1.254 \tag{3.46}$$

$$\text{Overshoot } (\%) = 5.521\frac{\gamma}{h} - 19.13 \tag{3.47}$$

It is also useful to have an idea of how uncertainty degrades performance. More concretely, next we analyze the effect of parametric uncertainty on the overshoot. Let us consider a certain amount (δ) of simultaneous uncertainty on each parameter of the FOPTD model. The worst case for this uncertainty profile is given by

$$\tilde{P} = K_g(1+\delta)\frac{e^{-s(1+\delta)h}}{(1-\delta)\tau s + 1} \tag{3.48}$$

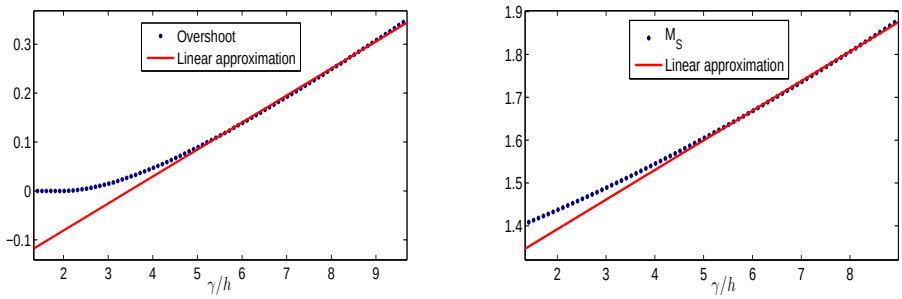

(a) Overshoot (b) M_S

Figure 3.5: Overshoot and M_S vs $\frac{\gamma}{h}$.

Thus, fixing δ is possible to determine the worst case overshoot as a function of $\frac{\gamma}{h}$. Figure 3.6 does so for different values of δ whereas Table 3.1 provides simple linear approximations.

Remark 3.5.1. *It is worth noting (see Figure 3.5(b)) that robustness decreases as we get closer to the regulator mode. The cancellation (3.33) (in conjunction with the waterbed effect (Skogestad and Postlethwaite, 2005)) increases the peak on S. This can be regarded as an inherent feature of a regulator-type tuning. In Figure 3.7 this point has been exemplified.*

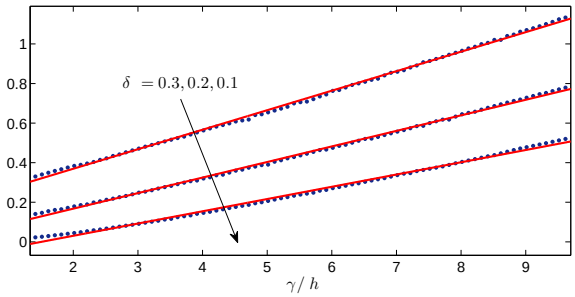

Figure 3.6: Maximum overshoots for different levels of parametric uncertainty with respect to the FOPTD model.

Table 3.1: Worst case (approximate) overshoots for different levels of parametric uncertainty.

uncertainty	worst case overshoot
$\delta = 0.1$	$6.2\gamma/h - 9.33$
$\delta = 0.2$	$7.86\gamma/h + 1.05$
$\delta = 0.3$	$9.86\gamma/h + 17.22$

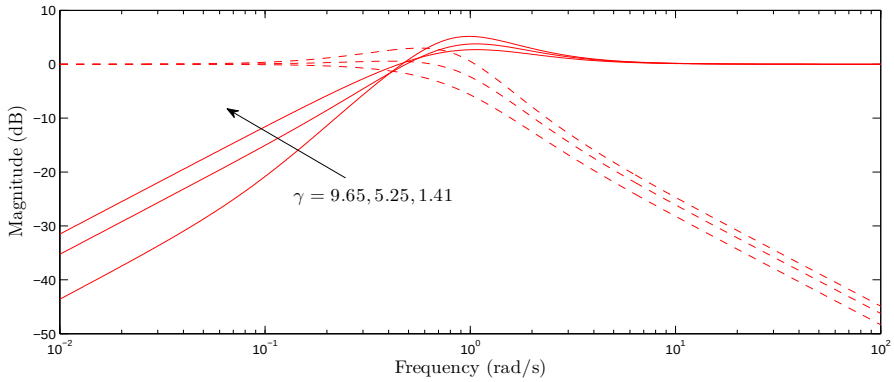

Figure 3.7: Shapes of the sensitivity (solid) and complementary (dash) sensitivity functions for $P = \frac{e^{-s}}{10s+1}$ and different tunings of γ. When $\gamma = \gamma_{ld} = 9.65$, condition (3.33) pushes up the peak of the sensitivity function.

3.6 Simulation examples

This section illustrates the presented method by considering two simulation examples.

3.6.1 Example 1

First, this example shows how the tuning of γ can be done quantitatively in terms of prescribed levels for the maximum overshoot. Second, it stresses the main feature of the suggested γ-tuning procedure: smooth control with adjustable operation mode. The following model will be used

$$P = \frac{e^{-0.073s}}{1 + 1.073s} \tag{3.49}$$

It will be assumed that the real plant consists of a FOPTD process. However, 20% of parametric uncertainty with respect to the model in (3.49) will be considered. Consequently, the worst case real plant is given by

$$P_1 = \frac{1.2e^{-0.0876s}}{1 + 0.858s} \tag{3.50}$$

The following controller specifications are given:

- Obtain the best possible load disturbance attenuation ensuring that the overshoot does not exceed 50%.

From (3.34), the best load disturbance attenuation is achieved for $\gamma = 0.764$. However, this tuning would lead to a high overshoot even in the nominal response. In fact, from (3.47) the nominal overshoot is approximately 40%. On the contrary, the worst load disturbance attenuation is given by $\gamma = 0.1032$, which leads to low overshoots. The value of γ satisfying the given requirement can be easily obtained from Table 3.1 (case $\delta = 0.2$). The exact value turns out to be $\gamma = 0.4036$. Figure 3.8 shows the time responses associated with the nominal model P. The responses for the case with 20% of parametric uncertainty can be seen in Figure 3.9. It is readily seen how the best possible disturbance rejection has been obtained while keeping the worst case overshoot below the prescribed value. It should be noted that in the case of the plant not being a FOPTD process, the quantitative formulae derived in this work are

not exact. In this case, the important point is that the general methodology continues to be valid as long as the plant can be adjusted well by a FOPTD model.

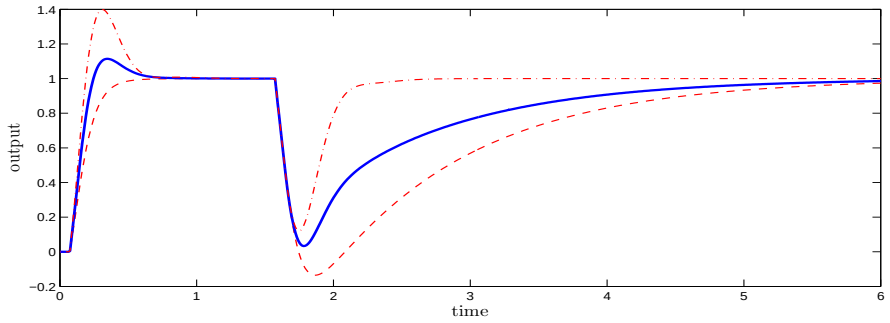

Figure 3.8: Nominal time responses for $\gamma = 0.1032$ (dash), $\gamma = 0.4036$ (solid) and $\gamma = 0.764$ (dash-dot).

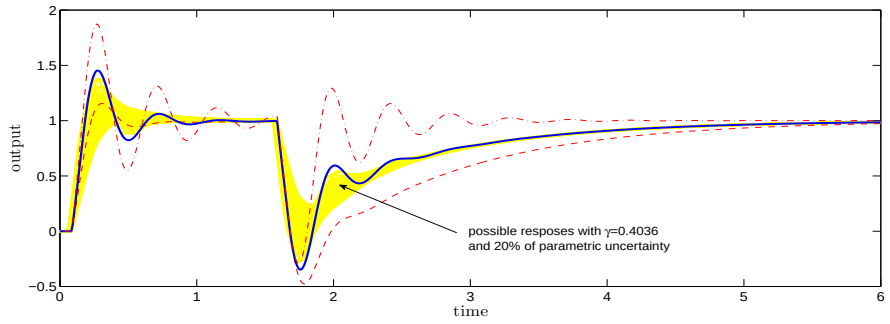

Figure 3.9: Worst case time responses in presence of 20% of parametric uncertainty with respect to P for $\gamma = 0.1032$ (dash), $\gamma = 0.4036$ (solid) and $\gamma = 0.764$ (dash-dot).

In (Skogestad, 2006), it is claimed that smooth control is probably the most common objective in industrial practice, where very high performance is not the main concern. Despite this, almost all published PID tuning rules aim at high performance (Skogestad, 2006). Even in direct synthesis approaches like IMC, which have the closed loop time constant λ as a tuning parame-

ter, the emphasis is to obtain a lower bound on λ (tight control). To clarify these points, we will consider the ISE-optimal tuning rules obtained numerically in (Zhuang and Atherton, 1993) for setpoint tracking and disturbance attenuation. In Figure 3.10, the responses associated with these rules and the proposed approach are compared. The tuning rules given in (Zhuang and Atherton, 1993) do not specify a value for N in (3.3); for the simulations, the value $N = 20$ has been used[2]. As it can be seen, the responses for the method in (Zhuang and Atherton, 1993) are extremely aggressive, resulting into poor robustness. It has been found that $M_S = 2.65$ for the set-point tuning, whereas $M_S = 21.22$ (!) for the regulatory tuning, indicating that no robustness consideration was taken into account. In contrast with these negative indicators, the proposed approach yields $M_S = 1.41$ ($\gamma = T_M = 0.1032$) and $M_S = 1.98$ ($\gamma = 0.755 \approx \gamma_{ld}$), adhering to the rule of thumb $M_S < 2$ for good robustness (Skogestad and Postlethwaite, 2005). The smoothness of the control action is also evident, and the performance level acceptable.

The IMC-based tuning in (Ali and Majhi, 2009) has also been evaluated in the load disturbance column of Figure 3.10. Following the work in (Ali and Majhi, 2009), we have adjusted the value of λ to obtain tight control, i.e., the best possible disturbance attenuation with acceptable robustness ($M_S < 2$). Taking $\lambda = 0.0321$ yields $M_S = 1.98$. For smaller values of λ, the robustness margins decrease. Therefore, the γ-tuning strategy allows to obtain considerably better regulatory performance with the same robustness level, only at the expense of a modest increment in the control effort.

3.6.2 Example 2

The aim of this example is twofold: on the one hand, it illustrates that the proposed general methodology continues to be valid when the plant is not a FOPTD system. On the other hand, it shows that the presented approach gives good results, in terms of smooth responses, when compared with a well-known tuning rule suggested in the literature. Let us consider the isothermal series/paralel Van de Vusse reaction (de Vusse, 1964) taking place in an isothermal continuous stirred tank reactor (CSTR). The rates of formation of A and B are assumed to be:

[2]It can be seen that $N = 10$, a more common value, yields even worse results.

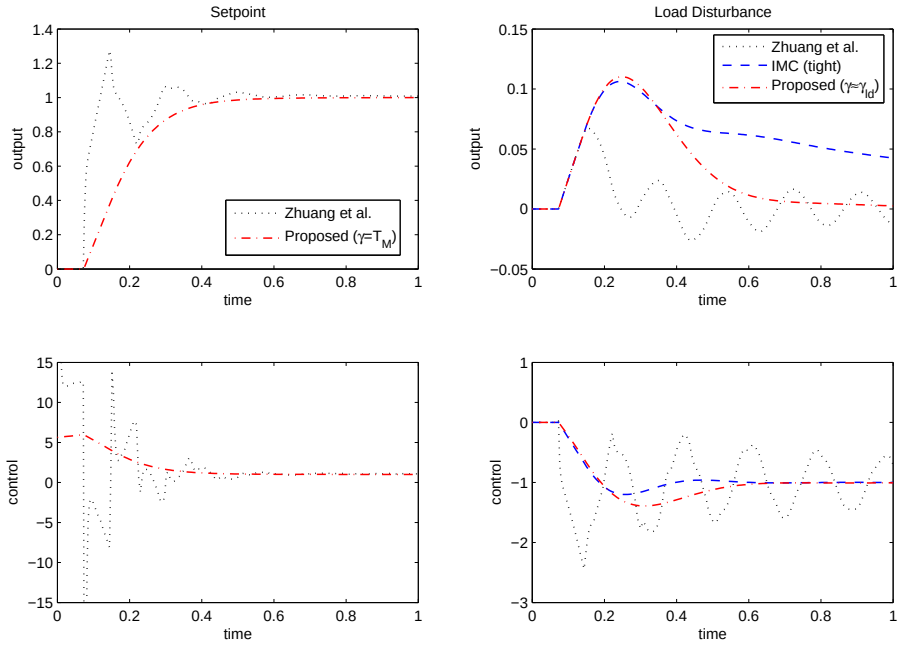

Figure 3.10: Setpoint and load disturbance responses.

$$\begin{aligned} r_A &= -k_1 c_A - k_3 c_A^2 \\ r_B &= k_1 c_A - k_2 c_A \end{aligned}$$

where $k_1 = 50h^{-1}$, $k_2 = 100h^{-1}$ and $k_3 = 10\ l(\text{gmol} \cdot h)^{-1}$ are the reaction rate constants. The feed steam consists of pure A. The mass balance for A and B is given by

$$\begin{aligned} V\frac{dc_A}{dt} &= F(c_{A_0} - c_A) + V(-k_1 c_A - k_3 c_A^2) \\ V\frac{dc_B}{dt} &= F(-c_B) + V(k_1 c_A - k_2 c_A) \end{aligned}$$

where F is the inlet flow rate of product A, V is the reactor volume which is kept constant during the operation, c_A and c_B are the concentrations of the

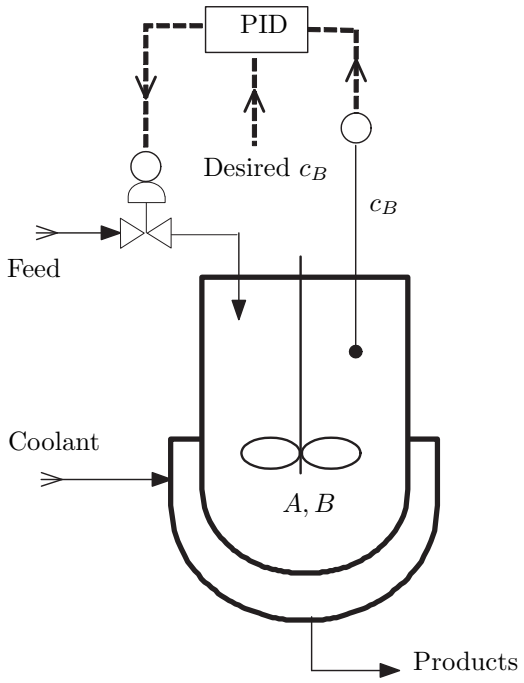

Figure 3.11: CSTR control system.

species A and B inside the reactor, respectively, and $c_{A_0} = 10$ gmol$\cdot l^{-1}$ is the concentration of A in the feed steam. We wish to maintain c_B at its set-point using the dilution rate F/V as the manipulated variable. Figure 3.11 depicts the CSTR control system under consideration. The system can be put in the standard form

$$\begin{aligned} \dot{x}_1 &= -k_1 x_1 - k_3 x_1^2 + (c_{A_0} - x_1)u \\ \dot{x}_2 &= k_1 x_1 - k_2 x_2 - x_2 u \\ y &= x_2 \end{aligned}$$

where $x_1 = c_A, x_2 = c_B, u = F/V, y = c_B$. Initially the system is at steady state with $x_1 = 2, x_2 = 0.851$. For control purposes, the non-linear system is approximated at the initial steady state by a FOPTD model with $K_g = 0.033, \tau = 0.02, h = 0.005$. Figure 3.12 shows the responses of the non-linear (real) system and the linear (FOPTD) approximation. Now we will turn our

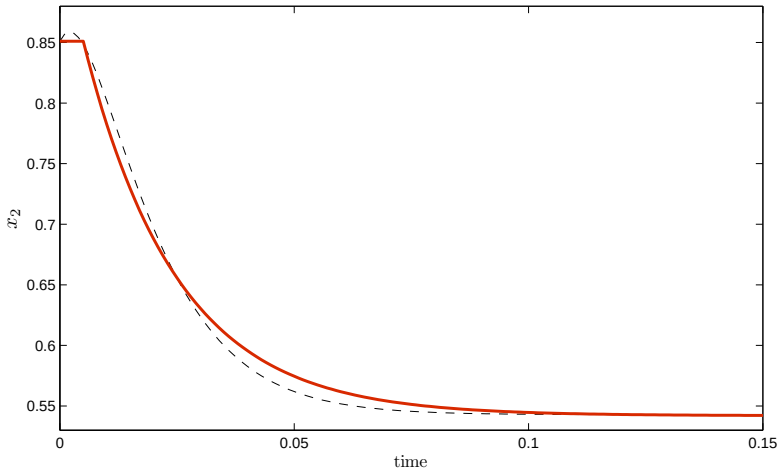

Figure 3.12: Real non-linear system (dashed) and FOPTD (solid) approximation.

attention to the control of the described plant. For comparison purposes, we will include the well-known AMIGO tuning rule in the simulations. As it is explained in (Astrom and Hagglund, 2004), the AMIGO tuning rule for the ISA PID controller was obtained to yield good disturbance attenuation along the lines the classical Ziegler-Nichols method, but with improved robustness.

In order to evaluate the performance obtained with the two methods at hand, the following standard measures will be used:

- *Output performance*: The Integrated Absolute Error (IAE) of the error $e = r - y$ will be computed.

  $$\text{IAE} = \int_0^\infty |e(t)|dt$$

- *Input performance*: To evaluate the manipulated input usage, the total variation (TV) of the control signal $u(t)$ will be computed.

  $$\text{TV} = \int_0^\infty |\dot{u}(t)|dt$$

In addition, the percent overshoot of the output $y(t)$, denoted by y_{ov}, will be taken into account for set-point output performance. The results obtained are depicted in Figure 3.13 and summarized in Table 3.2.

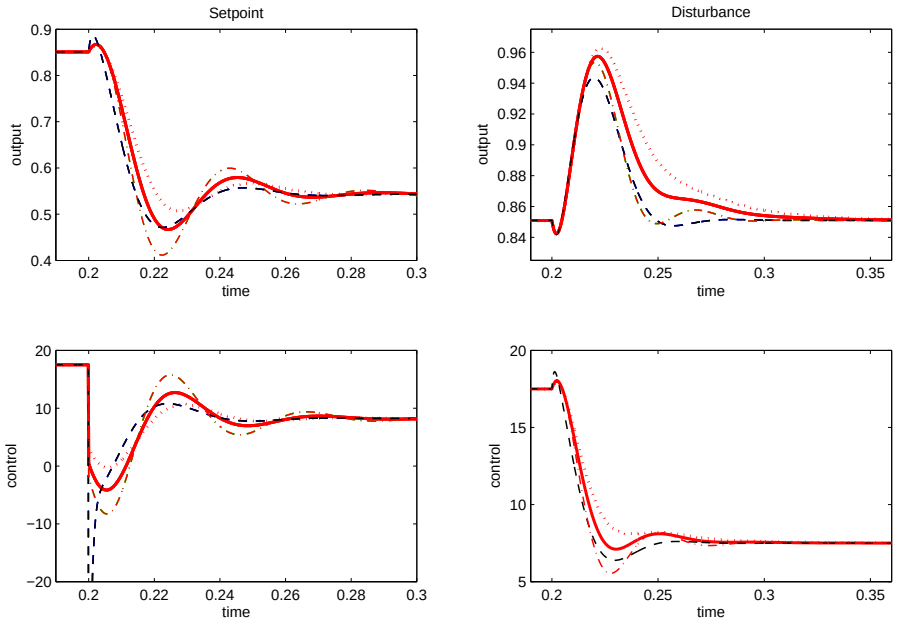

Figure 3.13: Time responses for the proposed: $\gamma = 0.0071 = T_M$ (dot), $\gamma = 0.032 = \gamma_{ld}$ (dash-dot), $\gamma = 0.0195$ (bold solid), and AMIGO (dashed) tuning rules.

It can be seen that the AMIGO tuning provides better results in general, the reason for this superior performance relies on the numerical, non-convex optimization approach on which it is based. However, it requires a more aggressive control effort in the set-point response. Overall, it can be observed that the proposed tuning yields smooth control, while allowing for an easy adjustment of the operation mode of the controller.

Table 3.2: Results for set-point and load disturbance.

	SP			LD	
Tuning method	IAE	y_{ov}	TV	IAE	TV
Proposed ($\gamma = 0.0071$)	0.048	7.02%	32.28	0.0044	11
Proposed ($\gamma = 0.032$)	0.060	31.85%	66.8	0.0024	16.96
Proposed ($\gamma = 0.0195$)	0.0051	16.23%	46.7	0.0034	13.03
AMIGO	0.0041	15.15%	158.86	0.0023	14.7

3.7 Summary

A model matching analytical approach to PID design assuming a FOPTD model for the plant has been presented and quantitatively analyzed. The studied method leads to a γ-tuning procedure in which the γ parameter is selected according to the desired operating mode for the PID controller. The servo and the regulator behaviours can be regarded as the extreme points of a curve, parameterized by γ, in the PID parameters space. If an intermediate value for γ is chosen, then a trade-off tuning is reached. Finally, quantitative tuning guidelines for γ in terms of popular robustness/performance indexes have been given, and simulation examples have confirmed the obtention of smooth responses with acceptable performance.

Chapter 4

λ-tuning versus γ-tuning

Based on (Alcántara et al.*, 2010*a*)*

Chapter 2 presented a simple (IMC-like) analytical design based on a weighted sensitivity problem (WSP). The tuning of the controller involved a single tuning parameter (λ), closely related to the closed-loop bandwidth. It was shown in Section 2.6 that, for lag-dominant processes, the disturbance attenuation was sluggish. On the other hand, Chapter 3 revised a model matching strategy for improving the load disturbance response. More concretely, a tuning parameter (γ) was used to account for a servo/regulator balance. This chapter compares the λ and γ-tuning methods from a servo/regulator point of view. Simulation examples clarify the discussion and confirm the effectiveness (and the limits) of each approach.

4.1 Introduction

The design revised in Chapter 3 conducted to the controller

$$K = \frac{1}{K_g(\rho+\gamma)} \frac{(1+\tau s)(1+\chi s)}{s(1+\frac{zT_M+h\chi}{\rho+\gamma}s)} \tag{4.1}$$

where K_g, τ, h constitute the FOPTD model information, $\chi = z+h-\rho+T_M-\gamma$ and z, T_M were fixed in (3.25). It was shown in Section 3.4 that if one considers disturbances entering at the output of the plant, choosing $\gamma = \gamma_o = 4.56h$

provides the best disturbance attenuation with respect to the ISE criterion. In addition, it was shown that if the disturbance occurs at the input of the plant, the disturbance rejection produced by taking $\gamma = \gamma_o = 4.56h$ may still be improved significantly. At the end, the following interval for γ was found

$$\gamma \in [\gamma_{sp} = \sqrt{2}h, \gamma_{ld}] \tag{4.2}$$

where

$$\gamma_{ld} \approx -\frac{12.36h(-\tau + \sqrt{2}h)}{h + \tau} \tag{4.3}$$

and extreme values for γ represent the tuning for *servo* ($\gamma = \gamma_{sp}$) and *regulator* ($\gamma = \gamma_{ld}$) operation. In general, the greater the value of γ, the greater the overshoot in the set-point response and the smaller the stability margins.

From the point of view of balanced servo/regulation operation, this chapter compares the control settings discussed in Chapter 3 (Alcántara *et al.*, 2010*b*) through the γ-tuning procedure with those obtained using the simpler IMC-like design of Chapter 2 (Alcántara *et al.*, 2010*c*). Within the latter method, the tuning parameter λ provides a means to adjust the *robustness/performance* trade-off. In this situation, we can distinguish between two tuning strategies (Skogestad, 2006; Ali and Majhi, 2009):

- *Smooth* control, which corresponds to the slowest possible control with acceptable disturbance rejection. In Chapter 2 (Alcántara *et al.*, 2010*c*), the value $\lambda = h$ was selected for smooth control, yielding $M_S \approx 1.42$.
- *Tight* control, which obeys the fastest possible control with acceptable robustness. This option implies a reduction in the value of λ which can be used to improve the regulatory performance.

How to tune λ for tight control is addressed in this chapter. Afterwards, a compromise between smooth and tight control is determined, corresponding to an intermediate value for λ.

The organization of this chapter is as follows. Section 4.2 proposes a tuning interval for λ, and suggests a value for balanced smooth/tight control. Section 4.3 is devoted to compare, from a servo/regulation point of view, the λ and γ-tuning approaches. Section 4.4 deals with some implementation aspects, whereas simulation examples are given in Section 4.5. Lastly, Section 4.6 summarizes the main ideas and draws some final conclusions.

4.2 *Smooth/Tight* interval for λ

Based on a FOPTD model, the controller obtained in Chapter 2 is given by

$$K = \frac{1}{K_g} \frac{(\frac{h}{2}s + 1)(\tau s + 1)}{s(\lambda^2 s + 2\lambda + \frac{h}{2})} \tag{4.4}$$

and depends on a single tuning parameter: λ. As in the standard IMC procedure (Morari and Zafiriou, 1989), the role of λ is to provide the necessary roll-off at high frequencies. First, let us consider the following question: How to choose λ for optimal load disturbance? We know from Chapter 2 that the optimal behaviour is recovered for $\lambda \to 0$. However, this would imply no robustness according to the detuning role of λ. It is easy to see (consult the Appendix 4A) that the value $\lambda \approx 0.22h$ provides the best disturbance rejection with respect to disturbances entering at the output of the plant and the ISE criterion. However, the corresponding robustness for $\lambda \approx 0.22h$ is poor. As it is shown in the Appendix 4A, augmenting λ increases the value of the ISE also for disturbances entering at the input. Consequently, according to the *tight* control concept, the idea is to select the smallest possible value (and consequently, the best possible load disturbance rejection) for λ providing acceptable robustness. Stated otherwise, since the IMC-like approach cannot produce the cancellation in (3.33), the best that it can be done to improve the load disturbance attenuation is making the closed-loop system faster. Sensitivity to modelling errors can be captured by the peak of the sensitivity function:

$$M_S \doteq \|S(j\omega)\|_\infty \doteq \max_\omega \left| \frac{1}{1 + L(j\omega)} \right| \tag{4.5}$$

By applying the Buckingham Pi Theorem (Balaguer *et al.*, 2009) from Dimensional Analysis, M_S can be determined in terms of a unique dimensionless parameter: λ/h. In concrete, $\lambda = 0.56h$ provides $M_S \approx 1.75$. We will consider this value of λ for *tight* control.

On the other hand, we saw in Chapter 2 (Alcántara *et al.*, 2010*c*) that by choosing $\lambda = h$, point on which $M_S \approx 1.42$, smooth set-point responses are obtained. The conclusion of the above analysis is that the interval to be considered for the *smooth/tight* trade-off is

$$\lambda = [\lambda_{ld} = 0.56h, \lambda_{sp} = h] \tag{4.6}$$

where the extreme values represent the *tight* ($\lambda = 0.56h$) and *smooth* ($\lambda = h$) tunings for the proposed controller.

Now, we will inspect when the λ-tuning approach is suitable to provide balanced *servo/regulator* operation, comparing it with the γ-tuning procedure. The first issue is how to adjust the value of λ, as Figure 4.1 illustrates. Let us

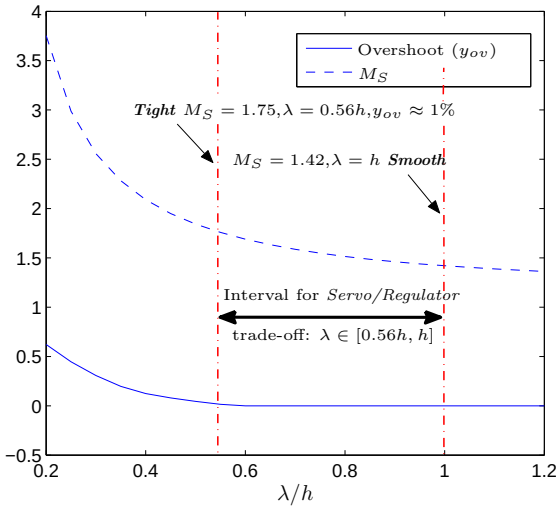

Figure 4.1: Sensitivity peak (M_S) and output overshoot against λ/h. *Smooth* & *Tight* control mode tuning.

define

$$\Delta(ISE)(\lambda/h) = \frac{ISE(\lambda/h, 1) - ISE(0.56, 1)}{ISE(0.56, 1)} \tag{4.7}$$

and

$$\Delta(M_S)(\lambda/h) = \frac{M_S(\lambda/h) - 1.42}{1.42} \tag{4.8}$$

as measures of the relative load disturbance performance and robustness degradation with respect to the corresponding optimal values. The ISE degradation index captures how the ISE due to a disturbance degrades with λ/h (consult the Appendix 4A for the details). In the case of load disturbance peformance, the minimum value is obtained for $\lambda = 0.56h$. As for the minimum value of M_S, it corresponds to 1.42. Now, it stands to reason to determine the trade-off

tuning λ value as

$$(\lambda/h)_{\text{trade-off}} = \arg\min_{\lambda/h} \max\{\Delta(ISE), \Delta(M_S)\} \tag{4.9}$$

Figure 4.2 displays the situation graphically. The trade-off value for λ is finally found to be $\lambda = 0.7h$. This value can be taken as a good rule of thumb as it will be seen later on.

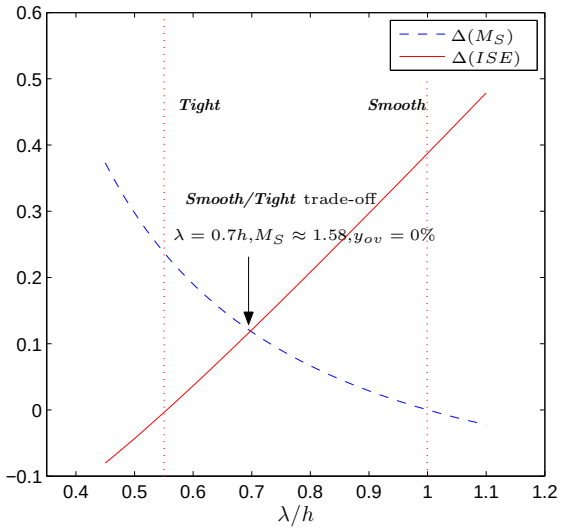

Figure 4.2: *Smooth/Tight* trade-off tuning. Normalized M_S and ISE degradations against λ/h.

In the next subsection, we explore in more depth the applicability of the suggested λ-tuning, comparing it with the γ-tuning strategy of Chapter 3.

4.3 Comparison of the λ and γ-tuning approaches

The λ-tuning strategy yields good set-point and disturbance responses when disturbances enter at the output of the plant. However, for lag-dominant plants, it provides sluggish (load) disturbance response. This way, in this comparison we will focus on load disturbance rejection capabilities. Let us

define the load disturbance performance degradation with respect to the γ-tuning method as follows

$$\Delta_{LD} = \frac{ISE(LD)_{\lambda-tuning} - ISE(LD)_{\gamma-tuning}}{ISE(LD)_{\gamma-tuning}} \tag{4.10}$$

Based on Dimensional Analysis (Balaguer *et al.*, 2009), it can be seen that Δ_{LD} only depends on $\frac{h}{\tau}$ once the values for λ and γ have been fixed. Remember that we are interested in obtaining a compromise between the servo and the regulator modes. In order to establish a comparison framework, let us assume that the maximum nominal overshoot is 10%. For a lag-dominant plant, it can be seen that this specification is met for $\gamma \leq 5.25h$. Figure 4.3 displays Δ_{LD} for $\gamma = 5.25h$ and $\lambda = 0.7h$. It can be observed that the λ-tuning provides

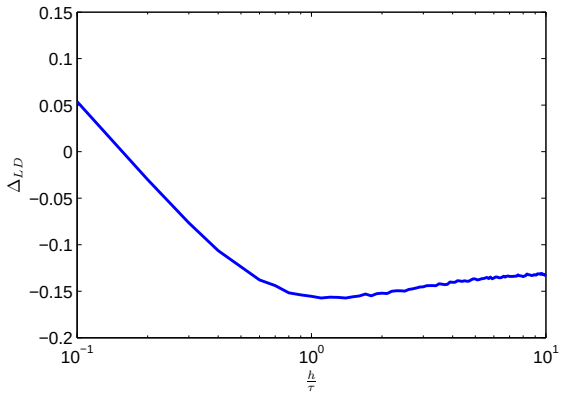

Figure 4.3: Load disturbance performance degradation of the λ-tuning method ($\lambda = 0.7h$) with respect to the γ-tuning one ($\gamma = 5.25h$) in *servo/regulator* trade-off mode.

better disturbance rejection than the γ-tuning design in the balanced lead/lag and lead-dominant cases. However, for $\frac{h}{\tau} < 0.175$ the γ-tuning method provides better disturbance attenuation. In order to outline the basic differences between the two approaches, let us take a look at the (approximate) sensitivity and complementary sensitivity functions depicted in Figure 4.4. It can be observed that the γ-tuning and the λ-tuning methodologies provide almost the same design when tuned in *servo* (*smooth*) mode, see Figure 4.4(c). As we move towards the *regulator* (*tight*) mode, it is clear that M_S increases for

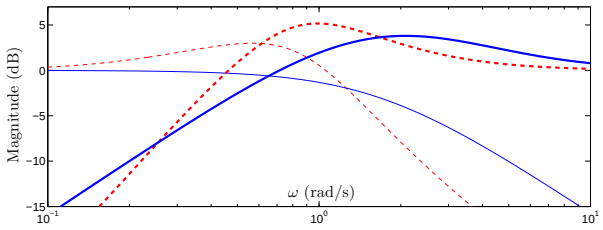

(a) *Regulator* (*Tight*) mode tuning: $\gamma = \gamma_{ld}, \lambda = 0.56h$

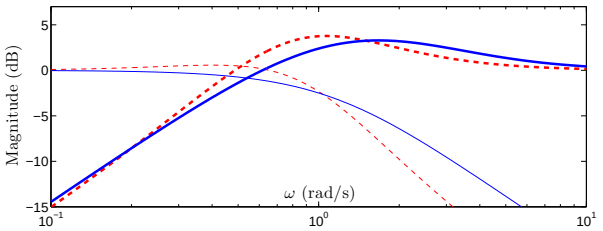

(b) *Servo/Regulator* trade-off tuning: $\gamma = 5.25h, \lambda = 0.7h$

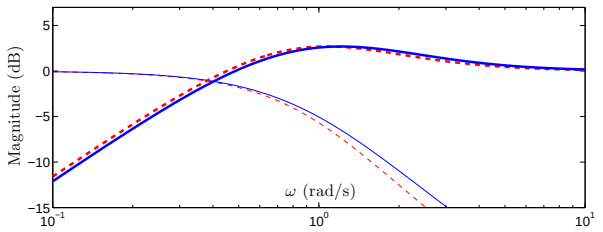

(c) *Servo* (*Smooth*) mode tuning: $\gamma = \gamma_{sp} = \sqrt{2}h, \lambda = h$

Figure 4.4: Sensitivity (thick) and Complementary Sensitivity (thin) functions for the γ-tuning (dashed) and λ-tuning (solid) approaches in *Regulator* (*Tight*), *Servo* (*Smooth*) and trade-off modes for the plant $P = \frac{-0.5s+1}{(0.5s+1)(10s+1)} \approx \frac{e^{-s}}{10s+1}$.

the γ-tuning approach. As it was discussed in Chapter 3, the reason for this greater peak can be attributed to condition (3.33).

4.4 Implementation aspects

So far in this chapter, the controller has been taken in the second order form

$$K = \frac{c_1 s^2 + c_2 s + c_3}{s(d_1 s + 1)} \tag{4.11}$$

where c_1, c_2, c_3, d_1 are assumed to be positive real constants. The controller above has four degrees of freedom and can be considered a *general* PID controller. However, for implementation purposes, it is desirable to cast this general form into practical PID realizations. In Chapters 2 and 3, the ISA PID structure (Astrom and Hagglund, 2005) was considered:

$$K = K_p \left(1 + \frac{1}{sT_i} + \frac{sT_d}{1 + s\frac{T_d}{N}} \right) \tag{4.12}$$

The controller above has the three modes (K_p, T_i, T_d) working additively and it is sometimes referred to as *noninteractive*, *ideal* or *parallel*. The derivative filter parameter N is typically fixed by the manufacturer, being $N = 10$ a typical value (O'Dwyer, 2006). However, as reported in (Isaakson and Graebe, 2002), fixing N independently of the other three parameters may not be a good idea. This can be observed by posing (4.12) in the general second order form (4.11)

$$K = K_p \frac{T_d \left(1 + \frac{1}{N}\right) s^2 + \left(1 + \frac{T_d}{T_i N}\right) s + \frac{1}{T_i}}{s\left(\frac{T_d}{N} s + 1\right)} \tag{4.13}$$

It is clear that the filter derivative parameter N has a big influence on the coefficients of the second order controller. Consequently, PID design should be a four-parameter design including N (Isaakson and Graebe, 2002) (this was also the case in Chapters 2 and 3). As it is claimed in (Luyben, 2001), the use of the fixed derivative filter parameter N explains in part the industrial myth that *derivative action does not work*. Another problem with the ISA

PID form can be detected if we convert from (4.11) to (4.12):

$$\begin{aligned} K_p &= c_2 - c_3 d_1 \\ T_d &= \frac{c_1}{K_p} - d_1 \\ T_i &= \frac{K_p}{c_3} \\ N &= \frac{T_d}{d_1} \end{aligned} \tag{4.14}$$

It is evident that there are combinations of c and d that cannot be described. For example, the tuning rule for the proposed controller with $\lambda = 0.7h$ is indicated in Table 4.1. It is easy to see that both N and T_d may become

Table 4.1: Tuning rule for the proposed controller assuming the ISA PID algorithm.

$\mathbf{K_p}$	$\mathbf{T_i}$	$\mathbf{T_d/N}$	$\mathbf{N+1}$
$\frac{0.53}{k_g}\frac{T_i}{h}$	$\tau + 0.25h$	$0.258h$	$1.94\frac{\tau}{T_i}$

negative, which is physically unfeasible and restricts the application of the proposed method. As pointed out in (Luyben, 2001) regarding model-based designs, the following practical form introduced in (Morari and Zafiriou, 1989) is preferable

$$K = K_p \left(1 + \frac{1}{T_i s} + T_d s\right) \frac{1}{T_F s + 1} \tag{4.15}$$

This alternative form provides a more straightforward parameterization of the second order controller (4.11):

$$\begin{aligned} K_p &= c_2 \\ T_d &= \frac{c_1}{K_p} \\ T_i &= \frac{K_p}{c_3} \\ T_F &= d_1 \end{aligned} \tag{4.16}$$

The corresponding tuning rule is given in Table 4.2. Note that it undergoes

Table 4.2: Tuning rule for the controller (4.4) in the ideal, output-filtered form ($\lambda = 0.7h$).

$\mathbf{K_p}$	$\mathbf{T_i}$	$\mathbf{T_d}$	$\mathbf{T_F}$
$\frac{1}{k_g}\frac{T_i}{1.9h}$	$\tau + \frac{h}{2}$	$\frac{\tau h}{2T_i}$	$0.2579h$

the limitations found in the ISA PID case. The advantages of using the four-parameter, parallel, output-filtered PID structure (4.15) in conjunction with the IMC method can be consulted in (Luyben, 2001). Due to all these considerations, the PID form (4.15) is the recommended one for the presented designs.

4.5 Simulation examples

The purpose of this section is to compare by example the λ and γ-tuning methods. The experimental setup is summarized in Table 4.3, and it has been taken from (Astrom and Hagglund, 2004) (Examples 1,3,4) and (Arrieta and Vilanova, 2007) (Example 2). As it can be seen, we will adopt a FOPTD model

Table 4.3: Experimental setup.

Example	Model	$\frac{h}{\tau}$	Real plant	
			CASE I	CASE II
1	$\frac{e^{-s}}{1+0.093s}$	10.75	$\frac{e^{-s}}{(1+0.05s)^2}$	$\frac{1.2e^{-1.2s}}{1+0.0744s}$
2	$\frac{e^{-0.99s}}{1+1.65s}$	0.6	$\frac{e^{-0.5s}}{(s+1)^2}$	$\frac{1.2e^{-1.188s}}{1+1.32s}$
3	$\frac{e^{-1.42s}}{1+2.9s}$	0.49	$\frac{1}{(s+1)^4}$	$\frac{1.2e^{-1.704s}}{1+2.32s}$
4	$\frac{e^{-0.073s}}{1+1.073s}$	0.068	$\frac{1}{(1+s)(1+0.1s)(1+0.01s)(1+0.001s)}$	$\frac{1.2e^{-0.0876s}}{1+0.8584s}$

for four different plants. Simulations will be shown for the nominal case — i.e., we will assume that the real plant corresponds exactly to the model — as well as for the uncertain scenario. Two cases will be distinguished here:

- CASE I: The real plant will not be a FOPTD model. This case will tackle the usual situation in which a simple model is used to represent a real (more complex) system, giving rise to neglected/unmodeled dynamics.
- CASE II: The real plant will be assumed to be perfectly described by the model. But 20% of parametric uncertainty will be taken into account.

The tuning of γ for the design of Chapter 3 will be done so as to get the best possible results limiting the nominal overshoot to a 10% value. This performance specification obeys the fact that in many processes an excessive overshoot is not acceptable. Figures 4.5,4.7,4.9 concern the lead-dominant and balanced lag and delay cases (Examples 1–3) and it is shown, especially for the lead-dominant plant (Example 1), that the λ-tuning is superior to the γ-tuning strategy, achieving a better trade-off tuning. The most interesting case is

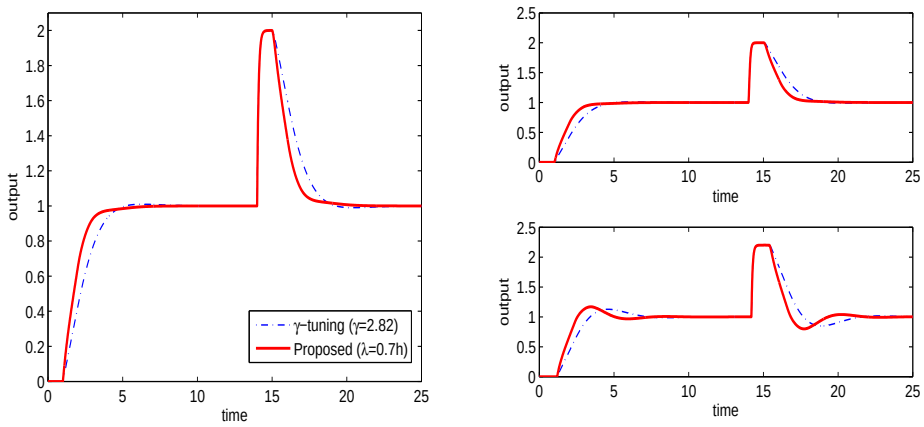

(a) Nominal case

(b) Uncertain case. Top: CASE I. Bottom: CASE II

Figure 4.5: Time responses for Example 1.

the *lag-dominant* one, which is dealt with in Example 4. The corresponding simulation results are captured in Figure 4.11. In this case, a trade-off tuning is more difficult to achieve. The γ-tuning produces excellent load disturbance attenuation by selecting $\gamma = \gamma_{ld} = 0.76$. Nevertheless, this choice produces an excessive nominal overshoot (40%). The value of γ needs to be decreased until $\gamma = 0.38$ in order to reduce the overshoot to approximately the 10%. When

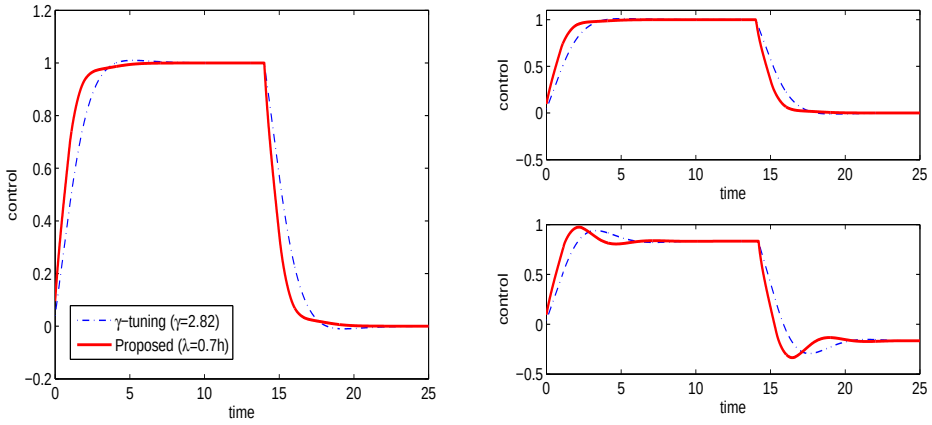

(a) Nominal case

(b) Uncertain case. Top: CASE I. Bottom: CASE II

Figure 4.6: Control effort for Example 1.

this is done, the load disturbance attenuation gets approximately the same as that obtained with the IMC-like approach. Regarding the set-point response, the suggested method provides clear superiority.

The results obtained for the examples 1–4 are collected and quantified in Tables 4.4 and 4.5 for the sake of a more precise comparison. Figures 4.6,4.8,4.10,4.12 plot the required control effort for the two methods at hand. It is noticeable that the γ-tuning results into less demanding controller generally. In spite of this, the manipulated variable movements are still quite acceptable for the IMC-like design tuned with $\lambda = 0.7h$. If strictly necessary, the control action *kicks* can be reduced by slightly augmenting the value of T_F in the tuning rule of Table 4.2. This is illustrated for Example 4. In this case, it can be seen that $T_F = 0.0188$. Figures 4.13 and 4.14 show that by increasing this value — corresponding to the d_1 coefficient with respect to (4.11) — the required control effort can be made equal to that of the γ-tuning method while still producing quite similar set-point and load disturbance responses. It has been verified that that $M_S = 1.618$ for $T_F = 0.0288$, whereas $M_S = 1.64$ for $T_F = 0.0388$.

Table 4.4: Performance evaluation for the nominal case.

Example	Tuning	$\underset{ISE}{SP}$	$\underset{ISE}{LD}$	M_S
1	λ-tuning ($\lambda = 0.7$)	1.48	1.44	1.58
	γ-tuning ($\gamma = 2.82$)	1.82	1.76	1.48
2	λ-tuning ($\lambda = 0.69$)	1.47	0.67	1.58
	γ-tuning ($\gamma = 4$)	1.72	0.85	1.55
3	λ-tuning ($\lambda = 0.99$)	2.1	0.85	1.58
	γ-tuning ($\gamma = 7$)	2.43	1	1.6
4	λ-tuning ($\lambda = 0.05$)	0.1085	0.0084	1.58
	γ-tuning ($\gamma = 0.38$)	0.1243	0.0077	1.62
	γ-tuning ($\gamma = 0.76$)	0.139	0.0026	1.99

Table 4.5: Performance evaluation for the uncertain case.

Example	Tuning	CASE I			CASE II		
		$\underset{ISE}{SP}$	y_{ov} (%)	$\underset{ISE}{LD}$	$\underset{ISE}{SP}$	y_{ov} (%)	$\underset{ISE}{LD}$
1	λ-tuning	1.49	0	1.45	1.59	16.8	2.23
	γ-tuning (γ=2.82)	1.82	1	1.78	1.86	12.7	2.63
2	λ-tuning	1.42	1.66	0.66	1.55	22.68	0.95
	γ-tuning (γ=4)	1.68	7.15	0.85	1.75	21.24	1.22
3	λ-tuning	2.25	14.2	0.95	2.24	24.36	1.16
	γ-tuning (γ=7)	2.66	23.2	1.17	2.56	29.2	1.43
4	λ-tuning	0.11	8.7	0.0085	0.1212	35	0.009
	γ-tuning (γ=0.38)	0.13	18.6	0.0078	0.144	43	0.009
	γ-tuning (γ=0.76)	0.15	46	0.0027	0.2366	86	0.0042

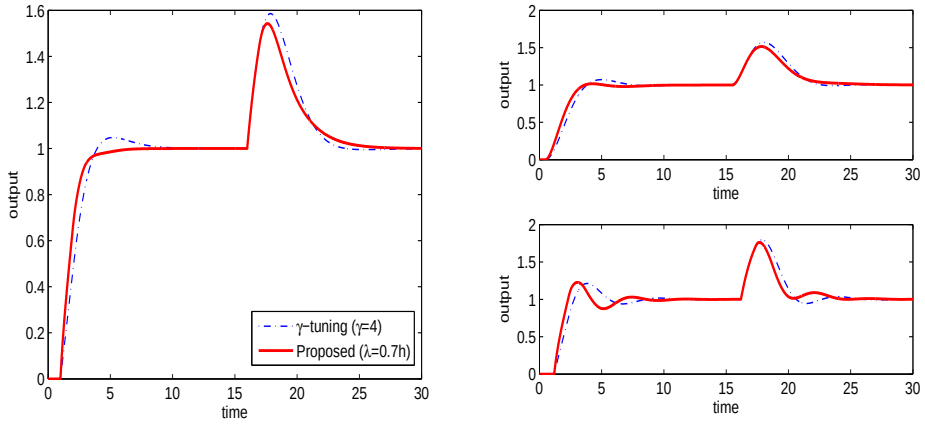

(a) Nominal case

(b) Uncertain case. Top: CASE I. Bottom: CASE II

Figure 4.7: Time responses for Example 2.

4.6 Summary

This chapter has compared the λ and γ-tuning approaches (Chapters 2 and 3). First, the rule $\lambda = 0.7h$ has been proposed for obtaining balanced performance between the servo and regulator modes based on a trade-off between smooth and tight control. The servo/regulator trade-off limits within the λ-tuning method have been explored; if the allowed nominal overshoot is required to be inferior to a 10%, the λ-tuning method provides in general both better servo and regulatory responses for plants such that $h/\tau \geq 0.1$. Nevertheless, for larger allowed overshoots and/or more lag-dominant plants, then the γ-tuning technique allows better (input) disturbance attenuation for a given degree of robustness.

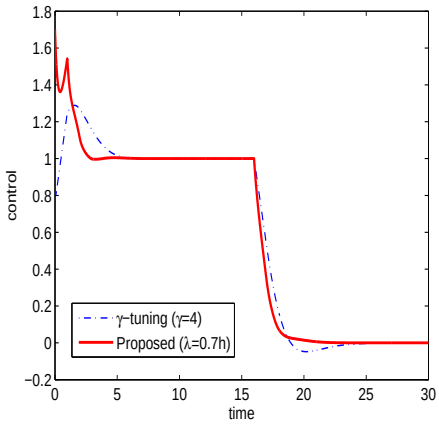

(a) Nominal case

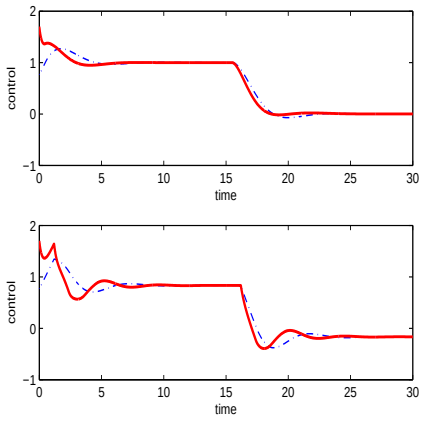

(b) Uncertain case. Top: CASE I. Bottom: CASE II

Figure 4.8: Control effort for Example 2.

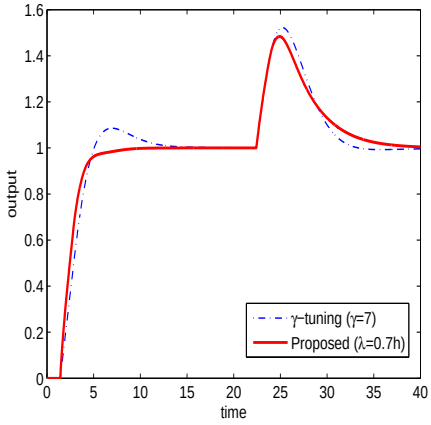

(a) Nominal case

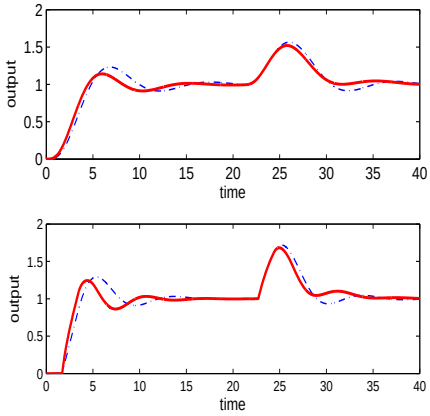

(b) Uncertain case. Top: CASE I. Bottom: CASE II

Figure 4.9: Time responses for Example 3.

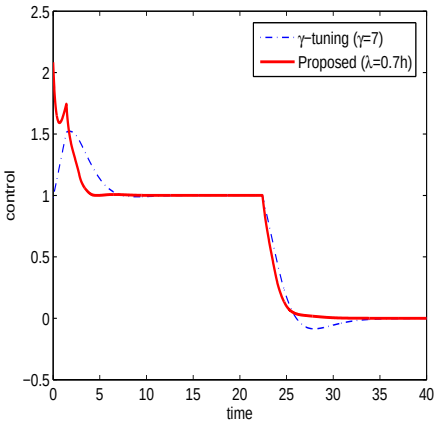

(a) Nominal case

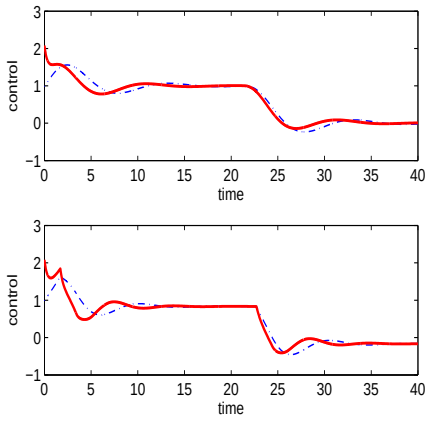

(b) Uncertain case. Top: CASE I. Bottom: CASE II

Figure 4.10: Control effort for Example 3.

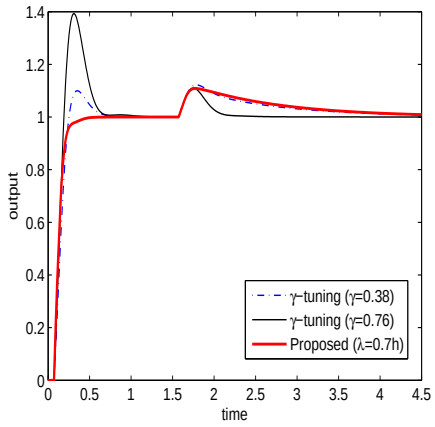

(a) Nominal case

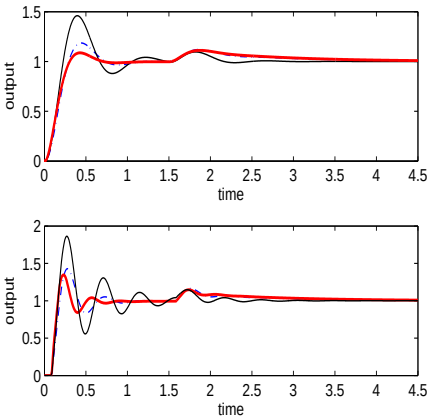

(b) Uncertain case. Top: CASE I. Bottom: CASE II

Figure 4.11: Time responses for Example 4.

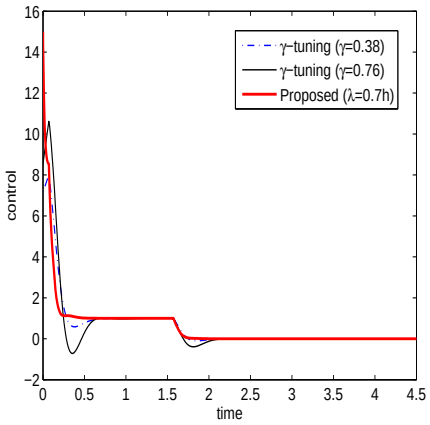

(a) Nominal case

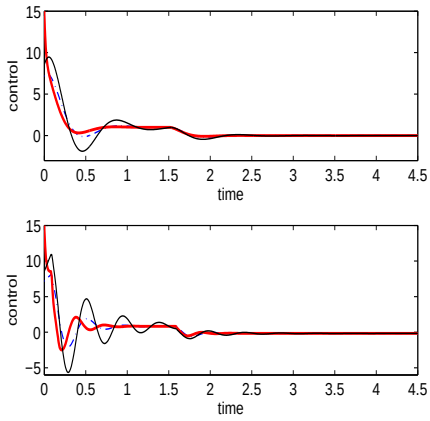

(b) Uncertain case. Top: CASE I. Bottom: CASE II

Figure 4.12: Control effort for Example 4.

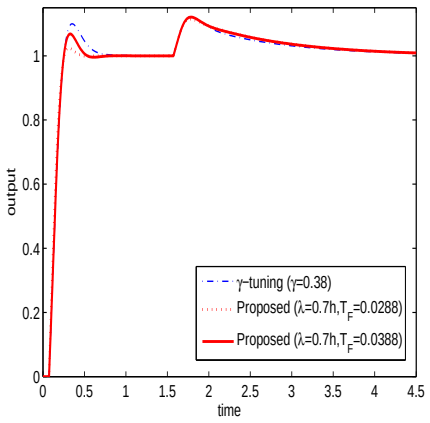

(a) Nominal case

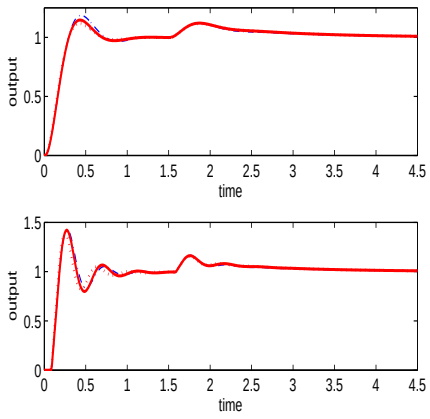

(b) Uncertain case. Top: CASE I. Bottom: CASE II

Figure 4.13: Time responses for Example 4 with increased value of T_F.

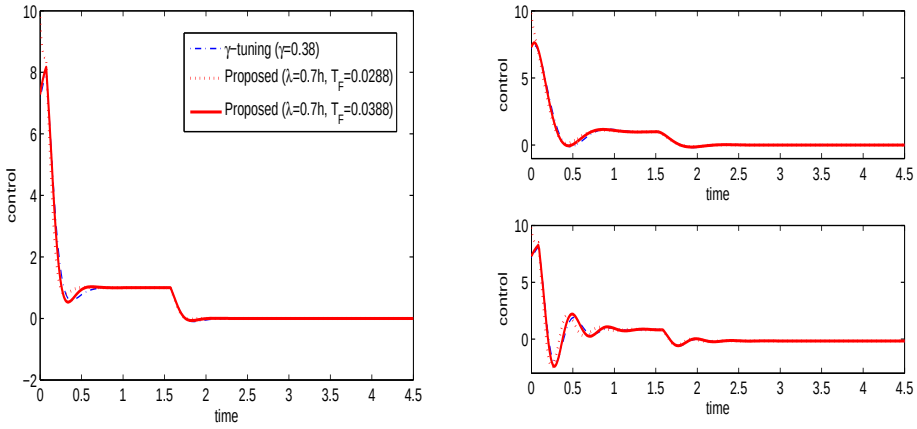

(a) Nominal case

(b) Uncertain case. Top: CASE I. Bottom: CASE II

Figure 4.14: Control effort for Example 4 with increased value of T_F.

Appendix 4A

From (2.4) and (2.20), we have that

$$y = (1 - PQ)d_o = \left(1 - \frac{-\frac{h}{2}s + 1}{(\lambda s + 1)^2}\right)\frac{1}{s} = \frac{\lambda^2 s + 2\lambda + \frac{h}{2}}{(\lambda s + 1)^2} \tag{4.17}$$

Along the lines of Section 3.4, the ISE criterion can be calculated as the sum of the residues of $y(s)y(-s)$ at its poles in the left half-plane (LHP):

$$ISE(\lambda, h) = \text{Res}\left(y(s)y(-s), -\frac{1}{\lambda}\right) = h\frac{20\left(\frac{\lambda}{h}\right)^2 + 1 + 8\frac{\lambda}{h}}{16\frac{\lambda}{h}} \tag{4.18}$$

The plot of ISE/h versus λ/h appears in Figure 4.15. Now, by taking the derivative with respect to λ, we can obtain the value that minimizes the ISE criterion

$$\frac{\partial ISE}{\partial \lambda} = 0 \Rightarrow \lambda = \frac{\sqrt{5}h}{10} \approx 0.22h \tag{4.19}$$

producing the following value

$$ISE_{op}(h) \approx 1.06h \tag{4.20}$$

Robustness associated with the tuning $\lambda = 0.22h$ is poor (M_S can be seen to be around 3). As commented in Section 4.2, for *Tight* control the idea is to increase λ so as to achieve acceptable robustness margins. This will provide the fastest possible closed-loop system since λ directly controls the closed-loop bandwidth. In concrete, this implies that the best disturbance attenuation will be obtained. Although only output disturbance has been explicitly considered, it is easy to check that the smaller the value of λ, the

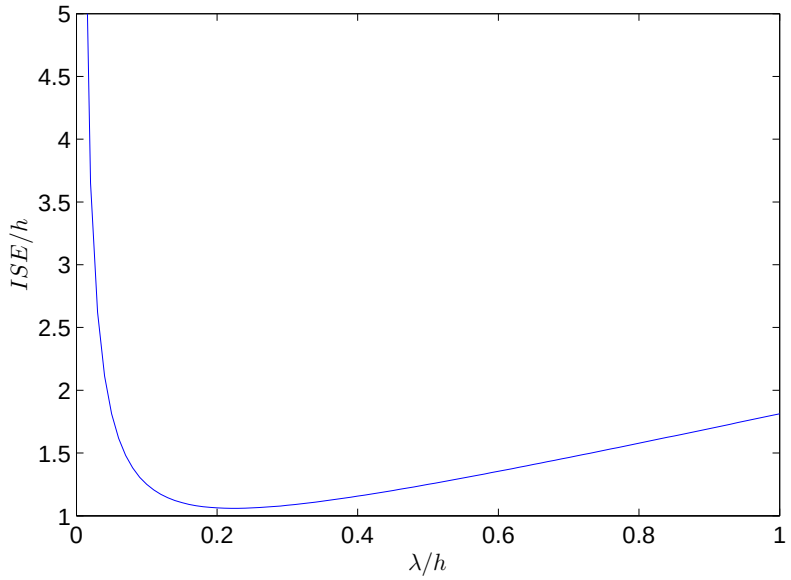

Figure 4.15: ISE/h versus λ/h.

better the load disturbance rejection as well. To see this, let us consider the output to a load disturbance[1]:

$$y = P(1 - PQ)d_i = \frac{(-\frac{h}{2}s + 1)(\lambda^2 s + 2\lambda + \frac{h}{2})}{(\frac{h}{2}s + 1)(\tau s + 1)(\lambda s + 1)^2} \tag{4.21}$$

Proceeding as before, the associated ISE can be computed as the sum of the residues of $y(s)y(-s)$ in its LHP poles:

$$ISE(\lambda, \tau, h) = \frac{1}{4}\frac{5\lambda^3 + 8\tau\lambda^2 + 2\lambda^2 h + \frac{1}{4}h^2\lambda + 4\tau\lambda + \frac{1}{2}\tau h^2}{(\lambda + \tau)^2} \tag{4.22}$$

Straightforward calculations yield

$$\frac{\partial ISE(\lambda, \tau, h)}{\partial \lambda} = \frac{20\lambda^3 + 60\tau\lambda^2 - h^2\lambda + 64\tau^2\lambda - 3h^2\tau + 16h\tau^2}{16(\lambda + \tau)^3} \tag{4.23}$$

[1] In what follows, we assume $K_g = 1$ in (2.4).

The sign of $\frac{\partial ISE}{\partial \lambda}$ is determined by the sign of the numerator in (4.23). Dividing it by h^3, the sign can be determined in terms of the following function:

$$f(\frac{\lambda}{h}, \frac{\tau}{h}) = 20\left(\frac{\lambda}{h}\right)^3 + 60\left(\frac{\lambda}{h}\right)^2 \frac{\tau}{h} - \frac{\lambda}{h} + 64\left(\frac{\tau}{h}\right)^2 \frac{\lambda}{h} - 3\frac{\tau}{h} + 16\left(\frac{\tau}{h}\right)^2 \quad (4.24)$$

The plot of f is shown in Figure 4.16. As it can be appreciated, f remains

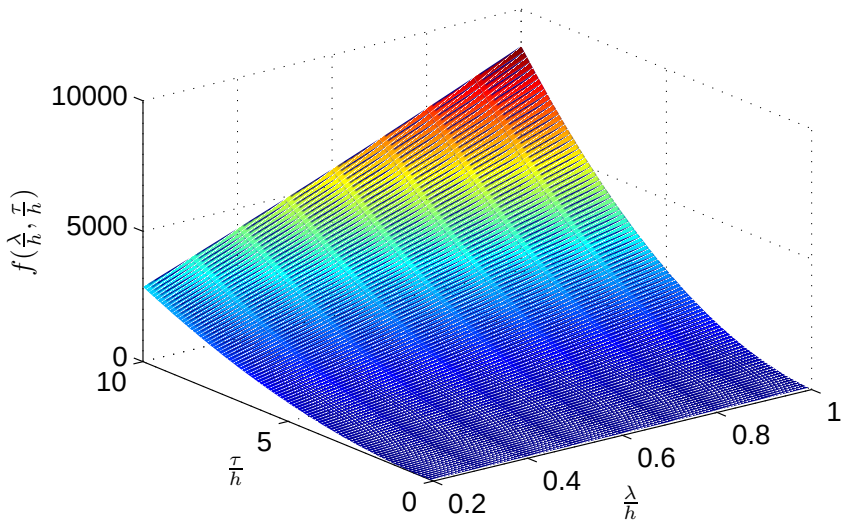

Figure 4.16: f versus λ/h and τ/h.

positive. This means that the ISE with respect to load disturbance is an increasing function of λ in the considered interval ($0.22 < \frac{\lambda}{h} \leq 1$).

Chapter 5

Combined $\lambda\gamma$ approach: a first $\mathcal{H}_\infty$ design

Based on (Alcántara et al.*, 2010*d*)*

Sometimes a 1DOF PID compensator operates in both *servo* and *regulator* mode. In this scenario, it is clear that it will be impossible to achieve both optimal set-point tracking and load disturbance attenuation. However, it would be desirable to possess a simple methodology to adjust a convenient compromise. This chapter presents a simple analytical PID design aimed at stable plants. Its distinguishing feature is that two design parameters allow adjustment of the *robustness/performance* as well as the *servo/regulator* trade-offs. The resulting unified design extends some previous approaches where only one of the aforementioned trade-offs is considered.

5.1 Introduction

The γ-tuning philosophy (recall Chapter 3) obeys the fact that sometimes a 1DOF PID compensator is to operate in both *servo* and *regulator* mode. It is well-known that within the 1DOF context is not possible to have both optimal *set-point* and *load disturbance* attenuation simultaneously (Skogestad and Postlethwaite, 2005). Thus, some kind of *servo/regulator* trade-off is necessary if the minimum overall performance degradation is sought. The name given to the technique comes from the fact that a single adjustable

parameter (γ) allows selection of the operating mode of the controller. Tuning γ appropriately results into a convenient *servo/regulator* compromise. The main shortcoming of the γ-tuning procedure is that it lacks the possibility of adjusting robustness easily.

On the other hand, it is well-known that the popular IMC design (Morari and Zafiriou, 1989) allows to trade-off between *robustness* and *performance* (understood as speed of response or closed-loop bandwidth) by means of adjusting a single parameter, normally denoted by λ. This approach leads to good *servo* responses. However, as reported in several works (Chien and Fruehauf, 1990; Horn *et al.*, 1996; Astrom and Hagglund, 2005), the conventional IMC design can exhibit poor disturbance rejection and it is therefore unsuitable for *regulator* purposes generally.

This chapter presents an analytical PID design which combines the two commented proposals (γ-tuning and λ-tuning) while avoiding their shortcomings. The resulting method involves two tuning parameters: λ and γ, which allow adjustment of the *robustness/performance* and the *servo/regulator* tradeoffs, respectively.

The chapter outline is given next. Section 5.2 introduces the control framework. The proposed design (called $\lambda\gamma$-tuning) is presented in Section 5.3, which also deals with robustness considerations and an interpretation in terms of IMC methodology. Section 5.4 illustrates the presented ideas by means of a simulation example. Finally, Section 5.5 makes a summary of the chapter.

5.2 The control framework

The conventional 1DOF scenario is assumed throughout this chapter and it is depicted in Figure 1.1. As usual, r, d, y denote, respectively, the reference, the disturbance and the output signals. On the other hand, $e = r - y$ is the tracking error. Step signals are assumed for both the reference and the disturbances. A simple FOPTD model of the plant is assumed:

$$P = K_g \frac{e^{-sh}}{\tau s + 1} \tag{5.1}$$

where K_g, τ, h denote, respectively, the gain, time constant, and delay (deadtime) of the process. For design purposes, it is convenient to approximate the

delay term in (5.1) so as to achieve a purely rational model. By using the first order Taylor expansion $e^{-sh} \approx 1 - sh$, (5.1) can be approximated as follows

$$P \approx K_g \frac{-sh+1}{\tau s+1} \tag{5.2}$$

Regarding the control law, the following practical PID forms are considered:

$$K = K_p \left(1 + \frac{1}{sT_i} + \frac{sT_d}{1+sT_d/N}\right) \tag{5.3}$$

and

$$K = K_p \left(1 + \frac{1}{sT_i} + sT_d\right) \frac{1}{T_F s+1} \tag{5.4}$$

The parameters K_p, T_i, T_d are known as the proportional gain, integral time and derivative time, respectively. The N parameter in the ISA form (5.3) is the derivative filter parameter, necessary to implement the derivative action. In the output-filtered form (5.4) introduced in (Morari and Zafiriou, 1989), T_F is an additional tuning parameter defining the first order filter that multiplies the output of the ideal PID. Instead of carrying out the design in the conventional setting of Figure 1.1, the Q-parameterization (1.23) will be used as in previous chapters.

5.3 Proposed $\lambda\gamma$-tuning

The proposed approach stems from considering the following weighted sensitivity problem (WSP) (Skogestad and Postlethwaite, 2005)

$$\min_{K \in \mathcal{C}} \|WS\|_\infty = \min_{Q \in \mathcal{RH}_\infty} \|WS\|_\infty \tag{5.5}$$

where $W(s)$ is a frequency weight which has to be designed. The problem above can be regarded as a min-max model matching problem (MMP) by expressing it in the form $\min_Q \|T_1 - T_2 Q\|_\infty$. A well-known solution of such a problem lies in optimal (Nevanlinna-Pick) interpolation theory (recall Lemma 1.2.1). For our purposes, however, it is not strictly necessary to invoke these results. By approximating the FOPTD plant (5.1) as in (5.2), the sensitivity transfer function is given by

$$S = 1 - PQ = 1 - K_g \frac{-hs+1}{\tau s+1} Q \tag{5.6}$$

It is clear that WS is analytical in the complex Right Half Plane (RHP) as long as S has zeros located at the unstable poles of W. In this case, the maximum modulus principle (Churchill and Brown, 1986) from complex variable guarantees that $|WS|$ attains its maximum over the imaginary axis. From (5.6), $S(1/h) = 1$, then

$$\|WS\|_\infty \geq |W(1/h)S(1/h)| = W(1/h) \triangleq \rho \tag{5.7}$$

Consequently, the optimal Q is such that

$$W\left(1 - PQ\right) = \rho \tag{5.8}$$

from where

$$\begin{aligned} Q &= P^{-1}\left(1 - \rho W^{-1}\right) \\ &= \frac{1}{K_g}\left(\frac{\tau s + 1}{-sh + 1}\right)\left(1 - \rho W^{-1}\right) \end{aligned} \tag{5.9}$$

Besides, the corresponding complementary sensitivity transfer function is

$$T = PQ = 1 - \rho W^{-1} \tag{5.10}$$

Note, from (5.9), that

$$\left(1 - \rho W^{-1}\right)|_{s=1/h} = 0 \tag{5.11}$$

because Q must be stable. In the light of (5.11), (5.10), (5.9), and (5.5), the following form for W is proposed

$$W = \frac{(\lambda s + 1)^2}{s(\alpha s + 1)} \tag{5.12}$$

The rationale behind this choice is as follows:

- From (5.10), the pole at the origin ensures integral action, that is, $T(0) = 1$, or equivalently, $S(0) = 0$.
- From (5.10), it is clear that the zeros of W are poles of the closed-loop. Assume now that $\alpha = \lambda$ in (5.12), then $W = \frac{\lambda s+1}{s}$ and $\rho = W(1/h) = \lambda + h$. Substituting these values into (5.10), the input-to-output relation becomes $T = \frac{-sh+1}{\lambda s+1}$. This way, λ is used to specify the closed-loop bandwidth. The smaller its value, the faster the closed-loop.

- The response to a disturbance is given by

$$y = SPd = SK_g \frac{-hs+1}{\tau s+1} d \tag{5.13}$$

Thus, when τ dominates over h, the slow dynamic $\frac{1}{\tau s+1}$ needs to be cancelled by S. Otherwise, the disturbance attenuation would be *sluggish*. That is, $S(-1/\tau) = 0$ is necessary for good *Regulator* behaviour. From (5.5), the pole at $s = -1/\alpha$ in (5.12) yields $S(-1/\alpha) = 0$. This way, $\alpha \in [\lambda, \tau]$ can be thought of as a tuning parameter in charge of adjusting the servo/regulator compromise. If $\alpha = \lambda$, $T = \frac{-sh+1}{\lambda s+1}$. From this point on, we can improve the disturbance attenuation by increasing the value of α. As commented, the best disturbance attenuation will be obtained for $\alpha = \tau$.

Now that we have designed W, we will proceed to the obtention of Q. From (5.12),

$$\rho = W(1/h) = \frac{(\lambda+h)^2}{\alpha+h} \tag{5.14}$$

and the optimal Q can be found from (5.9)

$$Q = \frac{1}{K_g} \frac{(\tau s+1)(\gamma s+1)}{(\lambda s+1)^2} \tag{5.15}$$

with

$$\gamma = \frac{h\alpha + 2\lambda\alpha - \lambda^2}{\alpha+h} \tag{5.16}$$

The sensitivity and the complementary sensitivity transfer functions become:

$$T = \frac{-hs+1}{\lambda s+1} \left(\frac{\gamma s+1}{\lambda s+1} \right) \tag{5.17}$$

$$S = \frac{(\lambda s+1) - (-hs+1)\left(\frac{\gamma s+1}{\lambda s+1}\right)}{\lambda s+1} \tag{5.18}$$

Elementary calculus shows that $\gamma \geq \lambda$ when $\alpha \geq \lambda$. More exactly, $\gamma = \lambda$ when $\alpha = \lambda$ and $\frac{\partial \gamma}{\partial \alpha} > 0$ for $\alpha \geq \lambda$. In this situation, the term $\frac{\gamma s+1}{\lambda s+1}$ is a *lead* network. When $\gamma = \lambda$ ($\alpha = \lambda$) we have that

$$T = \frac{-hs+1}{\lambda s+1} \qquad S = \frac{s(\lambda+h)}{\lambda s+1} \tag{5.19}$$

From (5.17), it is clear that improving the load disturbance attenuation by augmenting γ (equivalently α) will increase the overshoot in the input-to-output response. Finally, an equivalent unity feedback controller can be recovered from (1.23):

$$K = \frac{1}{K_g} \frac{(\tau s + 1)(\gamma s + 1)}{s\left((\lambda^2 + h\gamma)s + 2\lambda + h - \gamma\right)} \tag{5.20}$$

Regarding the PID form in (5.4), the following tuning rule is obtained

$$\begin{array}{rclcrcl} T_F & = & \frac{\lambda^2+h\gamma}{2\lambda+h-\gamma} & & T_i & = & \tau+\gamma \\ T_d & = & \frac{\tau\gamma}{\tau+\gamma} & & K_p & = & \frac{\tau+\gamma}{K_g(2\lambda+h-\gamma)} \end{array} \tag{5.21}$$

Remark 5.3.1. *It is noteworthy that in a Two-Degree-Of-Freedom (2DOF) setting, the servo (free-of-overshoot) response given by T in (5.19) can be recovered by simply adding the reference prefilter $f_R = \frac{\lambda s+1}{\gamma s+1}$.*

5.3.1 Robustness considerations in terms of λ and γ

The *lead* network $\frac{\gamma s+1}{\lambda s+1}$ appears in the transition from the servo to the regulator mode. We will inspect now how λ and γ influence robustness, which can be measured by looking at the peak of S, normally denoted by M_S. This value represents the inverse of the shortest distance from the Nyquist curve to the critical point: $-1 + 0j$. Figure 5.1 displays the magnitude of S for the plant $P = \frac{e^{-s}}{5s+1} \approx \frac{-s+1}{5s+1}$ when varying γ.

As it can be appreciated, augmenting γ leads to larger M_S. This can be explained generally by a *waterbed effect* (Skogestad and Postlethwaite, 2005) argument. When $\gamma > \lambda$ (equivalently $\alpha > \lambda$), the low frequency pole at $s = -1/\alpha$ pushes down $|S(j\omega)|$ at low frequencies. As a result, $|S(j\omega)|$ pops up at high frequencies, provoking a larger M_S. The peak on the magnitude of T: M_T, is also a robustness indicator. Obviously, because of the *lead* term $\frac{\gamma s+1}{\lambda s+1}$, the larger the value of γ in (5.17), the larger the value of M_T. Consequently, improving the disturbance rejection (augmenting γ) worsens robustness.

A robustness interpretation for λ comes from the well-known small gain theorem (Skogestad and Postlethwaite, 2005). If we suppose that the model is not perfect — this is, of course, the situation in practice — and assume the real plant belonging to the following set

$$\mathcal{F} = \left\{ \tilde{P} = P(1 + \Delta_m) \right\} \tag{5.22}$$

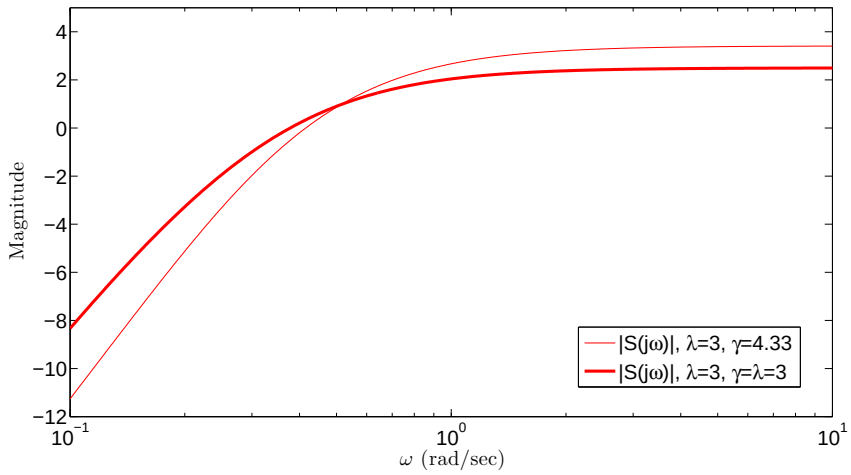

Figure 5.1: $|S(j\omega)|$ for different values of γ.

where Δ_m is the relative (multiplicative) model error

$$\Delta_m \doteq \frac{\tilde{P} - P}{P} \tag{5.23}$$

satisfying $|\Delta_m(j\omega)| \leq |W_m(j\omega)|$, with $W_m(s)$ a frequency weight bounding the modelling error, it is well-known (Skogestad and Postlethwaite, 2005; Morari and Zafiriou, 1989) that a controller that stabilizes the nominal plant P, also stabilizes all the plants in (5.22) provided that

$$\|W_m T\|_\infty < 1 \tag{5.24}$$

It is easy to see that the Robust Stability condition (5.24) holds if and only if

$$|T(j\omega)| < \frac{1}{|\Delta_m^*(j\omega)|} \ \forall\omega \tag{5.25}$$

where Δ_m^* denotes the worst relative error (5.23). Let us consider now that $P = \frac{e^{-s}}{5s+1} \approx \frac{-s+1}{5s+1}$ and assume the real plant affected by parametric uncertainty. As shown in Figure 5.2, considering $\gamma = 4.33$, the robust stability condition is satisfied for $\lambda = 4.25$, but not for $\lambda = 3$. Generally, the greater the value of λ, the slower (and the more robust) the closed-loop.

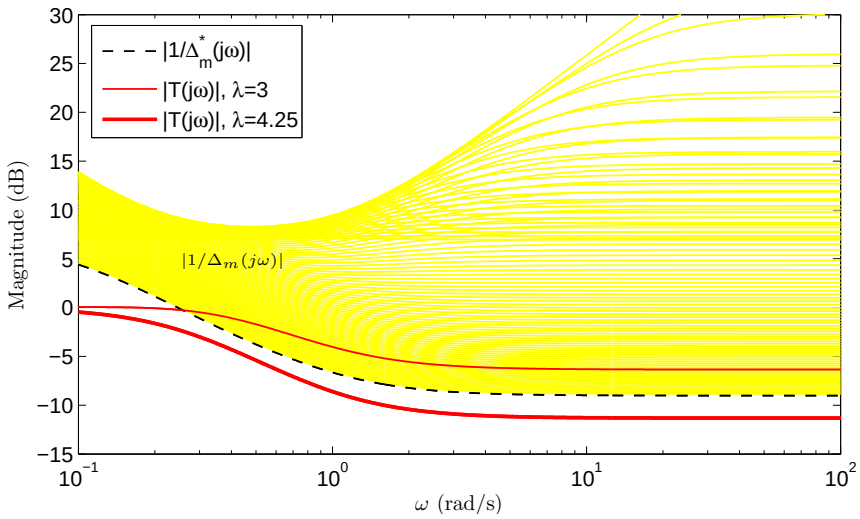

Figure 5.2: Robust Stability condition for $P_o = \frac{e^{-s}}{5s+1} \approx \frac{-s+1}{5s+1}$ and 45% of parametric uncertainty.

Remark 5.3.2. *In all the calculations, the nominal model has been taken as the FOPTD approximation in (5.2). Consequently, the real plant has been considered to belong to the set (5.22).*

5.3.2 IMC interpretation

The presented $\lambda\gamma$ approach can be interpreted within the IMC method (Morari and Zafiriou, 1989). Factor P in (5.1) according to the *inner-outer* factorization

$$P = P_m P_a \tag{5.26}$$

where $P_m = \frac{K_g}{\tau s+1}, P_a = e^{-sh}$ are the MP and all-pass portions. The optimal IMC controller Q minimizing the tracking Integrated Squared Error (ISE) is given by

$$Q = P_m^{-1} = \frac{\tau s + 1}{K_g} \tag{5.27}$$

However, the controller above is not proper. In order to make Q physically realizable it is necessary to extend it with a filter. By selecting

$$f_{sp} = \frac{1}{\lambda s + 1} \tag{5.28}$$

the following controller is finally obtained

$$Q_{sp} = Q f_{sp} = \frac{1}{K_g} \frac{\tau s + 1}{\lambda s + 1} \tag{5.29}$$

Note that the optimum Q is recovered as $\lambda \to 0$.

The controller Q_{sp}, obtained by means of using the filter f_{sp}, allows to trade-off between robustness and performance through the adjustment of the λ parameter. This is enough for set-point tracking purposes but fails to provide good disturbance attenuation for a *lag-dominant* plant (Chien and Fruehauf, 1990). Controller (5.29) is not able to produce $S(-1/\tau) = 0$ no matter how the λ parameter is chosen. In order to remedy the *sluggish* disturbance rejection obtained when using f_{sp}, the following alternative detuning filter can be considered (Horn *et al.*, 1996)

$$f_{ld} = \frac{\gamma s + 1}{(\lambda s + 1)^2} \tag{5.30}$$

Then, the resulting controller becomes

$$Q_{ld} = Q f_{ld} = \frac{1}{K_g} \frac{(\tau s + 1)(\gamma s + 1)}{(\lambda s + 1)^2} \tag{5.31}$$

If we try to recover a conventional unity feedback controller from (5.1), (5.31) and (1.23), a delay will appear in the denominator of K. By approximating this delay by its first order Taylor polynomial ($e^{-sh} \approx -sh + 1$), the controller in (5.20) is rederived. This way,

- λ has been inherited from the traditional IMC methodology, and is in charge of adjusting the *robustness/performance* trade-off.
- γ permits, once the robustness level has been specified with λ, to balance the performance conveniently between the *servo* and the *regulator* operation.

More concretely, $\gamma \in [\lambda, \gamma_{ld}]$, where

$$\gamma_{ld} \approx -\frac{\lambda^2 - 2\lambda\tau - h\tau}{h + \tau} \tag{5.32}$$

corresponds to $\alpha = \tau$ in (5.16), providing $S(-1/\tau) = 0$. In order to provide some guidelines for the tuning of λ and γ, Figure 5.3 shows how M_S depends on the ratio λ/h (assuming $\gamma = \lambda$). Besides, for each value of λ, the corresponding M_S value to $\gamma = \gamma_{ld}$ is shown. When $\gamma > \lambda$, M_S also depends on the ratio τ/h.

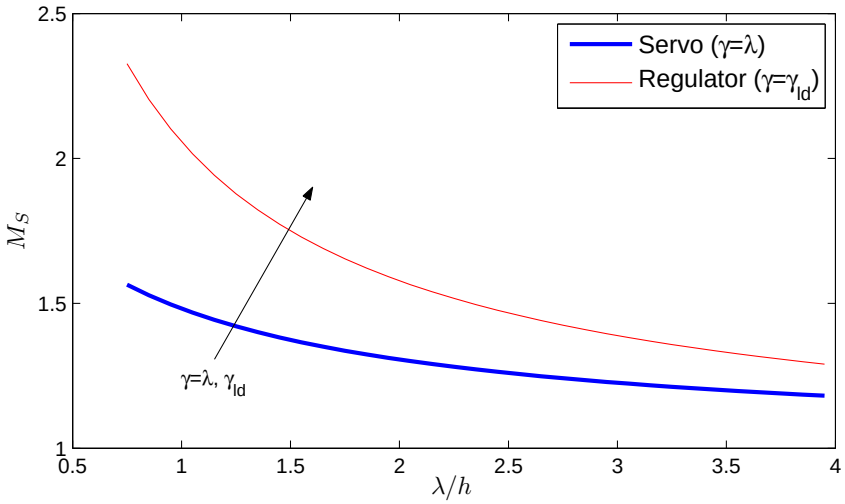

Figure 5.3: M_S for different values of λ/h. $P = \frac{e^{-s}}{10s+1}$.

5.4 Simulation example

Let us consider the FOPTD process

$$P = \frac{e^{-0.073s}}{1.073s + 1} \tag{5.33}$$

In (Zhuang and Atherton, 1993), optimal tuning rules for FOPTD systems were derived for both set-point and load disturbance response (the tuning rules

in (Zhuang and Atherton, 1993) were taken for servo and regulator operation in the numerical γ-tuning procedures (Arrieta and Vilanova, 2007; Arrieta *et al.*, 2010)). In particular, for the ISE criterion and (5.33), the parameters of (5.3) are $K_p = 11.6791, T_i = 0.9171, T_d = 0.0482$ (set-point) and $K_p = 19.9738, T_i = 0.1272, T_d = 0.0462$ (load disturbance). As for the N parameter, we take $N = 20$. Figure 5.4 and Figure 5.5 compare the tuning for set-point tracking with the proposed approach for $\lambda = h = 0.073$ and $\lambda = 2h = 0.146$. In order to obtain good results for the servo mode, we take $\gamma = \lambda$. From (5.4) and (5.21), it is easy to see that the corresponding servo-type controllers are of PI type, with $K_p = 7.3493, T_i = 1.073$ ($\lambda = h$) and $K_p = 4.896, T_i = 1.073$ ($\lambda = 2h$).

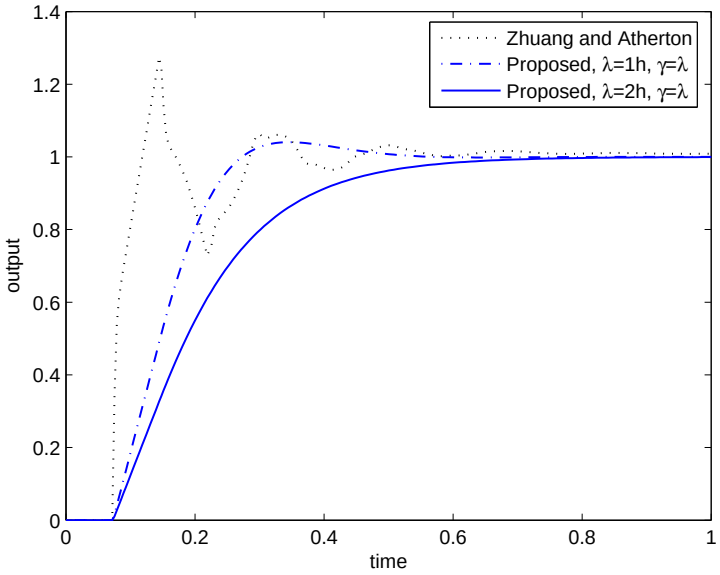

Figure 5.4: Set-point responses.

The tuning rules in (Zhuang and Atherton, 1993) achieve optimal performance at the expense of an aggressive control action. In accordance with this, the output response is somewhat oscillatory, indicating that robustness may be poor ($M_S = 2.65$). This type of responses is not desirable in industry, where *smoother* control is preferable. Within the proposed method, this is achieved by increasing the value of λ, which makes the control system slower and more

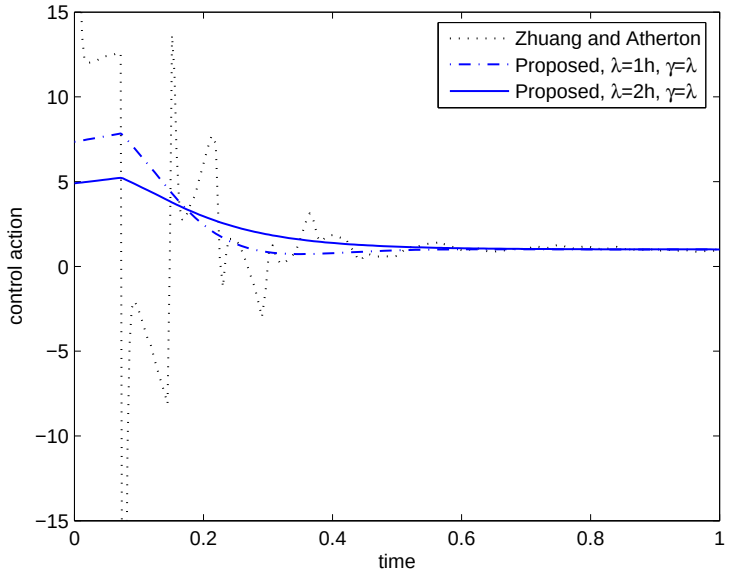

Figure 5.5: Control effort for the set-point responses.

robust. For $\lambda = h$ we obtain $M_S = 1.59$, whereas $\lambda = 2h$ leads to $M_S = 1.35$. Similarly, Figure 5.6 and Figure 5.7 depict the time responses for the regulator mode. Now, we select $\gamma = \gamma_{ld}$ to provide the best disturbance attenuation. The corresponding controllers are again of PI type: $K_p = 10.774, T_i = 0.2004$ ($\lambda = h$) and $K_p = 7.7215, T_i = 0.3231$ ($\lambda = 2h$) and provide, respectively, $M_S = 2.96$ and $M_S = 1.81$. It is clear from Figure 5.6 and Figure 5.7 that the optimal design given in (Zhuang and Atherton, 1993) results into an excessively high control action variation. Accordingly, it can be verified that $M_S = 21.23$, which is a very bad robustness indicator. Robustness can be improved by increasing N, for instance, if $N = 50$, $M_S = 14.06$, which continues to be too high, however. A typical value is $N = 10$ (O'Dwyer, 2006). For this value, we have that $M_S = 77.88$.

Let us turn our attention now to the standard IMC (Morari and Zafiriou, 1989) method. In (Ali and Majhi, 2009), the traditional PI tuning based on the IMC method is reexamined under the light of tight control and smooth control (Skogestad, 2006). The fastest possible control with acceptable robustness

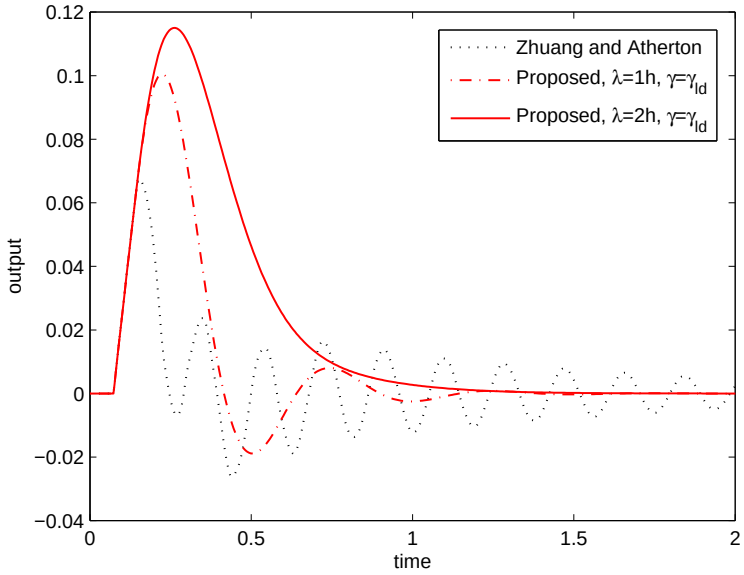

Figure 5.6: Load disturbance responses.

is achieved by tight control, whereas smooth control results in the slowest control subject to achieval of acceptable disturbance rejection. In (Ali and Majhi, 2009), the normalized IMC filter time constant (λ/h) is designed to achieve a particular value of M_S that results in smooth ($\lambda/h = 1.47$) and tight ($\lambda/h = 0.74$) control for stable FOPTD plants. In particular, the following PI settings are considered

$$K_p^{ti} = \frac{0.4\tau}{K_g h} \approx 5.88 \qquad T_i^{ti} = \tau = 1.073 \tag{5.34}$$

$$K_p^{sm} = \frac{0.57\tau}{K_g h} \approx 8.38 \qquad T_i^{sm} = \tau = 1.073 \tag{5.35}$$

respectively for tight and smooth control. In the smooth control case, $M_S = 1.38$, whereas in the tight control case, $M_S = 1.71$. In this approach, the basic idea is to improve the load disturbance rejection by means of making the system faster (and consequently less robust). This approach fails when

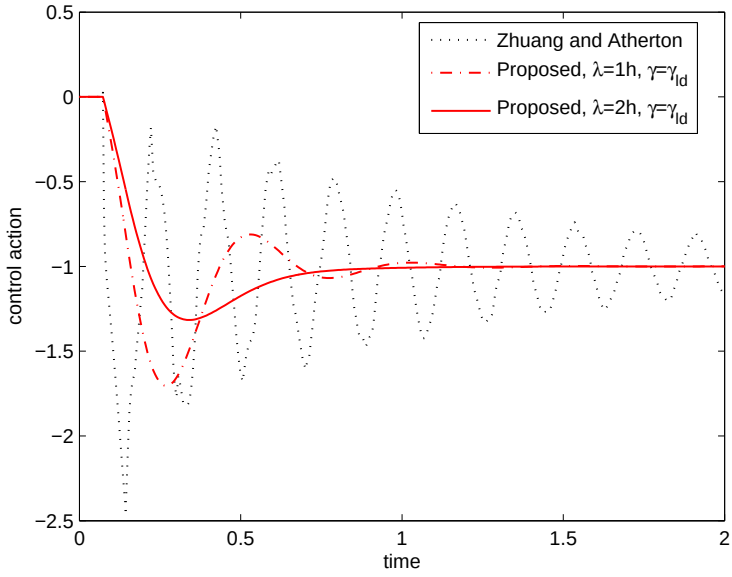

Figure 5.7: Control effort for the load disturbance responses.

considering lag-dominant plants. In Figure 5.8, the load disturbance responses associated with the smooth and tight PI settings in (Ali and Majhi, 2009) are compared with those obtained using the proposed method tuned with $\lambda = 2.4h = 0.1752, \gamma = \gamma_{ld}$, which leads to the PI controller $K_p = 6.8765, T_i = 0.3696$. This tuning of our $\lambda\gamma$ controller provides good disturbance attenuation and good robustness: $M_S = 1.6551$. As it can be seen, the approach in (Ali and Majhi, 2009) improves the disturbance rejection by making the system faster. In order to provide acceptable robustness, the system bandwidth is limited to that providing $M_S = 1.71$. Although the amplitude of the disturbance rejection response is attenuated, the response continues to be *sluggish* because the slow pole of the plant at $s = -1/\tau$ is not cancelled.

5.5 Summary

This chapter has presented a unified *servo/regulator* analytical design for robust PID tuning of stable plants. The design combines the basic ideas behind

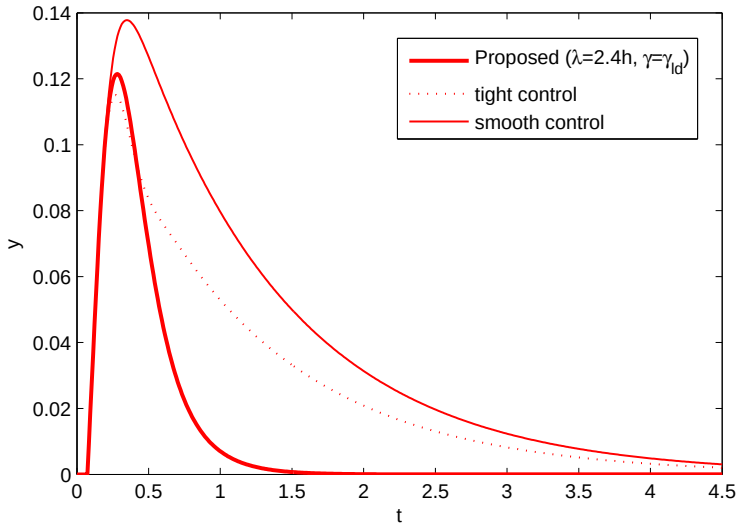

Figure 5.8: Load disturbance rejection for the proposed method and that in (Ali and Majhi, 2009) considering the FOPTD model (5.33).

the IMC and the γ-tuning approaches. A simulation example has verified the effectiveness of the proposed method. As a summary of this example, it has been shown how the proposed method allows for an easy adjustment of both the robustness margins (in contrast with some approaches focusing on the operating mode (Zhuang and Atherton, 1993; Arrieta *et al.*, 2010; Alcántara *et al.*, 2010*b*)) and the operating mode of the controller (in contrast with IMC and IMC-like procedures).

Chapter 6

An improved $\mathcal{H}_\infty$ design

Based on (Alcántara et al.*, 2011*c*; Alcántara* et al.*, 2011*b*)*

This chapter presents an $\mathcal{H}_\infty$ design that alleviates some difficulties with standard Internal Model Control (IMC), while still obeying the same spirit of simplicity. The controller derivation is carried out analytically based on a *weighted sensitivity* formulation. The corresponding frequency weight, chosen systematically, involves two tuning parameters with clear meaning in terms of common design specifications: one adjusts the *robustness/performance* trade-off as in the IMC procedure; the other one balances the *servo* and *regulatory* performance. For illustration purposes, the method is applied to analytical tuning of PI compensators. Due to its simplicity and effectiveness, the presented methodology is also suitable for teaching purposes.

6.1 Introduction

Simplicity is a desired feature of a control algorithm: we would like it to be widely applicable and easy to understand, involving as few tuning parameters as possible. Ideally, these parameters should possess a clear engineering meaning, making the tuning a systematic task according to the given specifications. As for implementation, low-order controllers are preferable.

In this line, the PID controller is recognized to be the bread and butter of automatic control, being by far the most dominating form of feedback in a wide range of industrial applications; the PID strategy is particularly effective in

process control, where a combination of benign process dynamics and modest performance requirements finds its place (Astrom and Hagglund, 2005). The ideal PID law is based on the present (P), past (I) and estimated future (D) error information. In accordance with this original conception, there are only three tuning parameters. Even for such a simple strategy, it is not easy to find good settings without a systematic procedure (Pedret *et al.*, 2002; Skogestad, 2003; Ogunnaike and Mukati, 2006).

During the last twenty years, there has been a revived interest in PID control, motivated by the advent of model predictive control, which requires well-tuned PID compensators at the bottom level, and the emergence of auto-tuning tools (Astrom and Hagglund, 2001). As a result, numerical (optimization-based) techniques have been suggested in the literature (Zhuang and Atherton, 1993; Visioli, 2001; Astrom and Hagglund, 2004; Toscano, 2005). In the same vein, analytically-derived tuning rules have appeared (He *et al.*, 2000; Lee *et al.*, 2000; Shamsuzzoha and Lee, 2007; Vilanova, 2008). Another reason for the PID revival has been the lack of results regarding stabilization of delayed systems (Silva *et al.*, 2002; Hohenbichler, 2009; Songa *et al.*, 2009; Ou *et al.*, 2009). These research efforts, specially the trend for analytical design, has incorporated into the PID arena the control theory mainstream developments, leaving aside more specific techniques.

Among the analytical methods, IMC (Morari and Zafiriou, 1989) has gained remarkable industrial acceptance due to its simple yet effective procedure (Skogestad, 2003; Dehghani *et al.*, 2006). Internal Model Control theory was first applied to PID control of stable plants in (Rivera *et al.*, 1986), solving the robustness problems associated with some early tunings like (Ziegler and Nichols, 1942). Although the IMC-PID settings (Rivera *et al.*, 1986) are robust and yield good set-point responses, they result in poor load disturbance rejection for integrating/lag-dominant plants (Chien and Fruehauf, 1990; Horn *et al.*, 1996). Alternative PID tuning rules aimed at good regulatory performance can be consulted in (Horn *et al.*, 1996; Shamsuzzoha and Lee, 2007). In (Skogestad, 2003), remarkably simple tuning rules which provide balanced servo/regulator performance are proposed based on a modification of the settings in (Rivera *et al.*, 1986). It is important to realize that the problems with the original IMC-based tunings come indeed from inherent shortcomings of the IMC procedure, thoroughly revised in (Dehghani *et al.*, 2006).

The purpose of this chapter is to present an $\mathcal{H}_\infty$ design which avoids some

of the limitations of the IMC method, while retaining its simplicity as much as possible. In particular, the method is devised to work well for plants of modest complexity, for which analytical PID tuning is plausible.

Roughly speaking, the design procedure associated with modern $\mathcal{H}_\infty$ control theory involves the selection of frequency weights which are used to shape prescribed closed-loop transfer functions. Many practitioners are reluctant to use this methodology because it is generally difficult to design the frequency weights properly. At the end of the day, it is quite typical to obtain high-order controllers, which may require the use of model order reduction techniques. Apart from the cumbersome design procedure, control engineers usually find the general theory difficult to master as well. To alleviate the above difficulties, we rely here on the plain $\mathcal{H}_\infty$ weighted sensitivity problem (WSP). By investigating its analytical solution, the involved frequency weight is chosen systematically in such a way that a good design in terms of basic conflicting trade-offs can be attained. The main contributions of the proposed procedure are:

1. The selection of the weight is *systematic* (this is not common in $\mathcal{H}_\infty$ control) and *simple*, only depending on two types of parameters:
   - One adjusts the robustness/performance trade-off as in the IMC approach.
   - The other one allows to balance the performance between the servo and regulator modes. As it will be explained, this can be interpreted in terms of a mixed S/SP sensitivity design.
2. The method is *general*: both stable and unstable plants are dealt with in the same way. This differs from other analytical $\mathcal{H}_\infty$ procedures.
3. The controller is derived *analytically*. For simple models, this leads to well-motivated PID tuning rules which consider the stable/unstable plant cases simultaneously.

The rest of the chapter is organized as follows: Section 6.2 presents the proposed design method, based on the $\mathcal{H}_\infty$ WSP, while Section 6.3 deals with its application to analytical tuning of PI controllers. Simulation examples are given in Section 6.4 to emphasize the new features of the proposed approach. Finally, Section 6.5 contains a summary of the chapter.

6.2 Proposed design procedure

The proposed approach stems from considering the WSP (Zames and Francis, 1983; Skogestad and Postlethwaite, 2005):

$$\begin{aligned} |\rho| &= \min_{K\in\mathcal{C}} \|\mathcal{N}\|_\infty \\ &= \min_{K\in\mathcal{C}} \left\| \mathcal{F}_l\left(\left[\begin{array}{c:c} W & -WP \\ \hdashline 1 & -P \end{array}\right], K \right) \right\|_\infty \\ &= \min_{K\in\mathcal{C}} \|WS\|_\infty \end{aligned} \tag{6.1}$$

6.2.1 Analytical solution

Before selecting W to shape S, we will look for an analytical solution of (6.1). The classical design found in (Francis, 1987; Doyle *et al.*, 1992) consists of transforming (6.1) into a Model Matching Problem (MMP) using the Youla-Kucera parameterization (Youla *et al.*, 1976). From an analytical point of view, the problem with this parameterization is the need of computing a coprime factorization when P is unstable. In order to deal with stable and unstable plants in a unified way, it would be desirable to avoid any notion of coprime factorization. Towards this objective, the key point is to use a possibly unstable weight:

Theorem 6.2.1. *Assume that P is purely rational (i.e., there is no time delay in P) and has at least one Right Half-Plane (RHP) zero. Take W as a MP weight including the unstable poles of P. Then, the optimal weighted sensitivity in problem (6.1) is given by*

$$\mathcal{N}^o = \rho \frac{q(-s)}{q(s)} \tag{6.2}$$

where ρ and $q = 1 + q_1 s + \cdots + q_{\nu-1} s^{\nu-1}$ (Hurwitz) are uniquely determined by the interpolation constraints:

$$W(z_i) = \mathcal{N}^o(z_i) \qquad i = 1 \ldots \nu, \tag{6.3}$$

being $z_1 \ldots z_\nu$ ($\nu \geq 1$) the RHP zeros of P.

Proof. The following *change of variable* (or IMC parameterization (Morari and Zafiriou, 1989))

$$K = \frac{Q}{1 - PQ} \tag{6.4}$$

puts $H(P, K)$ in the simpler form

$$H(P, K) = \begin{bmatrix} PQ & (1 - PQ)P \\ Q & 1 - PQ \end{bmatrix} \tag{6.5}$$

As shown in (Morari and Zafiriou, 1989), internal stability is then equivalent to

- $Q \in \mathcal{RH}_\infty$
- $S = 1 - PQ$ has zeros at the unstable poles of P

The weighted sensitivity $WS = W(1 - PQ) = \mathcal{N}^o$ in (6.2) is achieved by

$$Q_0 = P^{-1}(1 - \mathcal{N}^o W^{-1}) \tag{6.6}$$

First, we must verify that Q_0 is internally stabilizing. That $Q_0 \in \mathcal{RH}_\infty$ follows from the interpolation constraints (6.3). On the other hand, $S = 1 - PQ_0 = \mathcal{N}^o W^{-1}$ is such that $S = 0$ at the unstable poles of P (because W contains them by assumption). Now that internal stability has been verified, it remains to be proved that Q_0 (equivalently $\mathcal{N}^o$) is optimal. For this purpose, we use the result, proved in (Morari and Zafiriou, 1989), that the set of internally stabilizing Q's can be expressed as

$$\mathcal{Q} = \{Q : Q = Q_0 + \Upsilon Q_1\} \tag{6.7}$$

where $Q_1 \in \mathcal{RH}_\infty$ is any stable transfer function, and $\Upsilon \in \mathcal{RH}_\infty$ has (exclusively) two zeros at each closed RHP pole of P (the exact shape of Υ is not necessary for the proof). Hence, any admissible weighted sensitivity has the form

$$\begin{aligned} W(1 - PQ) &= W(1 - P[Q_0 + \Upsilon Q_1]) \\ &= W(1 - PQ_0) - WP\Upsilon Q_1 \\ &= \mathcal{N}^o - WP\Upsilon Q_1 \end{aligned}$$

Minimizing $\|\mathcal{N}^o - WP\Upsilon Q_1\|_\infty$ is a standard MMP in terms of Q_1, with $T_1 = \mathcal{N}^o \in \mathcal{RH}_\infty, T_2 = WP\Upsilon \in \mathcal{RH}_\infty$. From Lemma 1.2.1, the optimal error $\mathcal{E}^o = T_1 - T_2Q_1$ is all-pass and completely determined by the RHP zeros of T_2, which are those of P. More concretely, for each RHP zero of P, we have the interpolation constraint $\mathcal{E}^o(z_i) = \mathcal{N}^o(z_i)$. Obviously, this implies that $\mathcal{E}^o = \mathcal{N}^o$. Equivalently, the optimal solution is achieved for $Q_1 = 0$, showing that Q_0 is indeed optimal. □

Once the optimal weighted sensitivity has been determined, the following corollary of Theorem 6.2.1 gives the corresponding (complementary) sensitivity function and feedback controller:

Corollary 6.2.1. *Consider the following factorizations:*

$$P = \frac{n_p}{d_p} = \frac{n_p^+ n_p^-}{d_p^+ d_p^-} \qquad W = \frac{n_w}{d_w} = \frac{n_w}{d_w' d_p^+} \tag{6.8}$$

where n_p^+, d_p^+ contain the unstable (or slow in the case of d_p^+) zeros of n_p, d_p, respectively. Similarly, n_p^-, d_p^- contain the stable zeros of n_p, d_p. Then,

$$S = \mathcal{N}^o W^{-1} = \rho \frac{q(-s) d_w}{q(s) n_w} \tag{6.9}$$

$$T = 1 - \mathcal{N}^o W^{-1} = \frac{n_p^+ \chi}{q(s) n_w} \tag{6.10}$$

$$K = \left(\frac{1 - \mathcal{N}^o W^{-1}}{\mathcal{N}^o W^{-1}} \right) P^{-1} = \frac{d_p^- \chi}{\rho n_p^- q(-s) d_w'} \tag{6.11}$$

where χ is a polynomial such that

$$q(s) n_w - \rho q(-s) d_w = n_p^+ \chi \tag{6.12}$$

Proof. The optimal Weighted Sensitivity $\mathcal{N}^o$ corresponds to

$$S = \mathcal{N}^o W^{-1} \quad \text{and} \quad T = 1 - \mathcal{N}^o W^{-1} \tag{6.13}$$

From the definitions of S and T, the feedback controller can be expressed as

$$K = \frac{T}{S} P^{-1} = \frac{1 - \mathcal{N}^o W^{-1}}{\mathcal{N}^o W^{-1}} P^{-1} \tag{6.14}$$

Furthermore, the interpolation constraints (6.3) guarantee that $Q_0 \in \mathcal{RH}_\infty$. Thus, there exists a polynomial χ such that (6.6) can be rewritten as

$$Q_0 = \frac{d_p}{n_p^+ n_p^-}\left(\frac{q(s)n_w - \rho q(-s)d_w}{q(s)n_w}\right) = \frac{d_p \chi}{n_p^- q(s) n_w} \tag{6.15}$$

where the factorizations in (6.8) have been used. In terms of Q_0, we have that $S = 1 - PQ_0, T = PQ_0$ and $K = \frac{Q_0}{1-PQ_0}$. Finally, straightforward algebra yields the polynomial structure of equations (6.9)–(6.11). □

Remark 6.2.1. *It is noteworthy that the feedback controller (6.11) is realizable only if P is biproper. Hence, in practice, it may be necessary to add fictitious high-frequency zeros to the initial model to meet this requirement.*

6.2.2 Selection of W

Let us denote by $\tau_1, \ldots, \tau_k$ the time constants of the unstable or slow poles of P. Equation (6.9) reveals that, except by the factor ρ, $|S|$ is determined by $|W^{-1}|$ ($\mathcal{N}^o$ is all-pass). Based on (6.9) and (6.10), the following structure for the weight is proposed

$$W(s) = \frac{(\lambda s + 1)(\gamma_1 s + 1)\cdots(\gamma_k s + 1)}{s(\tau_1 s + 1)\cdots(\tau_k s + 1)} \tag{6.16}$$

where $\lambda > 0$, and

$$\gamma_i \in [\lambda, |\tau_i|] \tag{6.17}$$

The rationale behind the choice of W in (6.16) is further explained below:

- Let us start assuming that $k = 0$ (i.e., $W = \frac{\lambda s+1}{s}$). The integrator in W forces $S(0) = 0$ for integral action. From (6.10), the term $(\lambda s + 1)$ in the numerator of W appears in the denominator of the input-to-output transfer function. Consequently, the closed-loop will have a pole $s = -1/\lambda$. The idea is to use λ to determine the speed of response, as in standard IMC.

- If P has slow stable poles, it is necessary that S cancels them if disturbance rejection is the main concern. Otherwise, they will appear in the transfer function $T_{yd} = SP$, making the response sluggish. This is why W also contains these poles. As a result, slow (stable) and unstable poles

are treated basically in the same way. This unified treatment ensures internal stability in terms of the generalized $\mathcal{D}$-stability region of Figure 6.1.

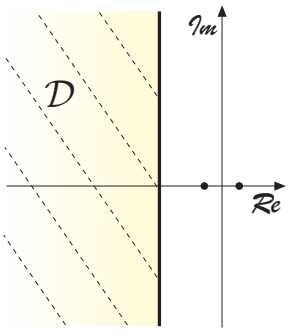

Figure 6.1: General stability region: slow and unstable poles are $\mathcal{D}$-unstable.

- As it has been said, producing $S(-1/\tau_i) = 0,\ i = 1, \ldots, k$ is necessary for internal stability and disturbance rejection. Notice, however, that these constraints mean decreasing $|S|$ at low frequencies. By a waterbed effect argument (Skogestad and Postlethwaite, 2005), recall the Bode's Sensitivity Integral:

$$\int_0^\infty |S(j\omega)| d\omega = \pi \sum_{i,\tau_i<0}^{k} |\tau_i|^{-1}, \tag{6.18}$$

  this will augment $|S|$ at high frequencies, maybe yielding an undesirable peak (M_S) on it. This, in turn, will probably augment the peak of $|T|$ (M_T) and the overshoot in the set-point response. In order to alleviate these negative effects, for each slow/unstable pole of P, we introduce a factor $(\gamma_i s + 1)$ in the numerator of W: as $\gamma_i \nearrow |\tau_i|$, $\left|\frac{\tau_i j\omega+1}{\gamma_i j\omega+1}\right| \searrow 1$; the resulting flatter frequency response will reduce the overshoot (improving the robustness properties, see Section 6.2.3) at the expense of settling time.

- We have supposed that $\lambda < |\tau_i|\ \forall k = 1 \ldots k$. In other words, we are considering relatively slow plants: for stable plants without slow poles,

the standard IMC procedure will provide good results in terms of tracking and disturbance rejection; there is no conflict between T_{yr} and T_{yd}. Note, in addition, that forcing $S = 0$ ($T = 1$) at high frequency is undesirable from a robustness point of view. This is why we discard rapid stable poles from the denominator of W. If the plant is unstable, there is no option and one has to force $S = 0$ ($T = 1$) at the rapid unstable poles, which imposes a minimum closed-loop bandwidth.

Essentially, there are two tuning parameters in W: λ is intended to tune the robustness/performance compromise. The set of numbers γ_i allow us to balance the performance between the servo and regulator modes. The latter point can be interpreted in terms of a mixed S/SP sensitivity design: let us assume that $\lambda \approx 0$. Then, when $\gamma_i = |\tau_i|$ (servo tuning), we have that $|WS| \approx |S/s|$ and we are minimizing the peak of $|S|$ ($= |T_{er}|$) subject to integral action. In the other extreme, if $\gamma_i = \lambda$ (regulator tuning), the poles of P appear in W. If the zeros of P are sufficiently far from the origin, we have that $|WS| \approx |SP/s|$ in the low-middle frequencies. Heuristically, we are minimizing the peak of $|SP|$ ($= |T_{yd}|$) subject to integral action.

Remark 6.2.2. *Let us consider that P has a RHP pole at $s = -1/\tau_i$ ($\tau_i < 0$) and a RHP zero at $s = z_i$. Then, from (6.3) and (6.16), it follows that*

$$\left|\frac{1}{\tau_i z_i + 1}\right| \left|\frac{(\lambda z_j + 1)\prod_{j=1}^{k}(\gamma_j z_j + 1)}{z_j \prod_{j=1, j\neq i}^{k}(\tau_j z_j + 1)}\right| = |\rho| \left|\frac{q(-z_i)}{q(z_i)}\right| \tag{6.19}$$

As the RHP pole $-1/\tau_i$ and the RHP zero z_i get closer to each other, $\tau_i z_i \to -1$, which makes the left hand side grow unbounded. Since $\left|\frac{q(-z_i)}{q(z_i)}\right| \leqslant 1$, $|\rho| \to \infty$. Note that this happens regardless the values of λ and the γ_j's, and obeys the fact that plants with unstable poles and zeros close to each other are intrinsically difficult to control (Morari and Zafiriou, 1989).

Remark 6.2.3. *For simplicity, the γ_i parameters could be determined from a single parameter $\gamma \in [0, 1]$ as indicated below:*

$$(\gamma_1, \ldots, \gamma_k)^T = (1 - \gamma)(\lambda, \ldots, \lambda)^T + \gamma(|\tau_1|, \ldots, |\tau_k|)^T \tag{6.20}$$

6.2.3 Stability and Robustness

Because of the assumptions in Theorem 6.2.1, the possible delay of the plant must be approximated by a non-minimum phase rational term. This approximation creates a mismatch between P (the purely rational model used for design) and the nominal model containing the time delay, let us call it P_o. The following sufficient condition for Nominal Stability can be derived from the conventional Nyquist stability criterion (Skogestad and Postlethwaite, 2005):

Proposition 6.2.1. *Assume that P is internally stabilized by K, and that P and P_o have the same RHP poles. Then, K internally stabilizes P_o if*

$$\left|\frac{L_o - L}{1 + L}\right| < 1 \ \forall \omega \in \Omega_{pc} \tag{6.21}$$

where $L = PK, L_o = P_oK$, and $\Omega_{pc} = \left\{\omega : \angle\left(\frac{L_o - L}{1+L}\right) = -\pi + 2\pi n,\ n \in \mathbb{Z}\right\}$ is the set of phase crossover frequencies of $\frac{L_o - L}{1+L}$.

Figure 6.2 illustrates the situation graphically for a stable plant: the distance from L to the point $(-1, 0)$ must exceed $|L_o - L|$ when the *vectors* $L_o - L$ and $-1 - PK$ are aligned. Rather than using Proposition 6.2.1, a more practical approach is to check Robust Stability with respect to P (Skogestad and Postlethwaite, 2005; Morari and Zafiriou, 1989), including P_o in the uncertain set under consideration (Vilanova, 2008). Generally, the way in which λ and γ_i influence robustness is:

- Augmenting λ decreases the closed-loop bandwidth, making the system more robust and less sensitive to noise.
- Decreasing γ_i improves the disturbance rejection, but increases the overshoot in the set-point response to the detriment of robustness.

These robustness implications can be understood in terms of the Robust Stability condition $\|\Delta T\|_\infty < 1$ (equivalently $|T| < 1/|\Delta|\ \forall\omega$), where Δ models the multiplicative plant uncertainty (Skogestad and Postlethwaite, 2005). Augmenting λ makes the system slower, which favours Robust Stability. On the other hand, decreasing γ_i increments the peak of $|T|$ (responsible for the overshoot increment), which limits the amount of multiplicative uncertainty.

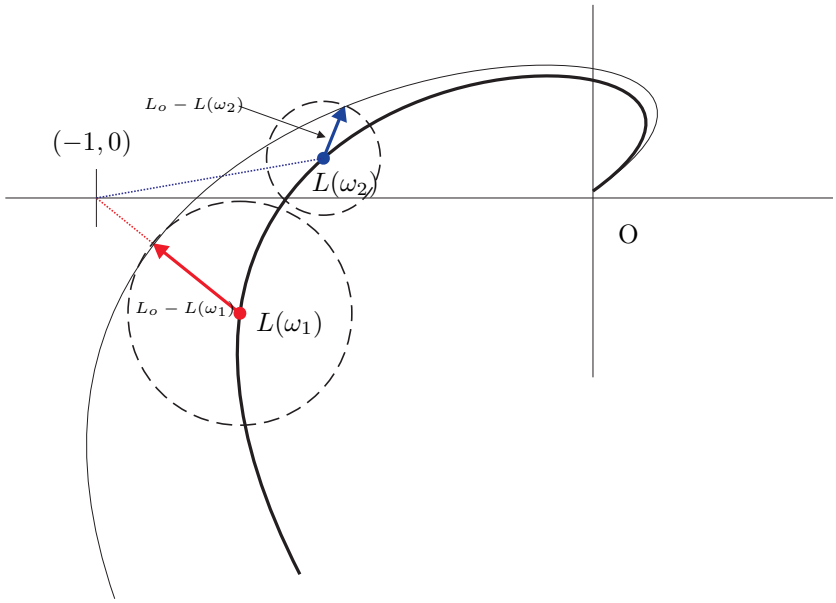

Figure 6.2: Stability condition for P_o in terms of P. The magnitude condition $|1 + L| > |L_o - L|$ must be true for ω_1 (which is a phase crossover frequency, i.e., $\omega_1 \in \Omega_{pc}$), but not for ω_2.

6.3 Application to PI tuning

This section deals with the application of the presented design method to the tuning of PI compensators.

6.3.1 Stable/unstable plants

Let us consider the First Order Plus Time Delay (FOPTD) model given by $P_o = K_g \frac{e^{-sh}}{\tau s+1}$, where K_g, h, τ are, respectively, the gain, the (apparent) delay, and the time constant — negative in the unstable case — of the process. For design purposes, we take

$$P = K_g \frac{-sh + 1}{\tau s + 1} \tag{6.22}$$

where a first order Taylor expansion has been used to approximate the time delay. From (6.16) and (6.22), with $k = 1$, the following weight results

$$W = \frac{(\lambda s + 1)(\gamma s + 1)}{s(\tau s + 1)} \tag{6.23}$$

where $\lambda > 0, \gamma \in [\lambda, |\tau|]$. The optimal weighted sensitivity is determined from (6.3). In this case, P has a single RHP zero ($\nu = 1$), and $\mathcal{N}^o$ becomes

$$\mathcal{N}^o = \rho = \frac{(\lambda + h)(\gamma + h)}{\tau + h} \tag{6.24}$$

From (6.11), the controller is finally given by

$$K = \frac{\chi}{K_g \rho s} \tag{6.25}$$

where

$$\chi = \frac{\tau(h + \lambda + \gamma) - \lambda\gamma}{\tau + h} s + 1 \tag{6.26}$$

The feedback controller (6.25) can be cast into the PI structure:

$$K = K_c \left(1 + \frac{1}{T_i s}\right) \tag{6.27}$$

according to the tuning rule in the first row of Table 6.1.

Table 6.1: Proposed PI tuning rules.

Model	K_c	T_i	
$K_g \frac{e^{-sh}}{\tau s+1}$	$\frac{1}{K_g} \frac{T_i}{\lambda+\gamma+h-T_i}$	$\frac{\tau(h+\lambda+\gamma)-\lambda\gamma}{\tau+h}$	$\lambda > 0, \gamma \in [\lambda, \lvert\tau\rvert]$
$K_g \frac{e^{-sh}}{s}$	$\frac{1}{K_g} \frac{T_i}{\lambda\gamma+hT_i}$	$h + \lambda + \gamma$	$\lambda > 0, \gamma \in [\lambda, \infty)$

Essentially, the trade-off between disturbance rejection and set-point tracking is controlled by T_i. This can be verified by considering the proposed PI settings for the extreme values of γ. This has been done in Table 6.2 for the stable plant case ($\tau > 0$). Certainly, T_i is the parameter which varies more with γ: K_c varies from $\frac{1}{K_g}\frac{\tau}{\lambda+h}$ to $\frac{1}{K_g}\frac{\tau}{\lambda+h}\left(\frac{h+2\lambda-\lambda^2/\tau}{h+\lambda}\right)$ as γ is decreased from τ to λ. This way, as we improve disturbance rejection, the controller gain

Table 6.2: PI tuning rules for the extreme values of γ.

$\gamma = \lambda$		$\gamma = \tau$	
K_c	T_i	K_c	T_i
$\frac{1}{K_g}\frac{\tau}{\lambda+h}\left(\frac{h+2\lambda-\lambda^2/\tau}{h+\lambda}\right)$	$\frac{\tau(h+2\lambda)-\lambda^2}{\tau+h}$	$\frac{1}{K_g}\frac{\tau}{\lambda+h}$	τ

increases. The multiplicative factor $\frac{h+2\lambda-\lambda^2/\tau}{h+\lambda}$ equals one when $\lambda = \tau$. If $\tau \gg h, \lambda$, then $\frac{h+2\lambda-\lambda^2/\tau}{h+\lambda} \approx \frac{h+2\lambda}{h+\lambda} < 2$, which shows that K_c augments moderately in the transition to the regulator mode. Based on these facts, it is reasonable to select $K_c = \frac{1}{K_g}\frac{\tau}{\lambda+h}$, and fix T_i for good servo/regulation tradeoff. This strategy is the essence of the SIMC tuning rule for stable plants (Skogestad, 2003).

Next, we will compare the input-to-output transfer functions achieved for the extreme values of γ. For small values of the time delay, $n_p^+ = -sh+1 \approx 1$, and equation (6.10) (with $q(s) = 1, \chi = \zeta s + 1, n_w = (\lambda s + 1)(\gamma s + 1)$) allows us to write:

$$|T(j\omega)| \approx \left|\frac{1}{\lambda j\omega + 1}\right| \left|\frac{\zeta j\omega + 1}{\gamma j\omega + 1}\right| \tag{6.28}$$

For a lag-dominant plant, the following approximations are valid:

- When $\gamma = \lambda$, the closed-loop magnitude is

$$|T(j\omega)| \approx \left|\frac{1}{\lambda j\omega + 1}\right| \left|\frac{\left(\frac{\tau(h+2\lambda)-\lambda^2}{\tau+h}\right) j\omega + 1}{\lambda j\omega + 1}\right| \approx \left|\frac{1}{\lambda j\omega + 1}\right| \left|\frac{(h+2\lambda) j\omega + 1}{\lambda j\omega + 1}\right| \tag{6.29}$$

- When $\gamma = |\tau|$, we have that

$$|T(j\omega)| \approx \left|\frac{1}{\lambda j\omega + 1}\right| \tag{6.30}$$

  for the stable plant case ($\tau > 0$). If P is unstable ($\tau < 0$), T is such that

$$\begin{aligned} |T(j\omega)| &\approx \left|\frac{1}{\lambda j\omega + 1}\right| \left|\frac{\left(\frac{\tau(h+\lambda+|\tau|)-\lambda|\tau|}{\tau+h}\right) j\omega + 1}{|\tau| j\omega + 1}\right| \\ &\approx \left|\frac{1}{\lambda j\omega + 1}\right| \left|\frac{(h+2\lambda+|\tau|) j\omega + 1}{|\tau| j\omega + 1}\right| \end{aligned} \tag{6.31}$$

Therefore, as the value of γ is increased, the pole and the zero of $\frac{\zeta s+1}{\gamma s+1}$ in (6.28) get closer to each other, reducing the overshoot and providing flatter frequency response.

6.3.2 Integrating plant case ($\tau \to \infty$)

If the plant under control is integrating, it can be modelled by an Integrator Plus Time Delay (IPTD) model: $P_o = \frac{K_g e^{-sh}}{s}$. For this case, we take

$$P = K_g \frac{-sh+1}{s} \tag{6.32}$$

The corresponding weight is chosen as

$$W = \frac{(\lambda s+1)(\gamma s+1)}{s^2} \tag{6.33}$$

where $\lambda > 0, \gamma \in [\lambda, \infty)$. The optimal weighted sensitivity becomes

$$\mathcal{N}^o = \rho = (\lambda + h)(\gamma + h) \tag{6.34}$$

From (6.11),

$$K = \frac{1}{K_g} \frac{\zeta' s + 1}{(\lambda\gamma + h\zeta')s} \tag{6.35}$$

where

$$\zeta' = h + \lambda + \gamma \tag{6.36}$$

The associated PI tuning rule can be consulted in the second row of Table 6.1. Alternatively, the tuning rules for the IPTD model could have been derived by taking the limit $\tau \to \infty$ in the FOPTD settings, considering the approximation $K_g \frac{e^{-sh}}{\tau s+1} = \frac{K_g}{\tau} \frac{e^{-sh}}{s+1/\tau} \approx \frac{K_g}{\tau} \frac{e^{-sh}}{s}$.

6.4 Simulation examples

This section evaluates the tuning rules given in Table 6.1 through four simulation examples. Examples 1–3 emphasize that the design presented in Section 6.2 generalizes standard IMC. The purpose of the fourth example is to illustrate that, for simple plants and modest specifications, the presented design overcomes basic limitations of IMC, thus not being advisable to embark on more complex strategies. A summary of the controller settings for Examples 1–4 can be consulted in Table 6.3.

6.4.1 Example 1

The IMC-based PI tuning rule for stable FOPTD processes is given by (Morari and Zafiriou, 1989):

$$K_c = \frac{1}{K_g}\frac{\tau}{\lambda + h} \qquad T_i = \tau \tag{6.37}$$

In this example, the following concrete process $\frac{e^{-0.073s}}{1.073s+1}$ is considered. Regarding the λ parameter, two different values are chosen in order to achieve *smooth* ($\lambda = 0.10731$) and *tight* ($\lambda = 0.05402$) control (Ali and Majhi, 2009), resulting into: $K_c^{sm} = 5.88, T_i^{sm} = 1.073$, and $K_c^{ti} = 8.38, T_i^{ti} = 1.073$. In the smooth control case, $M_S = 1.38$, whereas in the tight control case, $M_S = 1.71$. The associated disturbance responses are shown in Figure 6.3. As it can be seen,

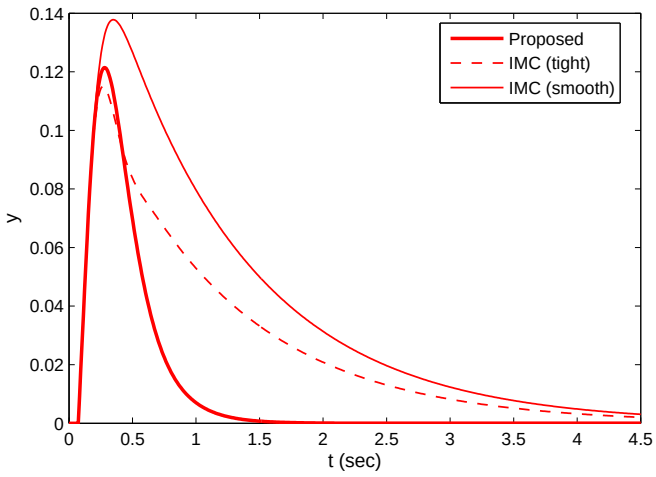

Figure 6.3: Load disturbance response for Example 1.

it is possible to reduce the magnitude of the disturbance rejection response by decreasing λ. However, the conventional IMC-based tuning continues to exhibit poor disturbance attenuation even for the tight case. To the detriment of robustness, decreasing further the value of λ would improve the regulatory performance a little, but the response would continue to be sluggish. Accordingly, it is not possible to get both good regulatory performance and good robustness for the process under examination.

In the design of Section 6.2, setting $\gamma = \lambda$ produces an improvement of the regulation performance. Consequently, the problem reduces now to finding a value for λ providing the prescribed robustness level. This is achieved for $\lambda = 0.1752$, which yields $M_S = 1.6551$. The corresponding time response is depicted in Figure 6.3.

It should be noted that the poor disturbance attenuation obtained through conventional IMC can be remedied in several (more *ad hoc*) ways. For example, approximating the process at hand by an integrating one (Chien and Fruehauf, 1990). Then, conventional IMC design gives satisfactory disturbance rejection. A limitation of this approach is that it does not consider the servo/regulator trade-off. Other IMC-based approaches for improved regulatory performance can be found in (Horn *et al.*, 1996; Shamsuzzoha and Lee, 2007). However, even for the simple FOPTD model, these approaches require a more complicated control structure (PID or PID plus filter). Overall, the presented tuning rules are simpler and more instructive.

Table 6.3: Tuning of λ, γ (and corresponding PI settings) for Examples 1–4.

Ex.	Model	λ	γ	K_c	T_i	Design type
1	$\frac{e^{-0.073s}}{1.073s+1}$	0.1752	0.1752	6.8765	0.3696	Regulator
2	$\frac{e^{-0.073s}}{1.073s+1}$	0.146	1.073	4.8995	1.0730	Servo (=IMC)
		0.146	0.4	5.8481	0.5286	Servo/Regulator
		0.146	0.146	7.7215	0.3231	Regulator
3	$\frac{e^{-s}}{-20s+1}$	2	2	-11.56	5.4737	Regulator (≈IMC)
		0.9	9	-11.9	11.9	Servo/Regulator
4	$\frac{-1}{-s+1} \approx \frac{-e^{-0.01s}}{-s+1}$	0.1	0.1	18.2	0.22	Regulator (≈IMC)
		0.1	1	10.9	1.22	Servo
		0.1	14	10.0642	15.667	Servo ($K \approx 10$)

6.4.2 Example 2

Generally speaking, the γ parameter allows to balance the performance between set-point tracking and disturbance rejection. To clarify this, we will

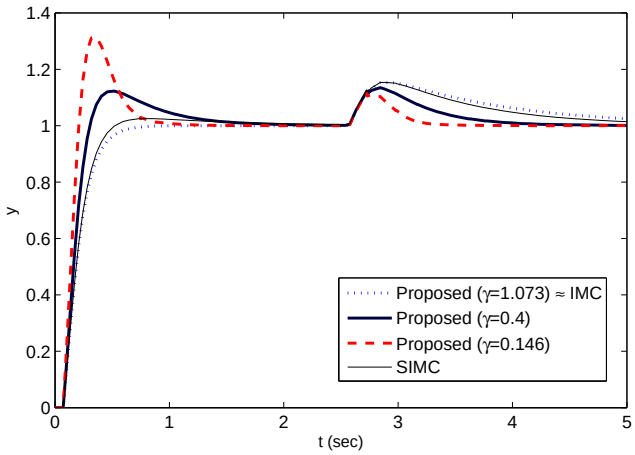

Figure 6.4: Tracking and disturbance responses for Example 2.

continue Example 1, selecting $\lambda = 2h = 0.146$ and considering three different values for γ. The first value is $\gamma = \tau = 1.073$ (servo tuning). The resulting design is identical to the conventional IMC one. The second value is $\gamma = \lambda = 0.146$ (regulator tuning). Finally, we set $\gamma = 0.4$ for balanced servo/regulator performance. Figure 6.4 shows the three time responses. We have also included the SIMC tuning rule (Skogestad, 2003):

$$K_c = \frac{1}{K_g}\frac{\tau}{\lambda + h} \qquad T_i = \min\left\{\tau, 4(\lambda + h)\right\}, \tag{6.38}$$

which was presented as a modification of the original settings (6.37) to improve the regulatory performance. Note, however, that in the *edge case* $\tau \approx 4(\lambda+h)$, there is no difference between (6.38) and (6.37). This is the situation in this example: $\tau = 1.073$ is close to $4(\lambda + h) = 0.876$. Looking at Figure 6.4, it is confirmed that the SIMC tuning gives approximately the same responses as conventional IMC. Lacking a rigorous analysis (this is not the intention here), the proposed PI tuning rule with $\gamma = 0.4$ seems to offer a better overall compromise. Finally, it is remarkable that, whereas the SIMC rule was derived only considering stable plants, the proposed tuning rule unifies the stable/unstable cases.

6.4.3 Example 3

For unstable plants, the IMC filter may cause large overshoot and poor robustness due to the large peak in the filter frequency response (Campi *et al.*, 1994; Dehghani *et al.*, 2006). The search of new filters to alleviate these shortcomings has resulted in more complicated (and application-specific) procedures (Campi *et al.*, 1994). In this example we deal with an unstable plant, analyzing how the proposed method, albeit simple, can mitigate these negative effects. Let us consider the unstable process $\frac{e^{-s}}{-20s+1}$. The IMC controller is such that $T = e^{-s}f$, where $f = \frac{a_1 s+1}{(\lambda s+1)^2}$ and $a_1 = 20\left(e^{1/20}(\lambda/20+1)^2 - 1\right)$. Suppose that $\lambda = 2$ produces the desired closed-loop bandwidth, then $a_1 = 5.4408$. The feedback controller is $K = (-20s+1)\frac{f}{1-e^{-s}f}$, which is not purely rational. Approximating $e^{-s} \approx -sh + 1$, we finally obtain

$$K_{imc} = \frac{-11.53s^2 - 1.542s + 0.1059}{s^2 - 0.04669s} \tag{6.39}$$

As for the proposed method, we start considering the initial tuning $\lambda = 2, \gamma = \lambda$. Figure 6.5 (Nominal Case) shows that this design is almost identical to the IMC one. Both K_{imc} and the proposed PI provide excellent disturbance rejection. However, it could be desirable to reduce the overshoot in the set-point response or improve the robustness properties. Within the IMC procedure, the only way to it is to roll-off the controller (increasing λ), making the system slower. Contrary to this, if we take $\lambda = 0.9, \gamma = 9 \in [0.9, 20] = [\lambda, |\tau|]$, it can be seen from Figure 6.5 (Nominal Case) that it is possible to reduce the overshoot (at the expense of disturbance attenuation and settling time) without slowing down the system. Figure 6.6 depicts the frequency response of $|S|$ and $|T|$. Recalling Section 6.2.3, the reduction of M_S and M_T confers more robustness and smoother control, as confirmed in Figure 6.5 (Uncertain Case), where the real plant delay is assumed to be $h = 1.6$ instead of one. Certainly, the new settings provide the best responses in both set-point tracking and disturbance attenuation.

6.4.4 Example 4

Finally, we revisit the design method in (Dehghani *et al.*, 2006) (briefly summarized in Section 1.1.3). This $\mathcal{H}_\infty$ procedure was devised to generalize IMC: in particular, for unstable plants, it allows to use a different filter from that

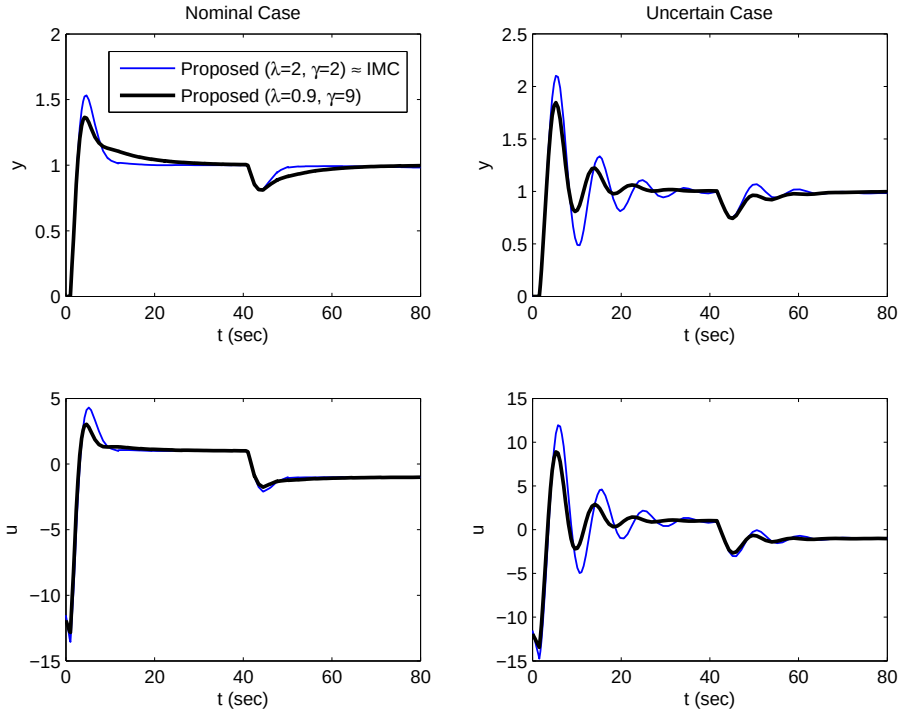

Figure 6.5: Tracking and disturbance responses for Example 3.

in (1.3), hence proving more flexible. The following design example, taken from (Dehghani *et al.*, 2006), makes it clear: given the unstable plant $\frac{-1}{-s+1}$ ($P_a = 1, P_m = \frac{-1}{-s+1}$), the controller is designed in order to achieve a closed-loop response similar to $\frac{1}{0.1s+1}$, that corresponds to $f = \frac{1}{0.1s+1}$ in problem (1.6). This specification is coherent, in the sense that the desired closed-loop bandwidth is considerably beyond the unstable pole frequency (Dehghani *et al.*, 2006). Note that $P_a f|_{s=1,0} \approx 1$, taking into account internal stability constraints and zero steady state error (unity low frequency gain). The desired closeness between T and $P_a f = \frac{1}{0.1s+1}$ is specified by the inequality $\|T - P_a f\|_\infty < \alpha$, with $\alpha = 0.1$. In addition, it is assumed that the actuators can pump up a maximum gain of 10 ($\beta_c = 10$). The frequency cost ϵ_1 is chosen to gradually reach the maximum gain $\alpha/10$ as the plant model loses

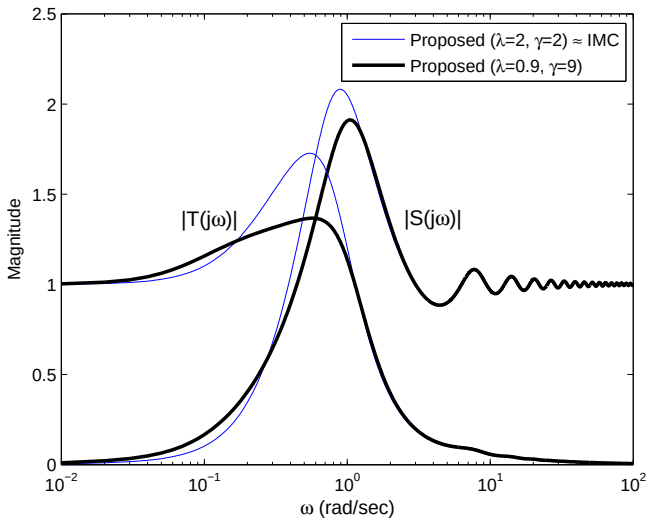

Figure 6.6: Magnitude frequency responses of S and T for Example 3. For $\lambda = 0.9, \gamma = 9$, the peaks of $|S|$ and $|T|$ are decreased without reducing the closed-loop bandwidth.

its bandwidth to the controller. Finally, $\epsilon_2 = 0$. Solving (1.6) leads to the $\mathcal{H}_\infty$ controller

$$K_\infty = \frac{1.099 \times 10^6 (s + 18.34)(s^2 + 6s + 9)}{(s + 1.15 \times 10^5)(s + 17.14)(s^2 + 5.94s + 8.85)} \tag{6.40}$$

and the flag $\rho = 0.1 \leqslant \alpha$. This (supported by the discussion in Section 1.1.3) means that the desired objectives have been achieved. Figure 6.7 depicts the results both in the frequency and the time domain[1]. In view of Figure 6.7, it is clear that K_∞ does not provide integral action, even if $f|_{s=0} = 1$. As claimed in (Lee and Shi, 2008), where this and other pitfalls in applying the design in (Dehghani *et al.*, 2006) are highlighted, there are two possible sources of difficulty: first, the fact that $f|_{s=1}$ is not exactly one, as required by the unstable plant pole at $s = 1$. Second, the fact that $\epsilon_1 \neq 0$ or $\epsilon_2 \neq 0$, as it is also the case in this example.

[1]These plots are absent in (Dehghani *et al.*, 2006).

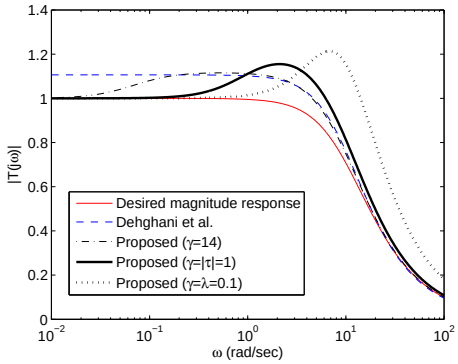

(a) Frequency responses.

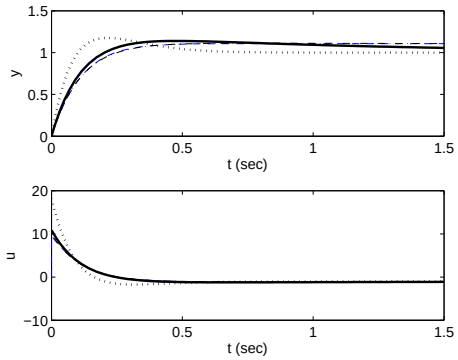

(b) Set-point responses.

Figure 6.7: Frequency and time responses for Example 4.

In what follows, we will inspect the results obtained with the proposed method, leaving the λ parameter fixed at $\lambda = 0.1$. Let us approximate $\frac{-1}{-s+1} \approx -\frac{e^{-0.01}}{-s+1}$ in order to apply the tuning rules of Table 6.1. We start by selecting $\lambda = 0.1, \gamma = \lambda$, but the actuator limits are violated. In order to adhere to the given specifications, we take $\gamma = 1$, which almost verifies the actuator restriction. As a matter of fact, we can make the closed-loop closer to $f = \frac{1}{0.1s+1}$ by increasing further the value of γ (the additional value $\gamma = 14$ has been considered). From Figure 6.7, it is evident that the proposed method always provides integral action. When $\gamma \to \infty$, a proportional controller $K = 10$ is

obtained, for which the closed-loop is $\frac{1}{0.1s+0.9} \approx \frac{1}{0.1s+1}$. It is remarkable that K_∞ can be handcrafted into such a plain gain too, yielding the same results as the original fourth-order controller. However, in (Dehghani *et al.*, 2006), the application of a model reduction algorithm only lowered the order of K_∞ to three. This point stresses that care has to be taken when using/implementing numerical designs. For the particular case at hand, $\gamma = 1$ gives a compromise between the desired magnitude response, control effort, controller complexity, and the inclusion of integral action in the loop. Obviously, the proposed design may be insufficient for more stringent specifications. In these cases, the more flexible procedure in (Dehghani *et al.*, 2006) reveals advantageous.

6.5 Summary

This chapter has presented an analytical $\mathcal{H}_\infty$ design method based on minimizing the weighted sensitivity function. The proposed weight, chosen in a systematic way, guarantees internal stability. This point helps unifying the treatment of stable/unstable plants, avoiding the notion of coprime factorization. Another important feature of the proposed procedure is that it allows to balance the performance between the *servo* and *regulator* modes, and not only the *robustness/performance* compromise as in the original IMC procedure. Both for stable and unstable plants, it has been shown that this extra degree of freedom circumvents basic shortcomings of IMC reported in the literature.

For illustration purposes, the application to analytical tuning of PI controllers has been considered based on FOPTD and IPTD models. The suggested methodology allows to tune the controller in terms of two intuitive parameters (λ and γ), therefore guiding the tuning process. Truly-PID rules (including derivative action) could be derived similarly for the most common first and second order models. These and other extensions, as providing $\lambda\gamma$-based auto-tuning, will be published elsewhere.

Appendix 6A

Application to reset-based control

The use of 2DOF controllers is the most common option to decouple set-point tracking and (load) disturbance rejection. For example, the following PI control law is commercially available

$$u(t) = K_c \left(br(t) - y(t) + \frac{1}{T_i} \int_0^t e(\tau) d\tau \right) \tag{6.41}$$

where b is the so-called set-point weight. If $b = 1$, (6.41) reduces to the conventional 1DOF PI controller. In general, the closed-loop system is described by the equation

$$y = \frac{K_2 P}{1 + K_1 P} r + \frac{P}{1 + K_1 P} d \tag{6.42}$$

where

$$K_1 = K_c \left(1 + \frac{1}{T_i s} \right) \qquad K_2 = K_c \left(b + \frac{1}{T_i s} \right) \tag{6.43}$$

This corresponds to the block diagram of Figure 6.8. Another possibility to combine good set-point and (load) disturbance processing is to switch between suitable controllers for each purpose (Visioli, 2002). The potential advantages of switched linear control have been reported in (Feuer *et al.*, 1997), among others. Consider the scheme of Figure 6.9.

- By default, the system operates in *Regulator* mode. Thus, K_1 is tuned using Table 6.1 ($\gamma = \lambda$).

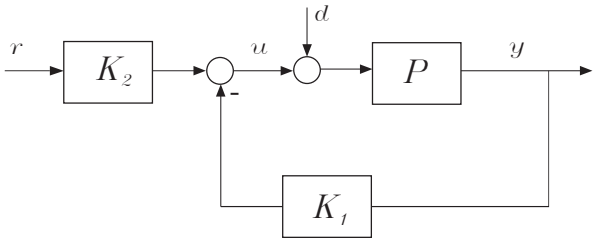

Figure 6.8: 2DOF control configuration.

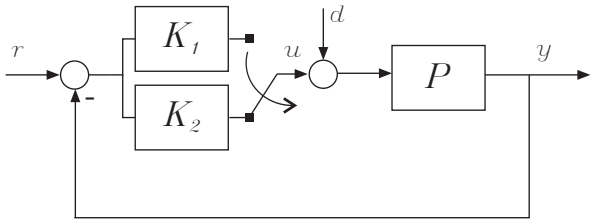

Figure 6.9: Switched feedback scheme.

- When a set-point change is signaled, we commute to K_2, which is tuned using Table 6.1 with $\gamma = |\tau|$. This way, during the set-point tracking, a *servo-type* tuning is used.
- After t_{sp} seconds, the system switches back to K_1.

If $t_{sp} = 0$, there is no switching and the scheme reduces to the conventional PI controller given by K_1 (K_2 is never active). By increasing t_{sp}, K_2 will be active for a longer period of time, reducing the overshoot after a reference change. Obviously, t_{sp} should be chosen, at maximum, equal to the settling time of the set-point response.

Reset controllers provide an alternative way to improve performance when controlling strongly traded-off plants. A reset controller operates most of the time as a linear system, but it performs a reset on its state when some condition holds. In the time domain, this mechanism has been proved to be useful for overcoming inherent limitations of linear controllers (Beker *et al.*, 2001). Also in the frequency domain, the advantages of the reset paradigm have been justified using different techniques such as describing function analysis (Baños and Vidal, 2007) or Poincare Maps (Barreiro and Dormido, 2011). The reset

idea has also been applied to improve the performance of linear observers (Paesa *et al.*, 2011).

Recently, PI control with reset action — or PI+CI, following the nomenclature introduced in (Baños and Vidal, 2007)—, has been proposed in different articles (Baños and Vidal, 2007; Bakkeheim *et al.*, 2008; Vidal and Baños, 2010). As depicted in Figure 6.10, the PI+CI controller can be regarded as a conventional PI compensator with two possible integral gains. Instead of using impulsive reset action based on the error signal as in (Baños

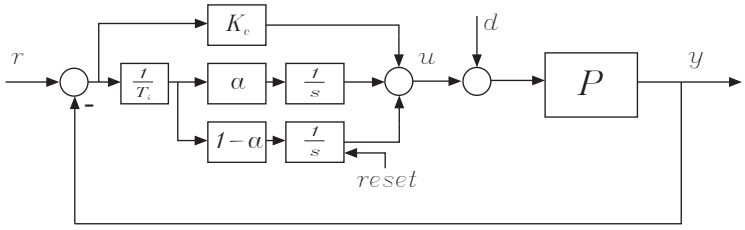

Figure 6.10: Unity feedback scheme using the PI+CI controller.

and Vidal, 2007; Bakkeheim *et al.*, 2008; Vidal and Baños, 2010), two alternative tunings based on switching and the proposed design are suggested in Table 6.4. By assuming that set-point changes occur at $t = 0$, the reset signal is:

$$\text{reset}(t) = \begin{cases} \text{ON} & \text{if} \quad 0 \leq t \leq t_{sp} \\ \text{OFF} & \text{if} \quad t > t_{sp} \end{cases} \tag{6.44}$$

The rationale behind Table 6.4 is explained next. Note that the PI+CI controller offers only a restricted implementation of the general switched scheme, since the reset mechanism just acts over the integral term. Therefore, T_i is chosen as in Table 6.1 ($\gamma = \lambda$) when the reset is inactive, and α is such that $\frac{\alpha}{T_i}$ is equal to the other extreme value of T_i given in Table 6.1 for $\gamma = |\tau|$. The idea is to recover the largest possible value of T_i when the reset is active. This way, during the set-point transient the integral gain is reduced to improve the tracking (diminishing the overshoot). As K_c is not altered by the reset mechanism, the two options in Table 6.4 correspond to selecting K_c using $\gamma = \lambda$ or $\gamma = |\tau|$. The first option chooses a *servo*-type tuning rule (Table 6.1, case $\gamma = |\tau|$) when the reset is active, and increases the integral gain for regulation purposes when the reset is inactive. On the other hand, option 2 uses a

regulator-type tuning rule (Table 6.1, case $\gamma = \lambda$) for normal operation, and reduces the integral gain to improve the set-point response.

Table 6.4: Tuning rules for the PI+CI controller.

Option	K_c	T_i	α
1	$\frac{1}{K_g}\frac{T_i}{\lambda+\lvert\tau\rvert+h-T_i}$	$\frac{\tau(h+2\lambda)-\lambda^2}{\tau+h}$	$\frac{\tau(h+2\lambda)-\lambda^2}{\tau(h+\lambda+\lvert\tau\rvert)-\lambda\lvert\tau\rvert}$
2	$\frac{1}{K_g}\frac{\tau}{\lambda+h}\left(\frac{h+2\lambda-\lambda^2/\tau}{h+\lambda}\right)$	$\frac{\tau(h+2\lambda)-\lambda^2}{\tau+h}$	$\frac{\tau(h+2\lambda)-\lambda^2}{\tau(h+\lambda+\lvert\tau\rvert)-\lambda\lvert\tau\rvert}$

Example 6.0.1. *For the plant* $P = \frac{e^{-s}}{10s+1}$, *Figure 6.11 (bottom) displays the results obtained using conventional 1DOF and 2DOF PI controllers, and the PI+CI controller using Option 1 in Table 6.4. In all the cases, the* feedback *tuning is the same:* $K_c = \frac{\tau}{K_g(\lambda+h)}, T_i = \frac{\tau(h+2\lambda)-\lambda^2}{\tau+h}$ *(*$\gamma = \lambda = 1.2$*). Substituting the concrete values into the tuning expressions, we get* $K_c = 4.545, T_i = 0.6512$. *Regarding the 2DOF PI controller,* $b = 0.25$ *(decreasing b further does not reduce the overshoot significantly). As for the PI+CI controller,* $\alpha = \frac{\tau(h+2\lambda)-\lambda^2}{\tau(h+\lambda+\lvert\tau\rvert)-\lambda\lvert\tau\rvert} = 0.1087$ *according to Table 6.4, and* $t_{sp} = 3$. *In this*

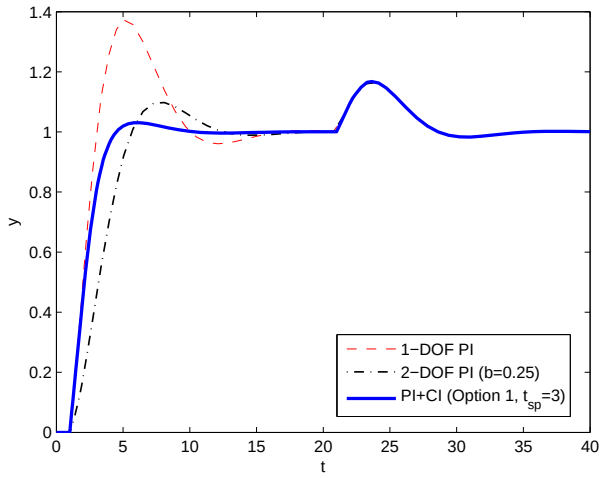

Figure 6.11: Time responses for 1DOF PI, 2DOF PI and PI+CI schemes.

particular example, it seems that the PI+CI controller may be advantageous

with respect to the 2DOF PI controller. In particular, a set-point response with shorter rise time and lower overshoot is attained. However, to establish this thesis completely, a more thorough study is necessary.

Chapter 7

The $\mathcal{H}_2$ counterpart

Based on (Alcántara et al.*, 2011*a*)*

Based on Internal Model Control (IMC), we present a design method to take into account both input and output disturbances. The proposed design provides generalized IMC filters that can be used to obtain good results in terms of output sensitivity (favouring output disturbances), or in terms of input sensitivity (therefore placing the emphasis on load disturbances). If both input and output disturbances are expected, the design offers the possibility of obtaining a balance that improves the overall disturbance rejection response.

7.1 Introduction

The objective of a control system is to make the output y behave in a desired way by manipulating the plant input u. There are basically two different problems (Pernebo, 1981; Skogestad and Postlethwaite, 2005): the *servo* problem, which concerns the tracking of the reference signal r, and the *regulator* problem, which aims at rejecting the disturbances d entering the control loop. In both cases, the controller K is designed to make the control error $e = y - r$ small.

This chapter deals exclusively with the *regulator* problem. Note that if the resulting tracking performance was not suitable, this could be fixed in a second step by introducing a reference prefilter (Morari and Zafiriou,

1989; Skogestad and Postlethwaite, 2005). More generally, the *servo* and the *regulator* problems can be solved independently by using a Two-Degree-Of-Freedom (2DOF) topology (Pernebo, 1981; Vilanova and Serra, 1997; Ibeas and Alcántara, 2010). In what follows, we will assume that disturbances cannot be measured and that can enter both at the input and at the output of the plant P. Therefore, a feedforward strategy (Faanes and Skogestad, 2004; Vilanova *et al.*, 2009*a*) is not advantageous in the considered scenario, where the feedback controller completely determines the disturbance response.

To cope with the input/output *regulator* problem, we rely here on the Internal Model Control (IMC) paradigm (Morari and Zafiriou, 1989). Historically, the inherent shortcomings of the IMC method have resulted in the search of new filters and/or alternative procedures: for minimum-phase (MP) unstable plants, Campi *et al.* (1994) suggested a filter which allows easy adjustment of the closed-loop bandwidth as well as a robustness improvement. For stable plants, Horn *et al.* (1996) modified the conventional filter for enhanced input disturbance attenuation. From a broader viewpoint, a simple IMC-based procedure applicable to both stable and unstable plants and aimed at input disturbances was presented by Lee *et al.* (2000). Some years later, Dehghani *et al.* (2006) reported the difficulties with the IMC procedure in an exhaustive manner and, in order to undergo them, devised a numerical design blending IMC and $\mathcal{H}_\infty$ ideas. Although the latter design offers great versatility, it requires judicious choices for some frequency weights and for the desired closed-loop response, which may lead to design pitfalls as noted in (Lee and Shi, 2008). Along these lines, a simpler IMC-like $\mathcal{H}_\infty$ design overcoming basic limitations of IMC has been reported by Alcántara *et al.* (2011*c*).

The analytical solution presented here can be seen as the $\mathcal{H}_2$ counterpart of that in Chapter 6 (Alcántara *et al.*, 2011*c*). With respect to (Alcántara *et al.*, 2011*c*), some assumptions have been removed: i.e., the plant model is not restricted to be purely rational nor to contain at least one Right Half-Plane (RHP) zero. In addition, plants with complex poles have been included in the discussion. An interesting aspect of the here-adopted $\mathcal{H}_2$ approach is that it unifies the previous designs (Campi *et al.*, 1994; Horn *et al.*, 1996; Lee *et al.*, 2000), resulting into a more general structure for the IMC filter. The distinguishing feature of the new filter is that it allows to balance the input/output regulatory performance in a simple manner. This is a fundamental trade-off, disregarded in (Campi *et al.*, 1994; Horn *et al.*, 1996; Lee *et al.*, 2000), that cannot be overcome using a 2DOF control configuration or a related approach

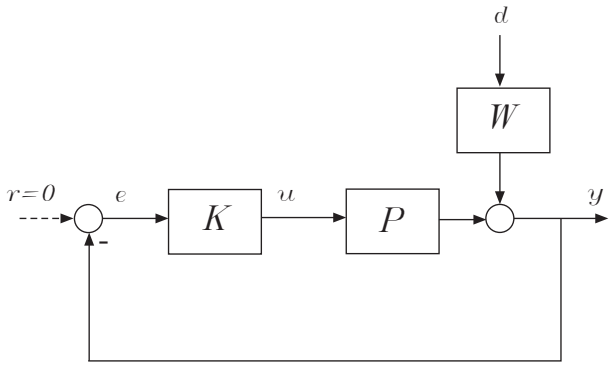

Figure 7.1: Basic setup for the input/output *regulator* problem.

as done in the works (Visioli, 2002; Shamsuzzoha and Lee, 2007; Shamsuzzoha and Lee, 2009).

An outline for the rest of the chapter is given next. Section 7.2 states the problem formally and reviews basic material about $\mathcal{H}_2$ optimization and IMC. The proposed design is introduced in Section 7.3, and is then illustrated by example in Section 7.4 to obtain different balances of input/output disturbance attenuation. Finally, Section 7.5 summarizes the main ideas and makes some concluding remarks.

7.2 Problem statement and background material

To set the problem, we make use of Single-Input Single-Output (SISO) linear models of the form

$$y = Pu + Wd \tag{7.1}$$

for which the corresponding feedback setup is depicted in Figure 7.1. In (7.1), W (which is not a physical component as P or K) represents a frequency weight that will be designed to make it easy to balance the disturbance response at the input and at the output of the plant. By absorbing the input type (e.g. step-like disturbances) into the weight W too, we will assume hereafter that d in Figure 7.1 is an impulse, i.e. $d(s) = 1$. To derive the feedback controller K, we will look at the structure of $\mathcal{H}_2$-optimal controllers. By an $\mathcal{H}_2$-optimal controller, we understand here one such that the integrated square

error

$$\|e\|_2^2 = \int_0^\infty e^2(t)dt \tag{7.2}$$

is minimized for a particular input. Bearing in mind that $e = -SWd = -SW$, where $S \doteq \frac{1}{1+PK}$ is the sensitivity function, we can state problem (7.2) in the frequency domain

$$\min_{K\in\mathcal{C}} \|e\|_2^2 = \min_{K\in\mathcal{C}} \frac{1}{2\pi} \int_{-\infty}^{\infty} |S(j\omega)W(j\omega)|^2 d\omega \tag{7.3}$$

where $\mathcal{C}$ denotes the set of *internally stabilizing* controllers. Internal stability is the requirement that all the closed-loop transfer functions are stable, implying that cancellation of unstable poles between the plant P and the controller K is not allowed. It is well-known that the IMC parameterization of the feedback controller(Morari and Zafiriou, 1989),

$$K = \frac{Q}{1 - PQ}, \tag{7.4}$$

allows to write all the closed-loop relations affinely in Q (e.g., $S = 1-PQ, T = PQ$). Then, in terms of Q, the following fundamental result solves (7.3):

Theorem 7.2.1 (Morari and Zafiriou, 1989, Theorem 5.2-1)**.** *Let us factor both the plant P and the weight W into an all-pass and a MP portion so that $P = P_a P_m$ and $W = W_a W_m$. Denote by l, k the number of integrators and unstable poles of P, respectively. Now, assume that the weight W contains $l' \geq l$ integrators and the first $0 \leq k' \leq k$ unstable poles of P and define:*

$$b_P = \prod_{i=1}^{k} \frac{-s + \pi_i}{s + \bar{\pi}_i} \quad \textit{and} \quad b_W = \prod_{i=1}^{k'} \frac{-s + \pi_i}{s + \bar{\pi}_i}, \tag{7.5}$$

being $\pi_1, \ldots, \pi_k$ the unstable poles of P. Then, the $\mathcal{H}_2$-optimal (internally stabilizing) Q is given by

$$Q = b_P (P_m b_W W_m)^{-1} \left\{ (b_P P_a)^{-1} b_W W_m \right\}_* \tag{7.6}$$

where the operator $\{\}_*$ denotes that after a partial fraction expansion (PFE) of the operand all terms involving the poles of P_a^{-1} are omitted.

Note that it is straightforward how to select W for the extreme cases at hand. For example, if only step output disturbances are considered, the weight should be $W = 1/s$, whereas $W = P/s$ for the case of step disturbances entering at the input of the plant. A more difficult problem is how to select W systematically for balanced operation. In addition, W should be such that it allows to adjust the robustness/performance trade-off. The selection of W will be fully addressed in Section 7.3. We end this section by observing the following facts:

Remark 7.2.1. *The optimal solution in (7.6) only depends on the MP part of W. Consequently, W can be restricted to be MP without loss of generality (i.e., $W = W_m$).*

Remark 7.2.2. *For MP (possibly unstable) plants ($P_a = 1$), the optimal solution in (7.6) becomes $Q = P_m^{-1}$, independently of W.*

7.3 Proposed input/output regulator design

This section first addresses the selection of a suitable weight W for the problem at hand (Section 7.3.1). After selecting W, an analytical solution for Q is given based on the $\mathcal{H}_2$ minimization criterion (Section 7.3.2). Finally, in Section 7.3.3 we examine the nominal performance, robust stability and robust performance properties of the derived controller.

7.3.1 Selection of W

Let us take $P = P_a P_m$ as in Section 7.2, and denote by d_d the generating polynomial of the disturbance (i.e., $d_d = s$ for steps, $d_d = s^2$ for ramps, etc). For the sake of clarity, it is temporarily assumed that $P_a \neq 1$ and that P has not any complex poles or zeros, nor any pole at the origin. We also assume that P has slow/unstable poles at $s = -1/\tau_1, \ldots, -1/\tau_k$. Then, we make the following choice of the (nonstrictly proper) weight:

$$W = \frac{(\lambda s + 1)^n}{d_d} \prod_{i=1}^{k} \frac{\gamma_i s + 1}{\tau_i s + 1} \tag{7.7}$$

with

$$n = \max\{1, \delta(d_d) + \delta(P) - 1\} \tag{7.8}$$

where $\delta(d_d), \delta(P)$ denote the degree of d_d and the relative degree of P, respectively. For the common case of step disturbances ($d_d = s$), (7.8) simplifies to $n = \max\{1, \delta(P)\}$. Finally, λ and $\gamma_1, \ldots, \gamma_k$ in (7.7) are tuning parameters verifying that

$$\lambda > 0 \quad , \quad \gamma_i \in [\lambda, |\tau_i|] \tag{7.9}$$

We recall here that the main objective of our design is to consider disturbances entering both at the input and at the output of the plant. In addition, the design has to account for model uncertainty. The rationale behind the selection of W in (7.7) is explained below:

- In order to explain the role of λ and γ_i separately, let us start considering that $\lambda = 0$. Then, we have that $W = \frac{1}{d_d}\prod_{i=1}^{k}\frac{\gamma_i s+1}{\tau_i s+1}$. Now, by making $\gamma_i = \lambda = 0, i = 1, \ldots, k$, the weight is $W = \frac{1}{d_d}\prod_{i=1}^{k}\frac{1}{\tau_i s+1}$. For this choice of γ_i, the design will provide good results in terms of input disturbance attenuation since we are including the slow/unstables poles of P in W. Stated otherwise, the disturbance passes through the conflicting poles of the plant (note that fast stable poles do not impose a trade-off between input/output regulatory performance).

- At this point, we can improve the output disturbance response by increasing the value of each γ_i. To see this, let us consider that γ_i is set to the upper bound of the interval (7.9), i.e., we take $\gamma_i = |\tau_i|$. It is then clear that $|W| = \frac{1}{|d_d|}$, for which (7.3) optimizes the ISE for output disturbances.

- So far, we have assumed that $\lambda = 0$. Let us suppose now that each γ_i has been fixed to a particular value. As we increase the value of λ, the minimization in (7.3) will penalize the magnitude of S at higher frequencies, resulting into a slower closed-loop. Therefore, λ can be used to adjust the robustness/performance trade-off. Regarding n, the value in (7.8) will ensure the properness of the final controller (this point will be clarified later).

Remark 7.3.1. *For simplicity, the γ_i parameters could be determined from a single parameter $\gamma \in [0, 1]$ as indicated below:*

$$(\gamma_1, \ldots, \gamma_k)^T = (1-\gamma)(\lambda, \ldots, \lambda)^T + \gamma(|\tau_1|, \ldots, |\tau_k|)^T \tag{7.10}$$

7.3.2 Analytical solution

The next step towards obtaining the IMC controller is to use Theorem 7.2.1. As $W = W_m$ in (7.7) contains the unstable poles of P, we have that $b_P = b_W$, and (7.6) simplifies to $Q = (P_m W)^{-1} \left\{ P_a^{-1} W \right\}_*$. This is a valid controller when P is nonminimum-phase (NMP) in the sense that it is internally stabilizing and proper. However, recalling the Remark 7.2.2, for MP plants (i.e., $P_a = 1$) the solution is $Q = P_m^{-1}$ regardless W. As a consequence, Q may be improper, and it would be necessary to extend Q by cascading a filter as in the conventional IMC procedure. We want to avoid this approach, and obtain a proper solution directly from the specified weight W. Towards this objective, we finally propose the following solution

$$Q = (P_m W)^{-1} \left\{ P_a^{-1} W \right\}_\star \tag{7.11}$$

where $\{\cdot\}_\star$ acts like $\{\cdot\}_*$, but also removing the non-strictly proper terms after the PFE. The $\{\cdot\}_\star$ operator gives the same result than $\{\cdot\}_*$ when the plant contains a delay. When P is delay-free, the actuation of $\{\cdot\}_\star$ can be understood in terms of $\{\cdot\}_*$ as follows:

$$\left\{ P_a^{-1} W \right\}_\star = \left\{ \left(\underbrace{P_a e^{-sh}}_{P_a'} \right)^{-1} W \right\}_* \Bigg|_{h=0}$$

That is to say, we consider a fictitious delay h, apply $\{\cdot\}_*$ and then evaluate at $h = 0$. The following example illustrates how to calculate (7.11):

Example 7.3.1. *Let us consider the (possibly unstable) First Order Plus Time Delay (FOPTD) model* $P = K_g \frac{e^{-sh}}{\tau s+1}$*, for which* $P_m = \frac{K_g}{\tau s+1}, P_a = e^{-sh}$*. We assume that* $|\tau| \gg h > 0$ *(*$k = 1$*). In addition, we assume step-like disturbances, i.e.* $d_d = s$*, and take* $n = 1$*. By substitution into (7.7), we get* $W = \frac{(\lambda s+1)(\gamma s+1)}{s(\tau s+1)}$*, with* $\lambda > 0, \gamma \in [\lambda, |\tau|]$*. If* $h > 0$*, the proposed controller*

(7.11) is identical to $\mathcal{H}_2$-optimal one:

$$\begin{aligned} Q &= \frac{(\tau s+1)^2 s}{K_g(\lambda s+1)(\gamma s+1)} \left\{ e^{sh} \frac{(\lambda s+1)(\gamma s+1)}{s(\tau s+1)} \right\}_\star \\ &= \frac{(\tau s+1)^2 s}{K_g(\lambda s+1)(\gamma s+1)} \left\{ e^{sh} \frac{(\lambda s+1)(\gamma s+1)}{s(\tau s+1)} \right\}_* \\ &= \frac{(\tau s+1)^2 s}{K_g(\lambda s+1)(\gamma s+1)} \left(\frac{1}{s} - \frac{\tau e^{-h/\tau} \tau (1-\lambda/\tau)(1-\gamma/\tau)}{\tau s+1} \right) \\ &= \frac{(\tau s+1)([\tau - \tau e^{-h/\tau}(1-\lambda/\tau)(1-\gamma/\tau)]s+1)}{K_g(\lambda s+1)(\gamma s+1)} \end{aligned} \tag{7.12}$$

If $h=0$, P becomes MP ($P_a=1$). In this case, we make $h=0$ in (7.12) and we arrive at

$$Q = \frac{(\tau s+1)([\tau - \tau(1-\lambda/\tau)(1-\gamma/\tau)]s+1)}{K_g(\lambda s+1)(\gamma s+1)} \tag{7.13}$$

In particular, note that $Q \to P_m^{-1} = (\tau s+1)/K_g$ as $\lambda \to 0$, implying that the $\mathcal{H}_2$-optimal solution is approached for small values of λ.

The following proposition summarizes the most basic properties of the proposed controller:

Proposition 7.3.1. *The IMC controller Q in (7.11) is such that:*

(P1) Q is $\mathcal{H}_2$-optimal if P contains a delay. If P is delay-free, Q tends to be $\mathcal{H}_2$-optimal when $\lambda \to 0$ provided that $\delta(d_d) \geq 1$.

(P2) Q is proper and stable.

(P3) $S = 1 - PQ = 0$ at the poles of W.

Proof.

(P1) The $\mathcal{H}_2$-optimal solution is given by $Q = (P_m W)^{-1} \left\{ P_a^{-1} W \right\}_*$. The difference with respect to the proposed solution amounts to the $\{\cdot\}_*$ operator. If P contains a delay, $\{\cdot\}_*$ and $\{\cdot\}_\star$ coincide because $\left\{ P_a^{-1} W \right\}_*$ is strictly proper. Thus, in this case, (7.11) is optimal (with respect to the selected W). When P is delay-free, $\left\{ P_a^{-1} W \right\}_\star \to \left\{ P_a^{-1} W \right\}_*$ when

$\lambda \to 0$. This is because $P_a^{-1}W$ tends to become strictly proper (the n zeros at $s = -1/\lambda$ of W move to infinity). By definition of $\{\cdot\}_*, \{\cdot\}_\star$, both yield the same result when applied to strictly-proper operands. Thus, the proposed Q tends to $Q = (P_m W)^{-1} \left\{P_a^{-1}W\right\}_* = P_m^{-1}$ when $\lambda \to 0$.

(P2) From (7.7) and (7.11), straightforward algebra shows that the structure of Q is given by

$$Q = \frac{P_m^{-1}\chi}{(\lambda s + 1)^n(\gamma_1 s + 1)\cdots(\gamma_k s + 1)} \tag{7.14}$$

where χ is a polynomial of degree $\delta_d(d_d) + k - 1$. Therefore, $\delta(Q) = n - \delta(P) - \delta(d_d) + 1$. Selecting n as in (7.8) provides $\delta(Q) \geq 0$, implying that Q is proper. Stability is also easy to check: the poles of Q are the Left Half-Plane (LHP) zeros of P, collected in P_m, and the zeros of W, which are also in the LHP.

(P3) Equivalently, we will show that $T = 1 - S = 1$ at the poles of W. The complementary sensitivity function is

$$T = PQ = (P_a^{-1}W)^{-1} \left\{P_a^{-1}W\right\}_\star \tag{7.15}$$

If W has a pole at $s = p$ of multiplicity m, then we can write $P_a^{-1}W = \frac{\phi(s)}{(s-p)^m}$, and (7.15) can be expressed as

$$T = \frac{(s-p)^m}{\phi(s)} \left(\cdots + \sum_{i=1}^{m-1} \frac{\alpha_i}{(s-p)^i} + \frac{\alpha_m}{(s-p)^m} + \cdots \right) \tag{7.16}$$

where $\alpha_m = \phi(p)$. It is clear then that $T|_{s=p} = \left(\frac{\alpha_m}{\phi(s)}\right)\Big|_{s=p} = 1$.

□

Property (P1) can be interpreted as the combination of the two steps of the IMC procedure into a single one. Properties (P2) and (P3) imply that Q is realizable and internally stabilizing (because W contains the poles of P). In addition, (P3) means asymptotic rejection of the disturbances (because the denominator of W contains the generating polynomial d_d, recall the *Internal Model Principle* (Morari and Zafiriou, 1989; Skogestad and Postlethwaite, 2005)).

Remark 7.3.2. *From (7.11) and Property (P3), Q and $1-PQ$ have zeros at the k slow/unstable poles of P. These zeros get cancelled when forming the equivalent unity feedback controller $K = \frac{Q}{1-PQ}$. This means that adjusting λ, γ_i in W does not change the structure of the final controller, but only its parameters.*

Remark 7.3.3. *Strictly speaking, properties (P2) and (P3) are not sufficient conditions for internal stability when P is a delayed unstable system. As explained in (Zhang* et al.*, 2006*a*), in this case there are irremovable RHP pole/zero cancellations in K that do not allow a direct implementation. In general, Q can be approximated by a practical controller K (e.g, PID type) by following different methodologies (Wang* et al.*, 2001; Shamsuzzoha and Lee, 2007; Shamsuzzoha and Lee, 2009).*

New insight into IMC filters

The proposed controller (7.11) can be expressed as

$$Q = P_m^{-1} f \tag{7.17}$$

with $f = W^{-1}\left\{P_a^{-1}W\right\}_\star$. Let us take $W = \frac{n_w}{d_w}$. Now, considering how $\{\cdot\}_\star$ acts and taking into account property (P3) in Proposition 7.3.1, we can alternatively express f as

$$f = \frac{\chi}{n_w} = \frac{\sum_{i=0}^{\delta(d_w)-1} a_i s^i}{(\lambda s+1)^n \prod_{i=1}^{k}(\gamma_i s+1)} \tag{7.18}$$

where $a_0, \ldots, a_{\delta(d_w)-1}$ are determined from the following system of linear equations

$$T|_{s=\pi_i} = P_a f|_{s=\pi_i} = 1 \qquad i = 1 \ldots \delta(d_w) \tag{7.19}$$

being $\pi_i, i = 1, \ldots, \delta(d_w)$ the poles of W. From (7.7), $\delta(d_w) = k + \delta(d_d)$ in general, except when P is stable and we take $\gamma_i = \tau_i$ for all i. In the latter case, the weight (7.7) simplifies to $W = \frac{(\lambda s+1)^n}{d_d}$, and $\delta(d_w) = \delta(d_d)$. Note that, as long as the a_i coefficients satisfy (7.19), the filter time constants λ and γ_i can be selected freely without any concern for nominal stability. In

more detail, (7.19) corresponds to

$$\begin{pmatrix} \pi_1^{\delta(d_w)-1} & \cdots & \pi_1 & 1 \\ \vdots & \ddots & \vdots & \vdots \\ \pi_{\delta(d_w)}^{\delta(d_w)-1} & \cdots & \pi_{\delta(d_w)} & 1 \end{pmatrix} \begin{pmatrix} a_{\delta(d_w)-1} \\ \vdots \\ a_0 \end{pmatrix} = \begin{pmatrix} P_a^{-1} n_w|_{s=\pi_1} \\ \vdots \\ P_a^{-1} n_w|_{s=\pi_{\delta(d_w)}} \end{pmatrix} \tag{7.20}$$

In the context of step-like inputs, the filter (7.18) generalizes some previously reported filters in the following way:

- For stable plants, by taking $\gamma_i = \tau_i$, the conventional IMC filter(Morari and Zafiriou, 1989) is obtained. However, if we take $\gamma_i = \lambda$, then the filter in (Horn *et al.*, 1996) results.
- Essentially, the filter suggested in (Campi *et al.*, 1994) for MP unstable plants corresponds to taking $\gamma_i \to \infty$ in (7.18). In the general unstable plant case, the filter in (Lee *et al.*, 2000) is recovered by choosing $\gamma_i = \lambda$.

Finally, by using Lagrange-Type interpolation theory (Morari and Zafiriou, 1989), it is possible to develop an expression[1] for (7.18) explicitly:

$$f = \frac{1}{n_w} \sum_{j=1}^{\delta(d_w)} (P_a^{-1} n_w)|_{s=\pi_j} \prod_{\substack{i=1 \\ i \neq j}}^{\delta(d_w)} \frac{s - \pi_i}{\pi_j - \pi_i} \tag{7.21}$$

Extension to plants with integrators or complex poles

It has been shown that we can reduce the proposed design to the selection of a proper filter f, so that $Q = P_m^{-1} f$. In this subsection, we detail the structure of such a filter (passing over W for brevity) when P has integrators and/or complex conjugate poles. To keep it simple, we address each situation at a time:

(i) P has (exclusively) l poles at the origin

Then, the corresponding filter is

$$f = \frac{\sum_{i=0}^{\delta(d_W)-1} a_i s^i}{(\lambda s + 1)^n \prod_{i=1}^{l} (\gamma_i s + 1)} \tag{7.22}$$

[1] The formula (7.21) is not valid for repeated poles.

where $\delta(d_W) = l+\delta(d_d)$. The only difference with respect to (7.18) is that now $\gamma_i \in [\lambda, \infty)$, whereas for slow/unstable poles we had $\gamma_i \in [\lambda, |\tau_i|]$. This can be easily understood, since an integrator corresponds to a pole with an infinitely large time constant.

(ii) P has (exclusively) m complex conjugate poles

Let us suppose that the m complex conjugate poles are at $-\xi_i\omega_{ni} \pm j\omega_{ni}\sqrt{1-\xi_i^2}$. Then, the structure of the filter is

$$f = \frac{\sum_{i=0}^{\delta(d_W)-1} a_i s^i}{(\lambda s+1)^n \prod_{i=1}^{m}(\gamma_{i,2}s^2+\gamma_{i,1}s+1)} \tag{7.23}$$

where $\delta(d_W) = 2m + \delta(d_d)$. For input disturbances, $\gamma_{i,2} = \lambda^2, \gamma_{i,1} = 2\lambda$ so that $\prod_{i=1}^{m}(\gamma_{i,2}s^2+\gamma_{i,1}s+1) = (\lambda s+1)^{2m}$. For output disturbances, we want $\prod_{i=1}^{m}(\gamma_{i,2}s^2+\gamma_{i,1}s+1)$ equal to $(1/{\omega_{ni}}^2)\prod_{i=1}^{m}(s^2+2|\xi_i|\omega_{ni}+{\omega_{ni}}^2)$, which is achieved for $\gamma_{i,2} = (1/\omega_{ni})^2, \gamma_{i,1} = 2|\xi_i|/\omega_{ni}$ (in this extreme case, only when P is stable, $\delta(d_W) = \delta(d_d)$). It is not so simple now to determine an interval for $\gamma_{i,1}, \gamma_{i,2}$ as in the real poles case (this will be illustrated in Section 7.4). An exception occurs if the complex poles are well-damped ($|\xi_i|$ close to one), in this case we can disregard the imaginary part and treat the complex conjugate pairs as double real poles at $s = -\omega_{ni}\xi_i$. This allows to simplify the filter structure to

$$f = \frac{\sum_{i=0}^{\delta(d_W)-1} a_i s^i}{(\lambda s+1)^n \prod_{i=1}^{m}(\gamma_i s+1)^2} \tag{7.24}$$

with $\gamma_i \in \left[\lambda, \frac{1}{|\omega_{n_i}\xi_i|}\right]$.

7.3.3 Nominal performance and robust stability/performance

In any practical design method, robust performance is the ultimate goal: we want the controller to work well under uncertain circumstances. Assuming that a condition for robust stability is met, the next subsection gives an upper bound for the performance degradation with respect to the nominal case. How the robustness/performance compromise is influenced by the tuning parameters λ and $\{\gamma_i\}_i$ is addressed later on.

General relations

From Section 7.2, the ISE for an output disturbance $d = 1/d_d$ is given by

$$\mathrm{ISE}_o = \int_0^\infty e^2(t)dt = \frac{1}{2\pi}\int_{-\infty}^{\infty} \left|Sd_d^{-1}(j\omega)\right|^2 d\omega \tag{7.25}$$

Similarly, when d enters at the input of the plant, the corresponding ISE is

$$\mathrm{ISE}_i = \int_0^\infty e^2(t)dt = \frac{1}{2\pi}\int_{-\infty}^{\infty} \left|PSd_d^{-1}(j\omega)\right|^2 d\omega \tag{7.26}$$

Equations (7.25) and (7.26) indicate the nominal performance achieved by the final design in terms of input/ouput disturbance attenuation. Robust stability can be assessed by the well-known condition (Morari and Zafiriou, 1989; Skogestad and Postlethwaite, 2005)

$$\|\Delta T\|_\infty = \sup_\omega |\Delta(\omega)T(j\omega)| < 1 \tag{7.27}$$

where $\Delta(\omega) \geq 0$ is a bound for the plant multiplicative uncertainty. In practice, nominal performance and robust stability alone are not enough because some plants in the uncertain set may be on the verge of instability, yielding very poor performance. It is therefore necessary to guarantee some degree of robust performance. To this aim, it is useful to have an upper bound for both ISE_i and ISE_o. The worst error is generated by the worst plant, which can be expressed as $P(1 + \delta(s)\Delta(\omega))$ for some $\delta(s)$ such that $|\delta(j\omega)| \leq 1$. By using the inequality $|1 + P(1 + \delta\Delta)K| \geq |1 + PK| - |PK|\Delta$, the actual sensitivity function $\mathcal{S}$ can be bounded as

$$|\mathcal{S}| = \left|\frac{1}{1 + P(1 + \delta\Delta)K}\right| \leq \left|\frac{1}{1 - |\Delta T|}\right| |S| \tag{7.28}$$

From (7.25), (7.26) and (7.28), the following upper bounds for the actual errors result

$$\mathrm{ISE}_o \leq \overline{\mathrm{ISE}_o} = \frac{1}{2\pi}\int_{-\infty}^{\infty} \left|\frac{1}{1 - |\Delta T|}\right|^2 |Sd_d^{-1}|^2 d\omega \tag{7.29}$$

$$\mathrm{ISE}_i \leq \overline{\mathrm{ISE}_i} = \frac{1}{2\pi}\int_{-\infty}^{\infty} \left|\frac{1}{1 - |\Delta T|}\right|^2 |PSd_d^{-1}|^2 d\omega \tag{7.30}$$

As it is logical, the modelling error increases the (finite) gap between ISE_i (ISE_o) and $\overline{\text{ISE}_i}$ ($\overline{\text{ISE}_o}$) as the stability boundary in (7.27) is approached, exhibiting the typical trade-off between nominal performance and performance degradation (Morari and Zafiriou, 1989; Zhou and Ren, 2001; Skogestad and Postlethwaite, 2005).

Tuning guidelines for λ and γ_i

In view of equations (7.25), (7.26), (7.29) and (7.30), Nominal Performance is captured in terms of S, whereas Robust Performance is expressed using T (which also determines Robust Stability (7.27)). The shape of these transfer functions depends on the values of the tuning parameters. The role of λ is the same as in the conventional IMC: basically, for a given value of each γ_i, increasing λ makes the system slower, to the detriment of ISE_o and ISE_i, but favouring the Robust Stability condition (7.27) by reducing the closed-loop bandwidth. Let us consider now that $\lambda, \gamma_j, j = 1..k, j \neq i$ have been fixed, and see which is the influence of γ_i. From earlier discussion, when $\gamma_i = \lambda < |\tau_i|$, W is asking for good load disturbance rejection by forcing $S = 0$ at $s = -1/\tau_i$, which may be responsible for a large peak on $|S|$ and $|T|$ and a somewhat aggressive response (Alcántara *et al.*, 2011*c*). As we increase γ_i, W specifies lower gains for $|S|$ at middle-high frequencies, which by a *waterbed effect* argument (Skogestad and Postlethwaite, 2005; Alcántara *et al.*, 2011*c*) is achieved augmenting $|S|$ at low frequencies. Consequently, augmenting γ_i has an *smoothing* effect. In particular, this means that improving the response to output disturbances will also make the system slower. As it will be shown in Section 4, after increasing γ_i, λ can be decreased to compensate for the reduction of the closed-loop bandwidth. In summary, tuning γ_i has also an effect on robustness, but it should be clear that the way of affecting the robustness properties is different: λ is more related to the closed-loop bandwidth, which by the Robust Stability condition (7.27) is responsible for robustness in the high frequency region (model uncertainty). On the other hand, the γ_i parameters affect the mid-frequency robustness properties altering the peaks of the sensitivity functions. More precisely, augmenting γ_i contributes to flatten out the frequency response.

7.4 Simulation examples

In this section, we consider three simulation examples to illustrate the features of the proposed procedure. For evaluating robustness, we use the peak of the sensitivity function

$$M_S \doteq \|S\|_\infty = \sup_\omega \left| \frac{1}{1+PK(j\omega)} \right| \tag{7.31}$$

Because M_S is the inverse of the shortest distance from the Nyquist curve of $L = PK$ to the critical point $-1 + 0j$, small values of M_S indicate good robustness. For a reasonably robust system, an upper bound for the M_S value can be fixed at around two (Skogestad and Postlethwaite, 2005). Another robustness indicator used throughout the examples is given by $M_T \doteq \|T\|_\infty \doteq \sup_\omega |T(j\omega)|$. The robustness interpretation for M_T (the peak of $|T|$) comes from the robust stability condition (7.27). To quantify the input usage, we compute the total variation (TV) of the input u:

$$\text{TV} \approx \sum_{i=1}^{\infty} |u_{i+1} - u_i| \tag{7.32}$$

where $\{u_i\}_{i=1}^{\infty}$ denotes a discretization sequence of u. In the examples that follow, we restrict our attention to (unity) step disturbances ($d_d = s$) as it is commonly done in the literature.

Example 1 The purpose of this preliminary example is to illustrate the different effect of the λ and γ parameters. We will consider the process $\frac{-(10s+1)(0.02s+1)}{(-100s+1)(s+1)(0.2s+1)}$, modeled as $P = -\frac{10s+1}{(-100s+1)(s+1)}$. The design of Section 7.3 yields $Q = P_m^{-1} f = P^{-1} f$, where

$$f = \frac{a_1 s + 1}{(\lambda s + 1)(\gamma s + 1)} \tag{7.33}$$

with $a_1 = 100\,[(1+\lambda/100)(1+\gamma/100) - 1]$ and $\gamma \in [\lambda, 100]$. For $\gamma = \lambda$, (7.33) coincides with the conventional IMC filter used in (Morari and Zafiriou, 1989; Lee *et al.*, 2000), which in this case favours input disturbances. As a consequence, the response for output disturbances may be undesirable. Figure 7.2 displays the time/frequency responses for $\lambda = \gamma = 0.15$. As it can be seen, the peak in $|T|$ ($M_T = 1.16$) degrades the robust stability margin and is

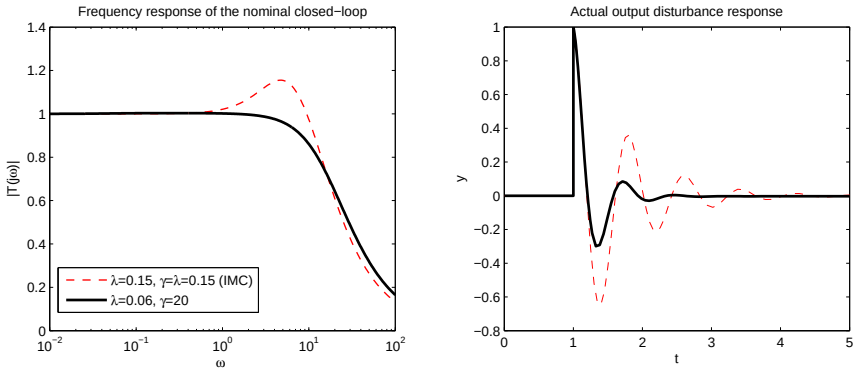

Figure 7.2: Frequency and time responses (Example 1).

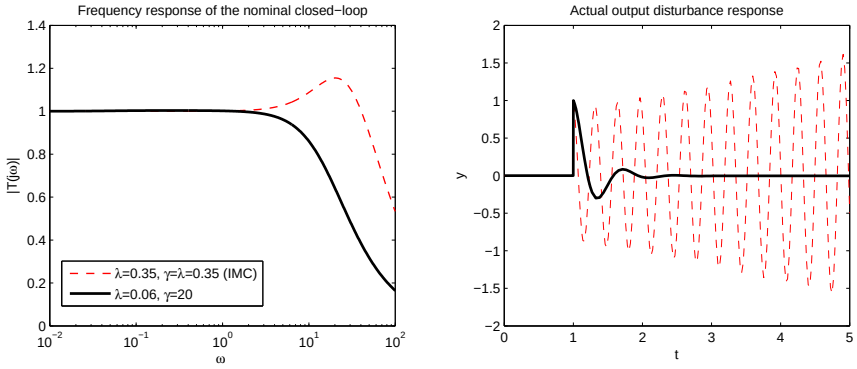

Figure 7.3: Frequency and time responses (Example 1).

responsible for the large oscillations in the response to the output disturbance. We know that by increasing γ (we take $\gamma = 20$) it is possible to improve this response. As stated in Section 7.3, this tends to make the system slower too. In order to preserve the original closed-loop bandwidth, the λ parameter can be decreased (we finally take $\lambda = 0.06$). As shown in Figure 7.2, this retuning allows to keep the original closed-loop bandwidth while avoiding the peak in $|T|$ (now, $M_T = 1$). The resulting outcome is better robustness and smoother output disturbance attenuation. It is remarkable that the peak in $|T|$ cannot be avoided using the classical filter in which $\gamma = \lambda$, as illustrated in Figure 7.3 and Figure 7.4. Clearly, if one uses the standard filter structure, the only

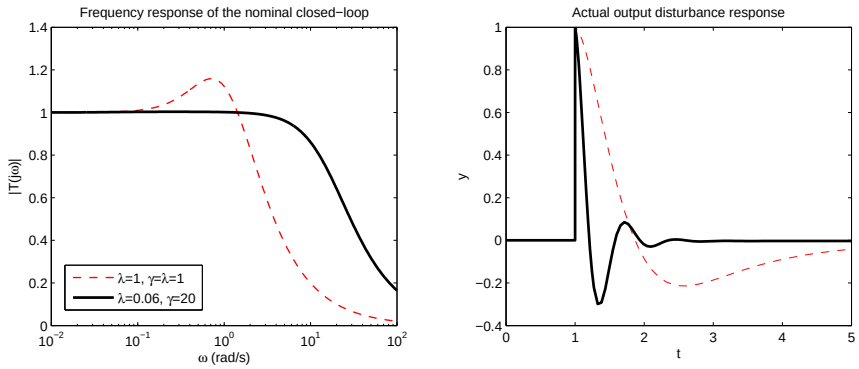

Figure 7.4: Frequency and time responses (Example 1).

reasonable option is to detune the controller, moving the peak in $|T|$ to lower frequencies (see Figure 7.4). This will improve robustness at the expense of nominal performance. In summary, even if there is an interaction between λ and γ, their roles are clearly different.

Example 2 As pointed out in the early work (Scali and Semino, 1991), an optimal controller designed for a specific type of disturbance (e.g., a step acting at the input of the plant) may result in very poor performance if the actual disturbance (e.g., a step acting at the output) is different from the one considered at the design stage. In this example, we examine how a balance between the response of input and output disturbances can be achieved, focusing on the FOPTD model $P = K_g \frac{e^{-sh}}{\tau s+1}$ ($K_g = 2, h = 1, \tau = 15$). The controller was already calculated in (7.13), and the corresponding filter has the same form as (7.33), taking now $a_1 = \tau - \tau(1 - \lambda/\tau)(1 - \gamma/\tau)$. Let us start by selecting $\lambda = \gamma = 1.75$, which provides $M_S = 1.69, M_T = 1.28, \mathrm{TV}_i = 2.98, \mathrm{TV}_o = 39.78$ ($\mathrm{TV}_i, \mathrm{TV}_o$ denote, respectively, the total variation with respect to the input and output disturbance). As shown by Figure 7.5(a), good attenuation of load disturbances is obtained. However, a somewhat large undershoot occurs for output disturbances. In the uncertain case ($h = 1.9$), we can see that the system becomes quite oscillatory ($\mathrm{TV}_i = 10.72, \mathrm{TV}_o = 82$), see Figure 7.5(b). By choosing $\gamma = \tau = 15$, we can avoid the undershoot in the output disturbance response, and improve the robustness margins, now $M_S = 1.33, M_T = 1, \mathrm{TV}_i = 2, \mathrm{TV}_o = 16.14$. As a result, the responses are smoother in the uncertain case ($\mathrm{TV}_i = 2.52, \mathrm{TV}_o = 18.6$), experiencing less

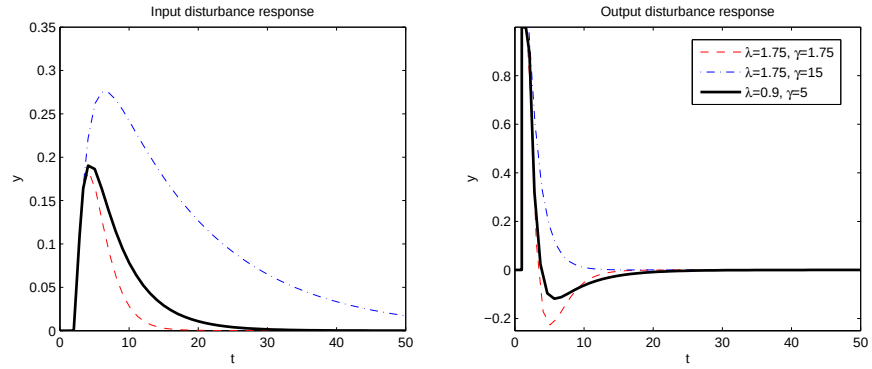

(a) Nominal case ($K_g = 2, h = 1, \tau = 15$).

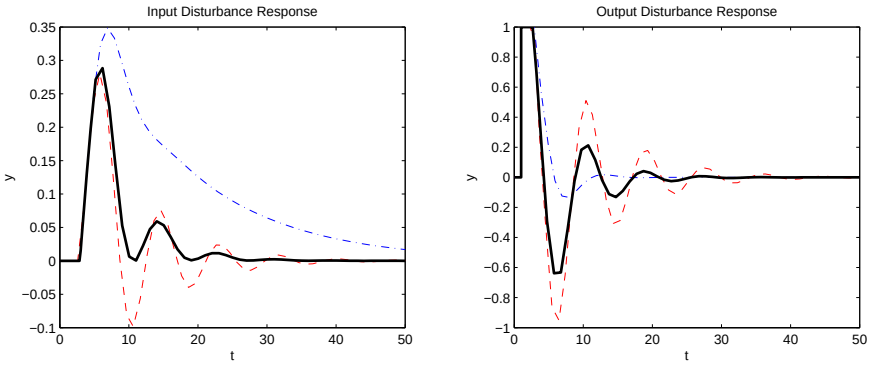

(b) Uncertain case ($K_g = 2, h = 1.9, \tau = 15$).

Figure 7.5: Input/Output step responses for Example 2.

performance degradation. However, the performance for load disturbances is poor, showing a sluggish return to steady state (this fact, sometimes referred to as *loss of integral action*, is specially relevant for very lag-dominant plants with high gain (Scali and Semino, 1991)). To reach a compromise, we finally retune the controller taking $\lambda = 0.9, \gamma = 5$. The latter values give $M_S = 1.6, M_T = 1.13, \mathrm{TV}_i = 2.55, \mathrm{TV}_o = 40.67$. In the uncertain case, $\mathrm{TV}_i = 6.73, \mathrm{TV}_o = 67.63$. The data concerning this example has been collected in Table 7.1.

Example 3 Lastly, we consider an stable second order system with a

Model: $K_g\frac{e^{-sh}}{\tau s+1}$			Nominal Case $K_g=2,h=1,\tau=15$				Uncertain Case $K_g=2,h=1.9,\tau=15$			
			Input dist.		Out. dist.		Input dist.		Out. dist.	
Tuning of (7.33)	M_S	M_T	TV	ISE	TV	ISE	TV	ISE	TV	ISE
$\lambda=\gamma=1.75$	1.69	1.28	2.98	0.17	39.78	2.39	10.72	0.31	82	6.3
$\lambda=1.75,\gamma=15$	1.33	1	2	0.66	16.14	2.34	2.52	0.69	18.6	3.06
$\lambda=0.9,\gamma=5$	1.6	1.13	2.55	0.21	60.67	2.71	6.73	0.29	67.63	5.92

Table 7.1: Data summary for Example 2.

pair of poorly damped poles. The model is given by $P=K_g\frac{e^{-sh}}{\left(\frac{s}{\omega_n}\right)^2+2\frac{\xi}{\omega_n}s+1}$ ($K_g=4,h=1,\omega_n=0.5,\xi=0.25$). Our design suggests the controller $Q=P_m^{-1}f=\left((s/\omega_n)^2+2\xi/\omega_n s+1\right)f$, where f has the following structure

$$f=\frac{a_2s^2+a_1s+a_0}{(\lambda s+1)^2\left(\gamma_{1,2}s^2+\gamma_{1,1}s+1\right)} \tag{7.34}$$

and the a_i coefficients satisfy that $P_af=e^{-s}f=1$ at the poles of $W=\frac{(\lambda s+1)^2(\gamma_{1,2}s^2+\gamma_{1,1}s+1)}{s((s/\omega_n)^2+2\xi/\omega_n s+1)}$. First, we select $\lambda=0.5$. For output disturbances, we then take $\gamma_{1,2}=(1/\omega_n)^2=4,\gamma_{1,1}=2\xi/\omega_n=1$, which results into $f=\frac{1}{(0.5s+1)^2}$. The associated responses can be seen in Figure 7.6 for both the nominal and the uncertain cases. The tuning $\lambda=0.5,\gamma_{1,2}=4,\gamma_{1,1}=1$ gives $M_S=1.62,M_T=1,\mathrm{TV}_i=4.91,\mathrm{TV}_o=140$ (Nominal Case) and $\mathrm{TV}_i=6.5,\mathrm{TV}_o=142$ (Uncertain Case). This design gives good results for output disturbances because the slightly damped poles are cancelled by the feedback controller. However, as no additional damping is really provided, these modes appear when excited from the input of the plant. Consequently, the response to load disturbances is quite oscillatory. To obtain much better performance for load disturbances, we select $\lambda=0.5,\gamma_{1,2}=\lambda^2=0.25,\gamma_{1,1}=2\lambda=1$. For these settings, the filter is $f=\frac{2.9658s^2+2.3389s+1}{(0.5s+1)^4}$. As desired, the response to load disturbances has been improved noticeably. However, a great undershoot appears for output disturbances, indicating that robustness has been seriously degraded: $M_S=3.88,M_T=2.96$. The corresponding input usage is given by $\mathrm{TV}_i=41.44,\mathrm{TV}_o=1840$ (Nominal Case) and $\mathrm{TV}_i=236.8,\mathrm{TV}_o=8365$ (Uncertain Case, $h=1.15$). A trade-off between the two designs considered so far can be obtained by selecting $\lambda=0.25,\gamma_{1,2}=3,\gamma_{1,1}=2$, which corresponds to the filter $f=\frac{4.682s^2+2.06s+1}{(0.25s+1)^2(3s^2+2s+1)}$. With this retuning, we finally

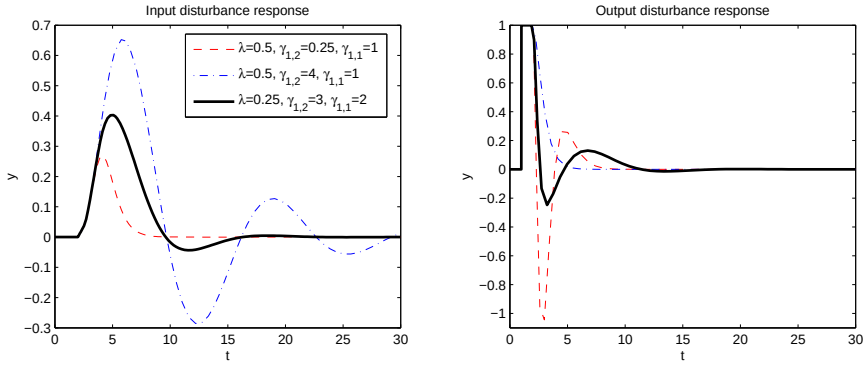

(a) Nominal Case ($K_g = 4, h = 1, \omega_n = 0.5, \xi = 0.25$).

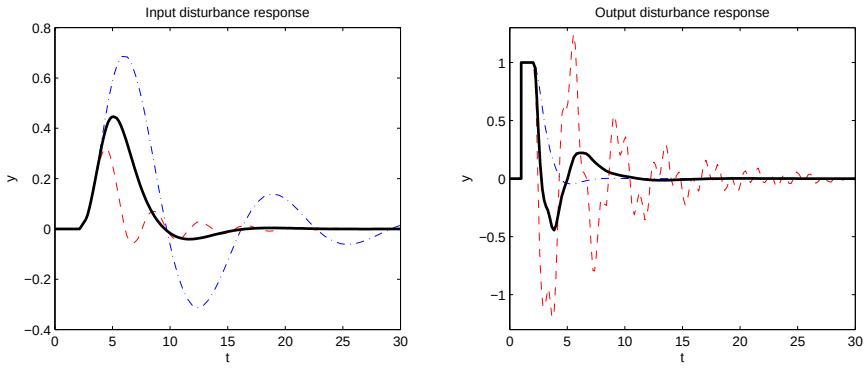

(b) Uncertain Case ($K_g = 4, h = 1.15, \omega_n = 0.5, \xi = 0.25$).

Figure 7.6: Input/Output step responses for Example 3.

get $M_S = 2.21, M_T = 1.35, \mathrm{TV}_i = 17.21, \mathrm{TV}_o = 903$ (Nominal Case) and $\mathrm{TV}_i = 24.4, \mathrm{TV}_o = 1121$ (Uncertain Case). The idea for selecting $\gamma_{1,2}, \gamma_{1,1}$ is to place the complex poles of f to the left of those of the plant P, and with increased damping factor. A summary of the results obtained can be consulted in Table 7.2 and Table 7.3.

To conclude this example, we will consider the simplified structure for f given by (7.24), which in the case at hand has the form

$$f = \frac{a_2 s^2 + a_1 s + a_0}{(\lambda s + 1)^2 (\gamma s + 1)^2} \tag{7.35}$$

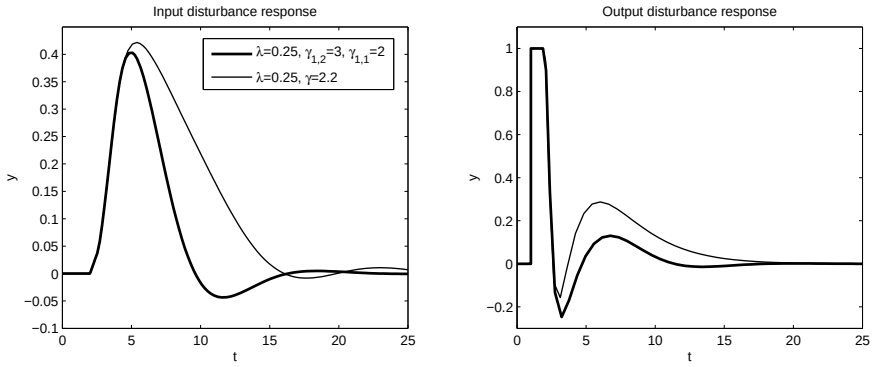

(a) Nominal Case ($K_g = 4, h = 1, \omega_n = 0.5, \xi = 0.25$).

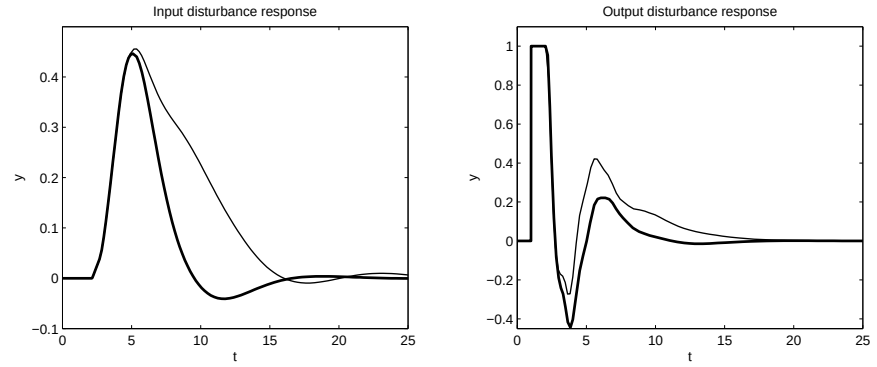

(b) Uncertain Case ($K_g = 4, h = 1.15, \omega_n = 0.5, \xi = 0.25$).

Figure 7.7: Time responses for Example 3 with simplified filter structure.

where the a_i coefficients satisfy that $P_a f = e^{-s} f = 1$ at the poles of $W = \frac{(\lambda s+1)^2(\gamma s+1)^2}{s((s/\omega_n)^2+2\xi/\omega_n s+1)}$. This filter has the same structure suggested by Campi *et al.* (1994) for MP unstable plants. If we choose $\gamma = \lambda$, we recover the design for input disturbances. The purpose now is to show that, although this filter can also be used to improve robustness with respect to the design for input disturbances, the robustness enhancement requires in general to sacrifice more nominal performance than when using the full-structure filter with $\gamma_{1,2}, \gamma_{1,1}$. Taking $\lambda = 0.25, \gamma = 2.2$, the concrete filter $f = \frac{8.354s^2+3s+1}{(0.25s+1)^2(2.2s+1)^2}$ results, for which $M_S = 2.24, M_T = 1.4$. These robustness indicators are only a little worse than those obtained for the previous trade-off tuning ($M_S =$

Model: $K_g \frac{e^{-sh}}{\left(\frac{s}{\omega_n}\right)^2+2\frac{\xi}{\omega_n}s+1}$			Nominal Case $K_g = 4, h = 1, \omega_n = 0.5, \xi = 0.25$			
			Input dist.		Output dist.	
Tuning of (7.34)	M_S	M_T	TV	ISE	TV	ISE
$\lambda = 0.5, \gamma_{12} = 0.25, \gamma_{11} = 1$	3.88	2.96	41.44	0.59	1840	11.55
$\lambda = 0.5, \gamma_{12} = 4, \gamma_{11} = 2$	1.62	1	4.91	3.78	140	8.19
$\lambda = 0.25, \gamma_{12} = 3, \gamma_{11} = 2$	2.21	1.35	17.21	2.14	903	9.78

Table 7.2: Data summary for Example 3 (Nominal Case).

Model: $K_g \frac{e^{-sh}}{\left(\frac{s}{\omega_n}\right)^2+2\frac{\xi}{\omega_n}s+1}$	Uncertain Case $K_g = 4, h = 1.15, \omega_n = 0.5, \xi = 0.25$			
	Input dist.		Output dist.	
Tuning of (7.34)	TV	ISE	TV	ISE
$\lambda = 0.5, \gamma_{12} = 0.25, \gamma_{11} = 1$	236.8	0.85	8365	33.82
$\lambda = 0.5, \gamma_{12} = 4, \gamma_{11} = 2$	6.5	4.73	142	8.34
$\lambda = 0.25, \gamma_{12} = 3, \gamma_{11} = 2$	24.4	2.62	1121	12.5

Table 7.3: Data summary for Example 3 (Uncertain Case).

$2.21, M_T = 1.35$). However, the overall performance is considerably worse as it can be appreciated from Figure 7.7. This shows the necessity of considering complex conjugate poles in the filter f for the best trade-off design.

7.5 Summary

In this chapter, we have presented a regulatory design method which considers whether the disturbances enter at the input or at the output of the plant. When both kind of disturbances are expected, the design allows to reach a balance. This is achieved by means of considering a weighted sensitivity problem where the weight is mostly guided by the input type and the conflictive poles of the plant. The final solution can be interpreted in terms of alternative IMC filters which allow to adjust both the robustness/performance and the input/output disturbance trade-offs. Simulation examples have shown that improving the rejection of input disturbances inherently requires larger peaks of the sensitivity functions, resulting into more aggressive responses. Further work will focus on the application to PID control.

Chapter 8

Conclusions and perspectives

8.1 Conclusions

This thesis deals with various aspects of the design of single-loop feedback compensators from an analytical point of view. The design methods that have been presented rely on a model of the process under control, given as a transfer function, and base the controller derivation on minimizing the weighted sensitivity function using standard system norms. The initial works in Chapters 2–4 motivate the usage of the $\mathcal{H}_\infty$ WSP for controller design, and the consideration of both robustness/performance and servo/regulator issues. A first attempt to select the weight systematically is made in Chapter 5. Afterwards, a refined selection of the weight is presented in Chapter 6, where the extension to unstable plants is carried out without using the notion of coprime factorization; this is achieved by considering possibly unstable weights. Finally, Chapter 7 applies the same design ideas to $\mathcal{H}_2$ optimization, while coping with some extensions such as plants with complex conjugate poles. In addition, in Chapter 7 an interpretation of the proposed solution in terms of generalized IMC filters is given.

In summary, the designs in Chapters 6 and 7 arise from a systematic choice of the weight in the WSP that explicitly captures the following control requirements: robustness, set-point (or output disturbance) response and load disturbance response. More precisely, a single parameter (λ) is used for detuning purposes, allowing adjustment of the robustness/performance trade-off as in IMC, whereas a set of parameters (γ_i) is used to balance the servo/regulator

performance. Tuning γ_i has also an effect on robustness, but it should be clear that the way of affecting the robustness properties is different: λ is more related to the closed-loop bandwidth, which by the Small-Gain Theorem is responsible for robustness in the high frequency region (model uncertainty). On the other hand, the γ_i parameters affect the mid-frequency robustness properties altering the peaks on the sensitivity functions (M_S and M_T). Stated otherwise, a regulatory design inherently requires larger values of M_S and M_T than a servo one for a fixed value of λ.

Apart from the considered ones, there are other essential requirements of a control system: noise sensitivity and required control activity. These points have not received specific attention in this thesis, for example, perfect measurement has been assumed. In practice, however, the sensitivity to measurement noise and the manipulated variable must be kept within prescribed bounds to reduce the actuator wear and tear. Although this may be conservative, augmenting λ to detune the controller implicitly decreases both the sensitivity to noise and the demanded control effort (Skogestad, 2006). The conservativeness of this approach is something that one may accept in the interests of mathematical convenience and simplicity. In this direction, if low-order models are used, the presented methodology can be applied to PID control as it has been done in Chapter 6. The resulting tuning rules are suitable for teaching purposes and have been found to yield good results compared with existing ones. The distinguishing feature of the derived tuning rules is that they unify the stable/unstable plant cases while introducing a servo/regulator consideration.

8.2 Perspectives

As always, there are improvements/extensions which can be addressed to continue the work done in this thesis. Some ideas are detailed below:

PID tuning

Revisiting the SIMC rules

Based on IMC principles, Skogestad (2003) presented remarkably simple and effective tuning expressions for PI/D controllers known as the SIMC rules.

Compared with the original IMC-based tuning rules (Rivera *et al.*, 1986), the SIMC settings provide an improvement of the regulatory performance in terms of load disturbance rejection. A limitation of the SIMC rules, as noted in the closely-related article (Shamsuzzohaa and Skogestad, 2010), is that they are only applicable to stable systems. In contrast, the tuning rules given in Chapter 6 include unstable plants too. Therefore, Chapter 6 constitutes a good framework to revisit the SIMC rules including unstable plants in the discussion. In this regard, some preliminary work can be found in (Alcántara *et al.*, 2011*b*).

Extension to fractional PID control

Fractional order control has received a considerable attention during the last years. Generally speaking, it has been shown that, although the tuning of the controller gets more involved, fractional order controllers outperform their integer order counterparts in general. Consult, for example, (Padula and Visioli, 2011) and the references therein for a deeper discussion in the particular context of fractional PID control. Although some analytic approaches have been extended to the fractional order setting, there is a lack of results (to the best of the author's knowledge) regarding the $\mathcal{H}_\infty$ weighted sensitivity approach. Thus, one could try to reformulate (in fractional order terms) the WSP used in Chapter 6 (will Lemma 1.2.1 still hold in the fractional order case?): for example, one may consider a fractional FOPTD model and a fractional weight. This could be used to obtain fractional order PID tuning rules. The resulting framework would allow a fair comparison between different cases arising from the use of fractional or integer order models for the plant and the controller. Along these lines, preliminary results have already been obtained in (Padula *et al.*, 2011).

Fixed-order single-loop controllers

The methods in Chapters 6 and 7 can be used as the first step towards the synthesis of fixed-order controllers. After giving suitable values to the tuning parameters λ and γ_i, the resulting feedback controller K may be of high order (this is the situation when a high order model for the plant is used). In a second step, a model order reduction scheme can be applied to find out a low order approximation $\hat{K}$ that matches the original controller as well as possible.

This would provide users with the option to achieve a specified approximation accuracy at the cost of complexity or retain a simple controller accepting some performance deterioration. It would also be useful to study when low-order controllers as those of PID type are suitable and when higher-order realizations are justified [1]. For the conventional IMC design procedure, these ideas are already implemented in (Wang *et al.*, 2001), where the following loss function is minimized

$$J^{(k)} = \sum_{i=1}^{M} \left| \hat{K}(j\omega_i) - K(j\omega_i) \right|^2 \tag{8.1}$$

using standard least-squares. In (8.1), k denotes the order of $\hat{K}$, and $J^{(k)}$ is (implicitly) a function of the parameters of $\hat{K}$ (e.g., K_c, T_i, T_d in the ideal PID case). Provided that K is internally stabilizing (and assuming that K and $\hat{K}$ have the same RHP poles), the stability issue for $\hat{K}$ can then be easily addressed with respect to K using standard robust control theory (Skogestad and Postlethwaite, 2005). Within this approach, two sources of uncertainty are considered: the real one (plant/model mismatch), and a fictitious one coming from the controller approximation error (Wang *et al.*, 2001). Because the mismatch between K and $\hat{K}$ is perfectly known (including phase information), a less conservative procedure would be to check first that $\hat{K}$ is internally stabilizing and, in a second step, tackle robust stability with respect to $\hat{K}$.

If the final aim is to get PID controllers, another popular option is to consider a Maclaurin series expasion of the original controller. If we express it as $K = f(s)/s$, then

$$K = \frac{1}{s}\left(f(0) + f'(0)s + \frac{f''(0)}{2}s^2 + \cdots \right) \tag{8.2}$$

With respect to an ideal PID controller, considering the first three terms yields the following tuning

$$K_c = f'(0) \quad T_i = \tfrac{f'(0)}{f(0)} \quad T_d = \frac{f''(0)}{2f'(0)} \tag{8.3}$$

[1] Other interesting approaches to fixed-order attanaible performance can be consulted in (Ibeas *et al.*, 2008; Larsson and Hagglund, 2011). Ibeas *et al.* (2008) presents a solution based on the Multiple-Model paradigm, whereas Larsson and Hagglund (2011) compares PID controllers with optimal ones, obtained through the use of the Youla-Kucera parameterization.

Of course, in order to get a PID compensator, one can also consider the specific structure of the controller from the very beginning and try a direct optimization as in the design reported in (Sanchís *et al.*, 2010). This (remarkably simple) direct approach avoids the inherent conservatism of using a low order model (like the FOPTD one) to represent the real process, and better performance can be obtained generally.

Independent tuning parameters and additional requirements

The design methods in Chapters 6 and 7 are based on adjusting the robustness/performance and servo/regualtor trade-offs through the λ and γ_i's parameters, respectively. These parameters are not independent in the sense that there is some interaction between them. For example, if the (load) disturbance attenuation is improved by increasing γ_i, this will also imply a robustness loss, which may require a retuning of λ if the new robustness margins are below the prescribed values. Although this makes sense because, in general, a regulatory design results in inferior robustness than a servo one (Skogestad and Postlethwaite, 2005, Chapter 2), it would be nice that the involved parameters were noninteracting so facilitate the tuning task. A MPC design which achieves this goal can be consulted in (Ogunnaike and Mukati, 2006), where three normalized tuning parameters are used to tune robustness, set-point response and disturbance suppression attributes *independently*.

On the other hand, there are important aspects that have not been explicitly considered in the adopted weighted sensitivity formulation. Two examples are measurement noise sensitivity and control effort constraints. Incorporating them into the design procedure is also left for future work. A recent numerical approach taking into account restrictions on the control signal and noise sensitivity is presented in (Larsson and Hagglund, 2011).

Alternatives to common 2DOF strategies

Although load disturbance regulation is often of primary concern, achieving a high performance in the set-point following task is also important in many applications. To address this problem, the typical approach is to adopt a 2-DOF strategy, namely to use a feedforward (linear) compensator to reduce the overshoot in the set-point response (Visioli, 2004). The common set-point weighting strategy (Astrom and Hagglund, 2005) falls within this framework.

The main limitation of this method is that the reduction of the overshoot is paid by a slower response (Visioli, 2004). In order to achieve low rise times and low overshoots simultaneously, different alternatives have been suggested in the literature. For example, a switched scheme is presented in (Visioli, 2002) based on IMC principles. Non-linear reference processing is used in (Visioli, 2004), whereas a non-causal approach based on dynamic inversion is taken in (Piazzi and Visioli, 2006). Other proposals are based on a reset mechanism (Baños and Vidal, 2007; Bakkeheim *et al.*, 2008) or on using a multi-loop control configuration (Tran *et al.*, 2007; Tahboub, 2011) .

According to (Visioli, 2002), in order to accommodate conflicting specifications (i.e., having both good set-point following and good load disturbance rejection at the same time), it seems sensible to use different control laws when a set-point change occurs and when the steady-state has to be maintained. In this direction, as the methods presented in Chapters 6 and 7 offer the possibility of adjusting the servo/regulator modes, they can be used to guide the selection of the controller for the extreme servo and regulator situations. In (Alcántara *et al.*, 2011*b*) (Appendix 6A), this idea is applied to the reset-based PI controller introduced by Baños and Vidal (2007), and the results are compared with those obtained using the classical set-point weighting strategy. Nevertheless, this work finds itself at an early stage and no firm conclusion has been reached yet.

MIMO extension

This work has concentrated on SISO systems. It is well-recognized that the design for the multivariable case, also referred to as Multiple-Input Multiple-Output (MIMO), is much more challenging. A simplistic approach with widespread use in industry is given by *decentralized control* (Skogestad and Postlethwaite, 2005). Roughly speaking, decentralized control is based on considering the multivariable plant diagonal, neglecting the interaction between the off-diagonals channels. Therefore, the design is simplified to that of n independent control loops. For MIMO plants with weak interactions, it is clear then that the presented designs can be easily applied along the lines of (Liu *et al.*, 2005; Vilanova *et al.*, 2009*b*).

The design gets more complicated when the interactions between the different channels are strong. In this case, one possibility is to use a *decoupling* strategy to make the plant nearly diagonal in a first step, and then use a

decentralized design. It is also possible to obtain decoupled (diagonal) responses in a single step (Zhang *et al.*, 2006*b*). The last possibility (for sure the most difficult one from an analytical point of view) is to adopt a *centralized* approach.

Further research to extend the presented ideas to the decoupling and centralized cases is necessary. A good starting point are the works in (Zhang *et al.*, 2006*c*; Zhang *et al.*, 2006*b*), where a SISO IMC-like design (Zhang *et al.*, 2006*c*) is extended to a decoupling MIMO design (Zhang *et al.*, 2006*b*).

Finally, the above-listed ideas should be put into practice to see whether they are beneficial to real-world control applications. As this thesis has only addressed design methods for continuous-time systems, the final solutions must be converted to discrete form for computer-based implementation.

Bibliography

Aguirre, L. A. (1992). PID tuning based on model matching. *Electronic Letters* **28**(25), 2269 – 2271.

Alcántara, S., C. Pedret and R. Vilanova (2010*a*). On the model matching approach to PID design: Analytical perspective for robust Servo/Regulator tradeoff tuning. *Journal of Process Control* **20**(5), 596 – 608.

Alcántara, S., C. Pedret, R. Vilanova and P. Balaguer (2010*b*). Analytical $\mathcal{H}_\infty$ Sensitivity matching approach to Smooth PID design: Quantitative Servo/Regulator tuning guidelines. Internal report.

Alcántara, S., C. Pedret, R. Vilanova and S. Skogestad (2011*a*). Generalized Internal Model Control for balancing input/output disturbance response. *Industrial & Engineering Chemistry Research* **50**(19), 11170–11180.

Alcántara, S., C. Pedret, R. Vilanova and W. Zhang (2009). Analytical $\mathcal{H}_\infty$ design for a Smith-type inverse response compensator. In: *Proc. of the American Control Conference*. pp. 1604–1609.

Alcántara, S., C. Pedret, R. Vilanova and W. Zhang (2010*c*). Simple Analytical min-max Model Matching Approach to Robust Proportional-Integrative-Derivative Tuning with Smooth Set-Point Response. *Industrial & Engineering Chemistry Research* **49**(2), 690 – 700.

Alcántara, S., C. Pedret, R. Vilanova and W. Zhang (2010*d*). Unified Servo/Regulator Design for Robust PID Tuning. In: *Proc. of IEEE Conference on Control Applications*. pp. 2432 – 2437.

Alcántara, S., S. Skogestad, C. Grimholt, C. Pedret and R. Vilanova (2011*b*). Tuning PI controllers based on $\mathcal{H}_\infty$ Weighted Sensitivity. In: *Proc. of the 19th Mediterranean Conference on Control and Automation*.

Alcántara, S., W.D. Zhang, C. Pedret, R. Vilanova and S. Skogestad (2011*c*). IMC-like analytical $\mathcal{H}_\infty$ design with S/SP mixed sensitivity consideration: Utility in PID tuning guidance. *Journal of Process Control* **21**(6), 976 – 985.

Ali, A. and S. Majhi (2009). PI/PID controller design based on IMC and percentage overshoot specification to controller setpoint change. *ISA Transactions* **48**, 10 – 15.

Amiri, M. S. and S. L. Shah (2009). Guidelines on robust PID controller tuning for FOPTD processes. In: *Proc. of the 8th World Congress of Chemical Engineering*.

Arrieta, O., A. Visioli and R. Vilanova (2010). PID autotuning for weighted servo/regulation control operation. *Journal of Process Control* **20**(4), 472 – 480.

Arrieta, O. and R. Vilanova (2007). Servo/regulation tradeoff tuning of PID controllers with a robustness consideration. *Proc of the 46th Conference on Decision and Control*.

Astrom, K. and T. Hagglund (2001). The future of PID control. *Control Engineering Practice* **9**(11), 1163 – 1175.

Astrom, K. and T. Hagglund (2004). Revisiting the Ziegler-Nichols step response method for PID control. *J. Process Control* **14**, 635–650.

Astrom, K. and T. Hagglund (2005). *Advanced PID control*. ISA - The Instrumentation, Systems, and Automation Society.

Astrom, K. J., H. Panagopoulos and T. Hagglund (1998). Design of PI controllers based on non-convex optimization. *Automatica* **34**, 585–601.

Bakkeheim, J., T. A. Johansen, Ø. N. Smogeli and A. J. Sørensen (2008). Lyapunov-Based Integrator Resetting With Application to Marine Thruster Control. *IEEE Trans. on Control Systems Technology* **16**(5), 908 – 917.

Balaguer, P., A. Ibeas, C. Pedret and S. Alcántara (2009). Controller Parameters Dependence on Model Information Through Dimensional Analysis. *Proc of the 48th Conference on Decision and Control*.

Baños, A. and A. Vidal (2007). Definition and tuning of a PI+CI reset controller. In: *Proc. of the European Control Conference*. pp. 4792 – 4798.

Barreiro, A. and A. Baños S. Dormido (2011). Reset Control Systems with Reset Band: Well-posedness and Limit Cycles Analysis. In: *Proc. of the 19th Mediterranean Conference on Control and Automation*.

Beker, O., C.V. Hollot and Y. Chait (2001). Plant with integrator: an example of reset control overcoming limitations of linear feedback. *Automatic Control, IEEE Transactions on* **46**(11), 1797 – 1799.

Bernstein, D. S. (2011). Exquisite Coupling. *IEEE Control Systems Magazine* **31**(2), 6 – 8.

Campi, M., W. S. Lee and B. D. O. Anderson (1994). New Filters for Internal Model Control Design. *International Journal of Robust and Nonlinear Control* **4**(6), 757 – 775.

Chien, I. L. and P. S. Fruehauf (1990). Consider IMC tuning to improve controller performance. *Chemical Engineering Progress* **86**(10), 33 – 41.

Churchill, R. and J. Brown (1986). *Complex Variable and Applications*. McGraw Hill.

de Vusse, J. G. Van (1964). Plug-flow type reactor versus tank reactor. *Chem. Eng. Sci.* **19**, 964.

Dehghani, A., A. Lanzon and B.O. Anderson (2006). $\mathcal{H}_\infty$ design to generalize internal model control. *Automatica* **42**(11), 1959 – 1968.

Doyle, J.C., B.A. Francis and A. Tanenbaum (1992). *Feedback Control Theory*. MacMillan Publishing Company.

El Rifai, Khalid (2009). Nonlinearly parameterized adaptive pid control for parallel and series realizations. In: *Proceedings of the American Control Conference*. pp. 5150–5155.

Faanes, A. and S. Skogestad (2004). Feedforward control under the presence of uncertainty. *European Journal of Control* **10**(1), 30 – 46.

Feuer, A., G. C. Goodwin and M. Salgado (1997). Potential benefits of hybrid control for linear time invariant plants. In: *Proc. of the IEEE American Control Conference*. Vol. 5. pp. 2790 – 2794.

Francis, B. A. (1987). *A course in $\mathcal{H}_\infty$ Control theory*. Springer-Verlag. Lecture Notes in Control and Information Sciences.

Ge, M., M. Chiu and Q. Wang (2002). Robust PID controller design via LMI approach. *J. Process Control* **12**, 3–13.

He, J., Q. Wang and T. Lee (2000). PI/PID controller tuning via LQR approach. *Chemical Engineering Science* **55**, 2429 – 2439.

Hoagland, M. B. and B. Dodson (1995). *The Way Life Works*. Times Books.

Hohenbichler, N. (2009). All stabilizing PID controllers for time delay systems. *Automatica* **45**(11), 2678 – 2684.

Horn, I. G., J. R. Arulandu, C. J. Gombas, J. G. VanAntwerp and R. D. Braatz (1996). Improved Filter Design in Internal Model Control. *Industrial & Engineering Chemistry Research* **35**(10), 3437 – 3441.

Ibeas, A. and S. Alcántara (2010). Stable genetic adaptive controllers for multivariable systems using a two-degree-of-freedom topology. *Engineering Applications of Artificial Intelligence* **23**(1), 41 – 47.

Ibeas, A., P. Balaguer, R. Vilanova and C. Pedret (2008). On-Line Model Selection Techniques By Using Multiple Models And Supervision Algorithms. In: *IEEE International Symposium on Intelligent Control*. pp. 631 – 636.

Isaakson, A. and S. Graebe (2002). Derivative filter is an integral part of PID design. *IEE Proc. Part D* **149**, 41 – 45.

Kano, M. and M. Ogawa (2010). The state of the art in chemical process control in Japan: Good practice and questionnaire survey. *Journal of Process Control* **20**(9), 969 – 982.

Kristiansson, B. and B. Lennartson (1998). Optimal PID controllers for unstable and resonant plants. In: *Proc. of the IEEE Conference on Decision and Control*. pp. 4380–4381.

Kristiansson, B. and B. Lennartson (2006). Robust tuning of PI and PID controllers: using derivative action despite sensor noise. *IEEE Control Systems Magazine* **26**(1), 55 – 69.

Kwok, W.W. and D.E. Davison (2007). Implementation of stabilizing control laws - how many controller blocks are needed for a universally good implementation?. *Control Systems Magazine, IEEE* **27**(1), 55–60.

Larsson, Per-Ola and Tore Hagglund (2011). Control Signal Constraints and Filter Order Selection for PI and PID Controllers. In: *Proc. of the American Control Conference*.

Lee, W. S. and J. Shi (2008). Improving $\mathcal{H}_\infty$ to Generalize Internal Model Control with Integral Action. In: *Proc. of the Chinese Control and Decision Conference (CCDC)*.

Lee, Y., J. Lee and S. Park (2000). PID controller tuning for integrating and unstable processes with time delay. *Chemical Engineering Science* **55**(17), 3481 – 3493.

Leva, A. and M. Maggio (2011). A systematic way to extend ideal PID tuning rules to the real structure . *Journal of Process Control* **21**(1), 130 – 136.

Liu, Tao, Weidong Zhang and Danying Gu (2005). Analytical Multiloop PI/PID Controller Design for Two-by-Two Processes with Time Delays. *Industrial & Engineering Chemistry Research* **44**, 1832 – 1841.

Luyben, W. (2001). Effect of derivative algorithm and tuning selection on the PID control of dead-time processes. *Industrial & Engineering Chemistry Research* **40**, 3605 – 3611.

McFarlane, D. C. and K. Glover (1992). A loop shaping design procedure using $\mathcal{H}_\infty$ synthesis. *IEEE Trans. Automat. Contr.* **37**(6), 759 – 769.

Morari, M. and E. Zafiriou (1989). *Robust Process Control*. Prentice-Hall International.

O'Dwyer, A. (2006). *Handbook of PI and PID controller tuning rules*. 2nd edition ed.. Imperial College Press.

Ogunnaike, B. and K. Mukati (2006). An alternative structure for next generation regulatory controllers: Part I: Basic theory for design, development and implementation. *Journal of Process Control* **16**(5), 499 – 509.

Ou, L., W. Zhang and L. Yu (2009). Low-Order Stabilization of LTI Systems With Time Delay. *IEEE Trans. Automat. Contr.* **54**(4), 774 – 787.

Padula, F. and A. Visioli (2011). Tuning rules for optimal PID and fractional-order PID controllers. *Journal of Process Control* **21**(1), 69 – 81.

Padula, F., R. Vilanova and A. Visioli (2011). $\mathcal{H}_\infty$ Optimal Interpolation for Fractional First Order Plus Dead Time Systems. Submitted.

Paesa, D., C. Franco, S. Llorente, G. Lopez-Nicolas and C. Sagues (2011). Reset observers applied to MIMO systems. *Journal of Process Control* **21**(4), 613 – 619.

Panagopoulos, H., K.J. Astrom and T. Hagglund (2002). Design of PID controllers based on constrained optimisation. *Control Theory and Applications, IEE Proceedings* - **149**(1), 32 –40.

Pannocchia, Gabriele, Nabil Laachi and James B. Rawlings (2005). A candidate to replace PID control: SISO-constrained LQ control. *AIChE Journal* **51**(4), 1178–1189.

Pedret, C., R. Vilanova, R. Moreno and I. Serra (2002). A refinement procedure for PID controller tuning. *Computers & Chemical Engineering* **26**(6), 903 – 908.

Pernebo, L. (1981). An Algebraic Theory for the Design of Controllers for Linear Multivariable Systems-Part II: Feedback Realizations and Feedback Design. *IEEE Transactions on Automatic Control* **26**(1), 183 – 194.

Piazzi, A. and A. Visioli (2006). A noncausal approach for PID control. *Journal of Process Control* **16**(8), 831 – 843.

Rivera, Daniel E., Manfred Morari and Sigurd Skogestad (1986). Internal model control: PID controller design. *Industrial & Engineering Chemistry Process Design and Development* **25**(1), 252 – 265.

Sanchís, R., J. A. Romero and P. Balaguer (2010). Tuning of PID controllers based on simplified single parameter optimisation. *International Journal of Control* **83**(9), 1785 – 1798.

Scali, C. and D. Semino (1991). Performance of Optimal and Standard Controllers for Disturbance Rejection in Industrial Processes. In: *Conference of the IEEE Industrial Electronics Society (IECON).*

Shamsuzzoha, M. and M. Lee (2007). IMC-PID Controller Design for Improved Disturbance Rejection of Time-Delayed Processes. *Industrial & Engineering Chemistry Research* **46**(7), 2077 – 2091.

Shamsuzzoha, M. and M. Lee (2009). Enhanced disturbance rejection for open-loop unstable process with time delay. *ISA Transactions* **48**(2), 237 – 244.

Shamsuzzohaa, M. and S. Skogestad (2010). The setpoint overshoot method: A simple and fast closed-loop approach for PID tuning. *Journal of Process Control* **20**(10), 1220 – 1234.

Silva, G. J., A. Datta and S. P. Bhattacharyya (2002). New results on the synthesis of pid controllers. *IEEE Transactions On Automatic Control* **47**(2), 241 – 252.

Skogestad, S. (2003). Simple analytic rules for model reduction and PID controller tuning. *J. Process Control* **13**, 291–309.

Skogestad, S. (2006). Tuning for smooth PID control with acceptable disturbance rejection. *Industrial & Engineering Chemistry Research* **45**, 7817 – 7822.

Skogestad, S. and I. Postlethwaite (2005). *Multivariable Feedback Control*. Wiley.

Sánchez, J., A. Visioli and S. Dormido (2011). A two-degree-of-freedom PI controller based on events. *Journal of Process Control* **21**(4), 639 – 651.

Songa, Y., M. Tadñe and T. Zhang (2009). Stabilization and algorithm of integrator plus dead-time process using PID controller. *Journal of Process Control* **19**(9), 1529 – 1537.

Tahboub, K. A. (2011). Suitability of PID Controllers for Unstable Processes. An issue to be tackled in Undergraduate Control Education.. In: *Proc. of the 19th Mediterranean Conference on Control and Automation*.

Tavakoli, S., I. Griffin and P. Fleming (2007). Robust PI Control Design: A Genetic Algorithm Approach. *Int. Journal of Soft Computing* **2**(3), 401–407.

Toscano, R. (2005). A simple PI/PID controller design method via numerical optimization approach. *J. Process Control* **15**, 81–88.

Tran, T. H., Q. P. Ha and H. T. Nguyen (2007). Robust Non-Overshoot Time Responses Using Cascade Sliding Mode-PID Control. *Journal of Advanced Computational Intelligence and Intelligent Informatics* **11**(10), 1224 – 1231.

Vidal, A. and A. Baños (2010). Reset compensation for temperature control: Experimental application on heat exchangers. *Chemical Engineering Journal* **159**(1 – 3), 170 – 181.

Vidyasagar, M. (1985). *Control System Synthesis. A factorization approach*. MIT Press. Cambridge, Massachusetts.

Vilanova, R. (2008). IMC based Robust PID design: Tuning guidelines and automatic tuning. *Journal of Process Control* **18**, 61–70.

Vilanova, R. and I. Serra (1997). Realization of two-degree-of-freedom compensators. *IEE Proceedings. Part D.* **144**(6), 589–596.

Vilanova, R. and I. Serra (1999). Model reference control in two-degree-of-freedom control systems: Adaptive min-max approach. *IEE Proceedings. Part D.* **146**, 273–281.

Vilanova, R. and O. Arrieta (2007). PID design for improved disturbance attenuation: min max Sensitivity matching approach. *IAENG International Journal of Applied Mathematics*.

Vilanova, R., O. Arrieta and P. Ponsa (2009*a*). IMC based feedforward controller framework for disturbance attenuation on uncertain systems. *ISA Transactions* **48**(4), 439 – 448.

Vilanova, R., P. Balaguer, A. Ibeas and C. Pedret (2009*b*). Expected Interaction Analysis for Decentralized Control on TITO Systems: Application to IMC based PI/PID controller selection. *International Journal Of Innovative Computing, Information and Control* **5**(10B), 3439 – 3456.

Visioli, A. (2001). Optimal tuning of PID controllers for integral and unstable processes. *IEE Proceedings. Part D* **148**(2), 180 – 184.

Visioli, A. (2002). Improving the load disturbance rejection performances of IMC-tuned PID controllers. In: *Proc. of the 15th IFAC Triennial World Congress*.

Visioli, Antonio (2004). A new design for a PID plus feedforward controller. *Journal of Process Control* **14**(4), 457 – 463.

Wang, Q-G., C. hang and X-P. Yang (2001). Single-loop controller design via IMC principles. *Automatica* **37**(12), 2041 – 2048.

Youla, D., H.A. Jabr and J. Bongiorno (1976). Modern Wiener-Hopf design of optimal controllers, part II: The multivariable case. *IEEE Trans. Automat. Contr.* **21**(6), 319–338.

Zames, G. and B. Francis (1983). Feedback, minimax sensitivity, and optimal robustness. *IEEE Trans. Automat. Contr.* **AC-28**(5), 585 – 601.

Zhang, W., F. Allgower and T. Liu (2006*a*). Controller parameterization for SISO and MIMO plants with time delay. *Systems & Control Letters* **55**(10), 794 – 802.

Zhang, W., Y. Xi, G. Yang and X. Xu (2002). Design PID controllers for desired time-domain or frequency-domain response. *ISA Transactions* **41**(4), 511 – 520.

Zhang, Weidong, Chen Lin and Linlin Ou (2006*b*). Algebraic Solution to H2 Control Problems. II. The Multivariable Decoupling Case. *Industrial & Engineering Chemistry Research* **45**(21), 7163 – 7176.

Zhang, Weidong, Linlin Ou and Danying Gu (2006*c*). Algebraic Solution to H2 Control Problems. I. The Scalar Case. *Industrial & Engineering Chemistry Research* **45**(21), 7151 – 7162.

Zhong, Q.-C. (2003). Robust stability analysis of simple systems controlled over communication networks. *Automatica* **39**(7), 1309–1312.

Zhou, K. and Z. Ren (2001). A new controller architecture for high performance, robust and fault tolerant control. *IEEE Trans. Automat. Contr.* **46**(10), 1613–1618.

Zhuang, M. and D. Atherton (1993). Automatic tuning of optimum PID controllers. *IEE Proceedings. Part D* **140**(3), 216–224.

Ziegler, L. G. and N. B. Nichols (1942). Optimum settings for automatic controllers. *ASME* **64**, 759–768.